



# Ultra precise mass measurements at PENTATRAP

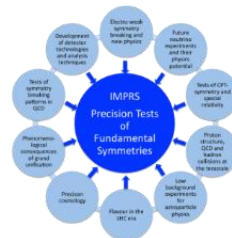
Menno Door

Max-Planck-Institut für Kernphysik, Heidelberg

2022/09/02



Max Planck Society



IMPRS-PTFS



DFG FOR 2202



ERC AdG 832848 - FunI



European Research Council  
Established by the European Commission



DFG SFB 1225

# Experiment PENTATRAP

Max-Planck Institute for Nuclear Physics (Heidelberg)  
Division “Stored and Cooled Ions” (Prof. Blaum)

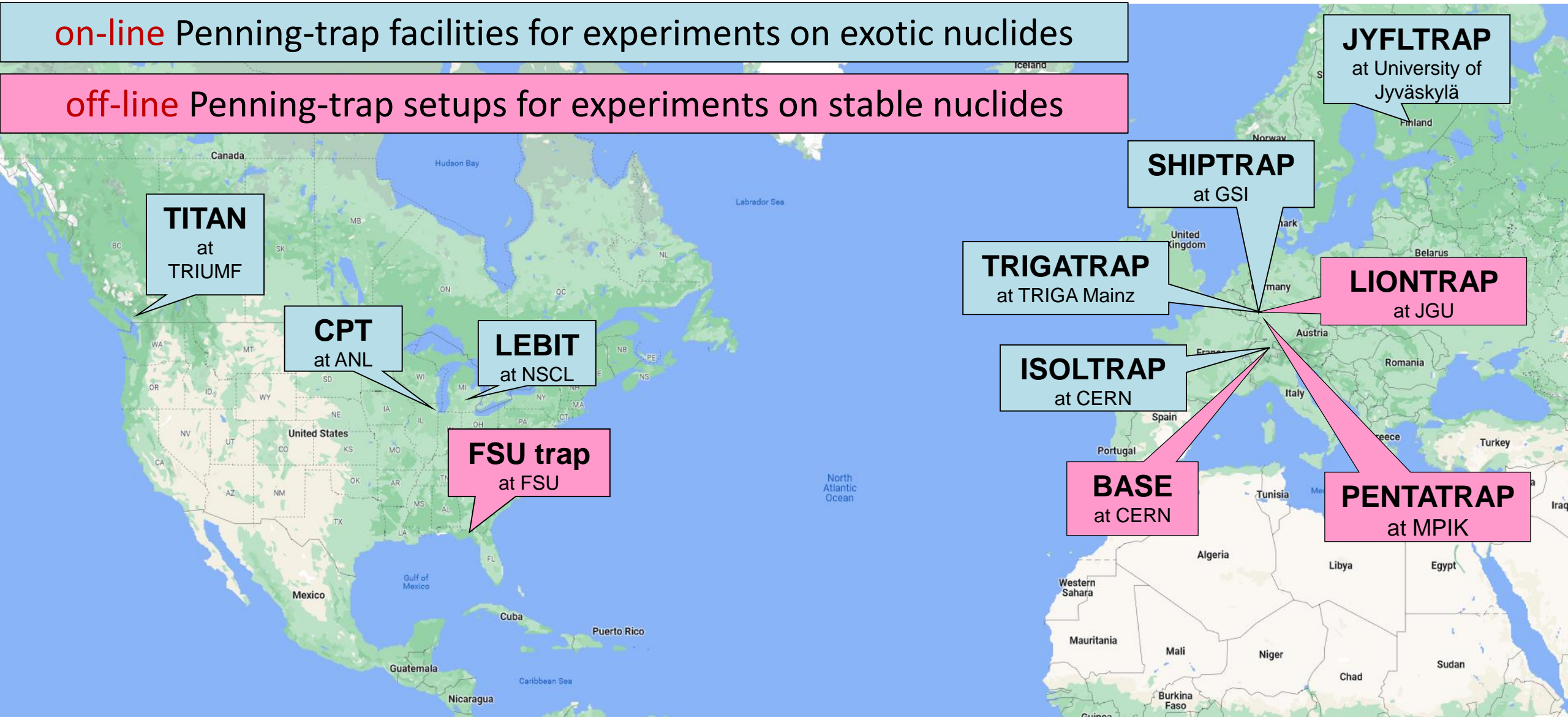


mass ratios of long-lived & stable nuclides  
with an uncertainty  $< 10^{-11}$

# High-Precision Penning Traps Worldwide

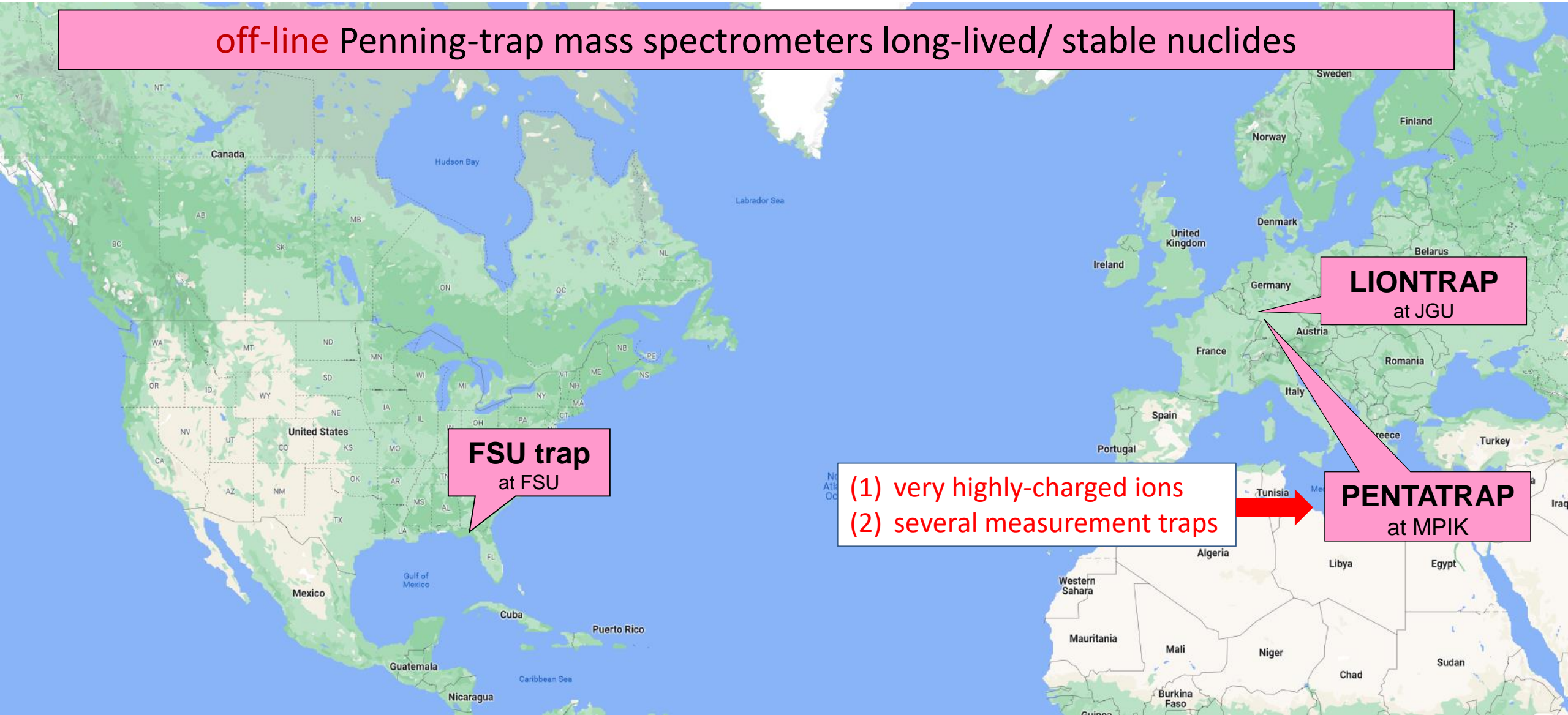
**on-line** Penning-trap facilities for experiments on exotic nuclides

**off-line** Penning-trap setups for experiments on stable nuclides



# High-Precision Penning Traps Worldwide

**off-line** Penning-trap mass spectrometers long-lived/ stable nuclides



**FSU trap**  
at FSU

**LIONTRAP**  
at JGU

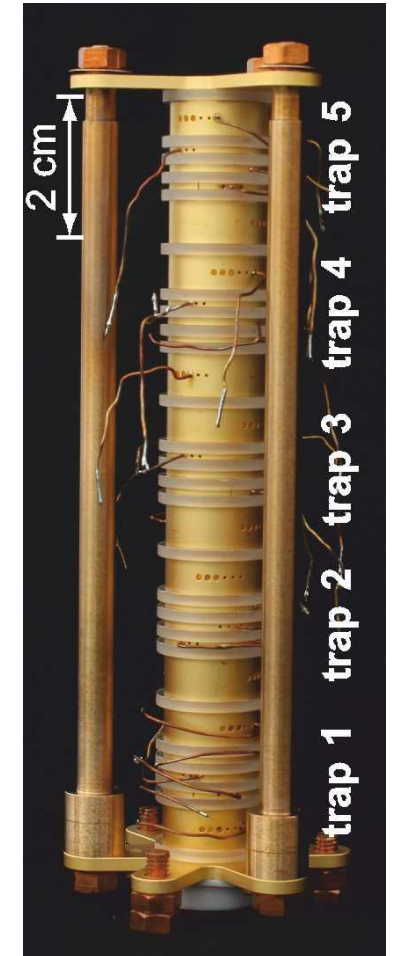
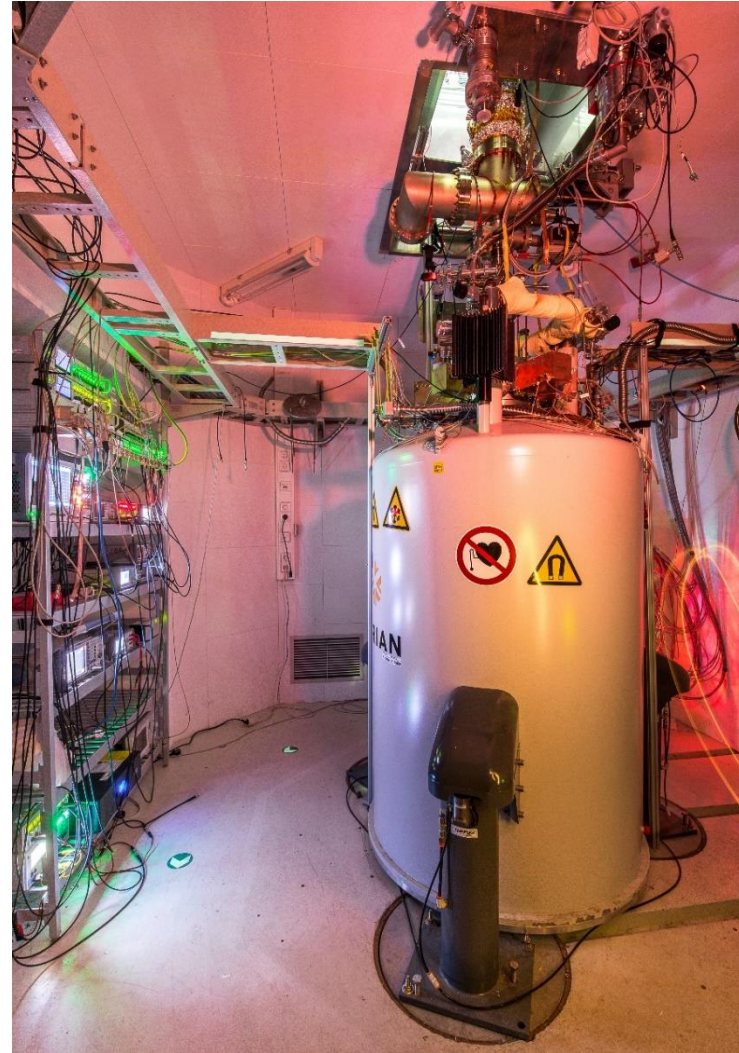
(1) very highly-charged ions  
(2) several measurement traps

**PENTATRAP**  
at MPIK

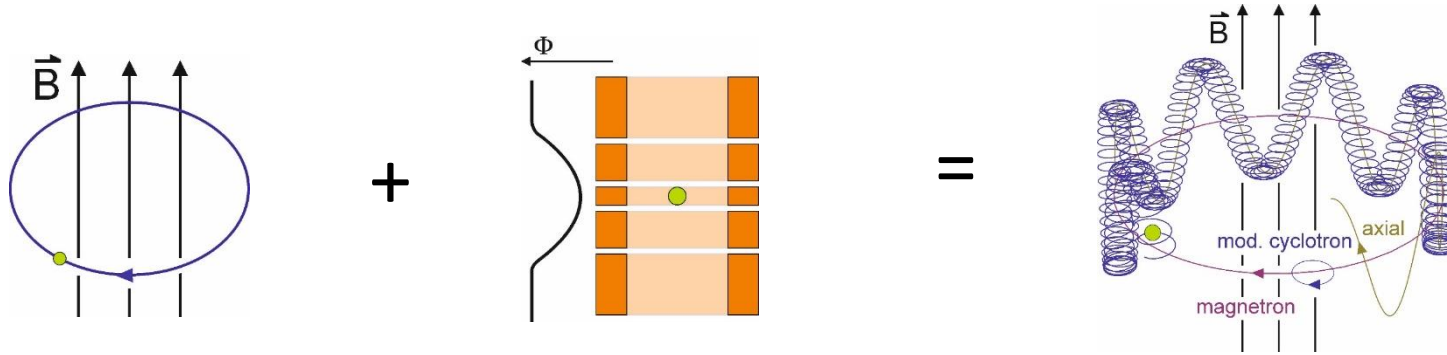


# Outline

- Measurement principles
- Pentatrap setup
- Physics with Pentatrap



# Penning-trap mass measurement



Free-space  
cyclotron frequency

Harmonic electrical  
potential

3 Eigenmotions in trap

$$\omega_c = \frac{qB}{m}$$

$$\omega_z = \sqrt{\frac{2qC_2}{md^2} U}$$

Measurement of all Eigenfrequencies

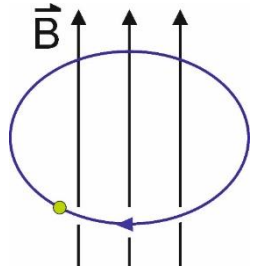
$$\omega_c^2 = \omega_+^2 + \omega_z^2 + \omega_-^2$$

Rev. Mod. Phys. 58, 233 (1986)

$$\omega_+ = \frac{\omega_c}{2} + \sqrt{\frac{\omega_c^2}{4} - \frac{\omega_z^2}{2}}$$

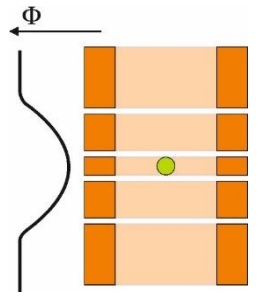
$$\omega_- = \frac{\omega_c}{2} - \sqrt{\frac{\omega_c^2}{4} - \frac{\omega_z^2}{2}}$$

# Penning-trap mass measurement



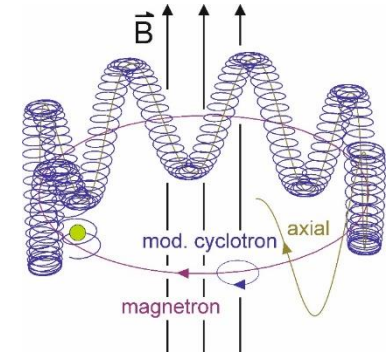
Free-space cyclotron frequency

$$\omega_c = \frac{qB}{m}$$



Harmonic electrical potential

=

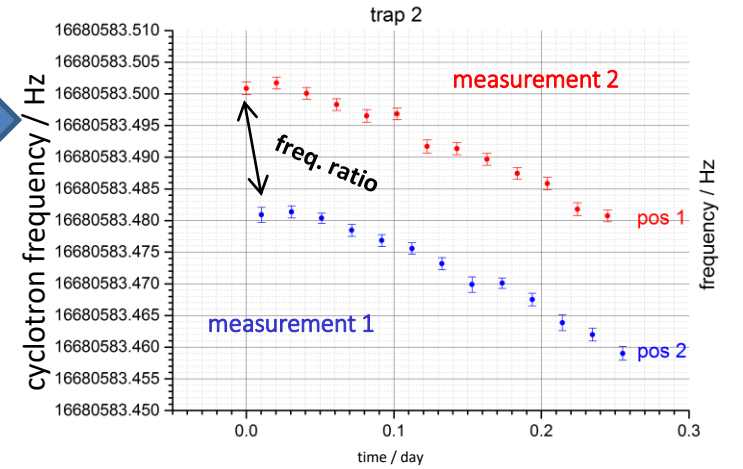
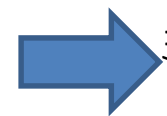


3 Eigenmotions in trap

$$\omega_z = \sqrt{\frac{2qC_2}{md^2} U}$$

$$\omega_+ = \frac{\omega_c}{2} + \sqrt{\frac{\omega_c^2}{4} - \frac{\omega_z^2}{2}}$$

$$\omega_- = \frac{\omega_c}{2} - \sqrt{\frac{\omega_c^2}{4} - \frac{\omega_z^2}{2}}$$



Mass ratio:

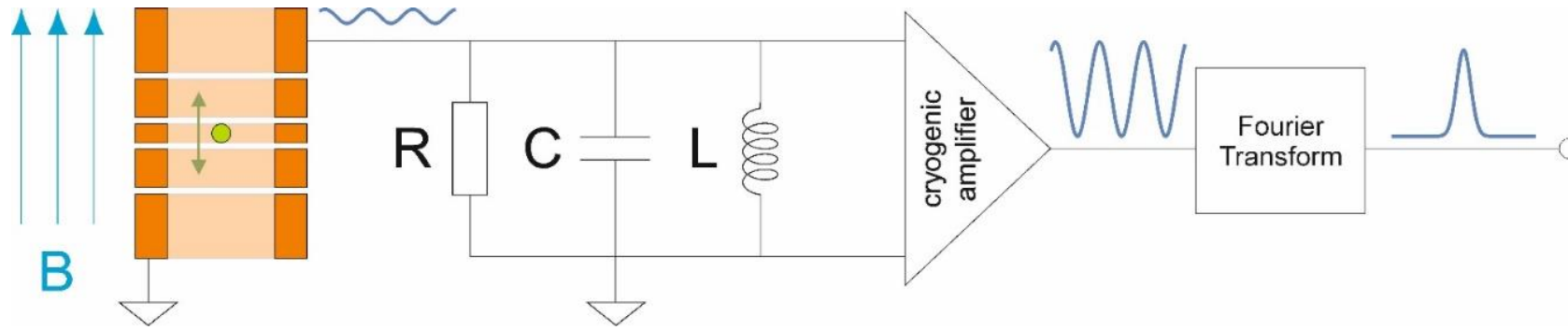
$$R = \frac{\omega_c^A}{\omega_c^B} = \frac{q^A m^B}{q^B m^A}$$

Measurement of all Eigenfrequencies

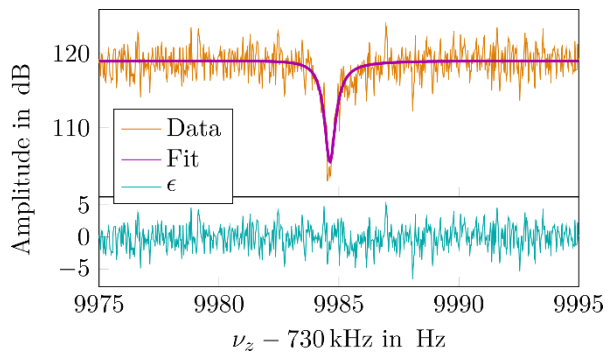
$$\omega_c^2 = \omega_+^2 + \omega_z^2 + \omega_-^2$$

Rev. Mod. Phys. 58, 233 (1986)

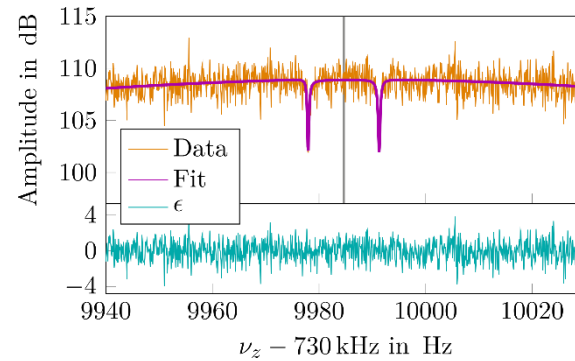
# Fourier transform ion cyclotron resonance – FT-ICR



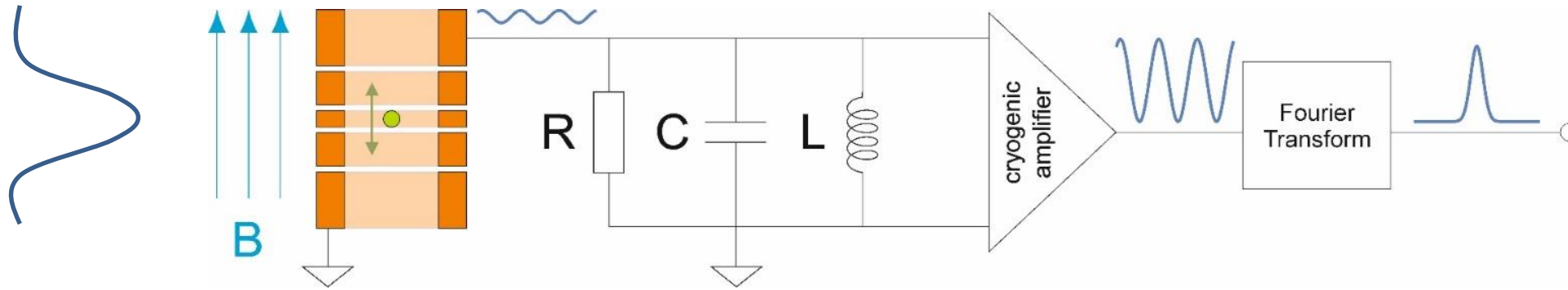
Direct measurement  
of  $\omega_z$  by dip method



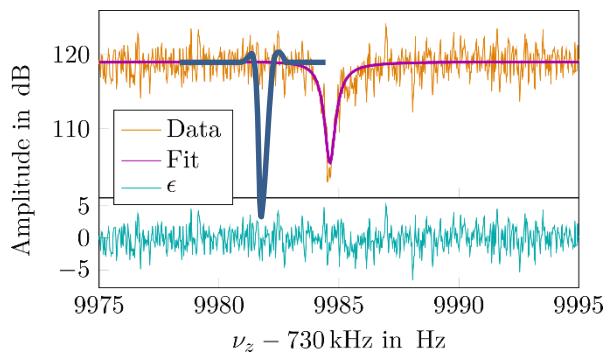
Sideband  
Coupling  $\omega_-$  to  $\omega_z$



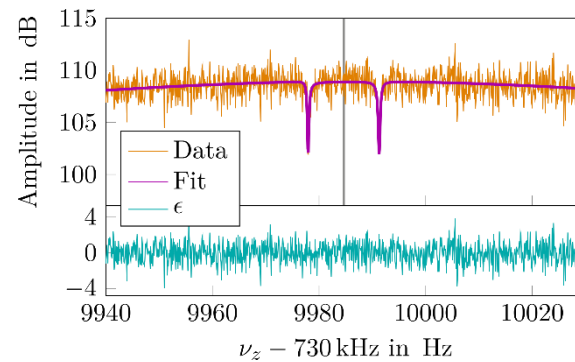
# Fourier transform ion cyclotron resonance – FT-ICR



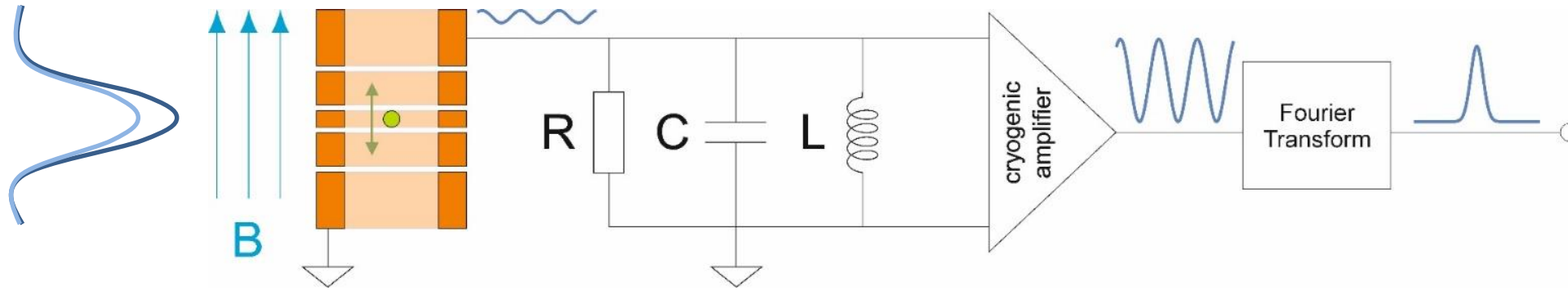
Direct measurement  
of  $\omega_z$  by dip method



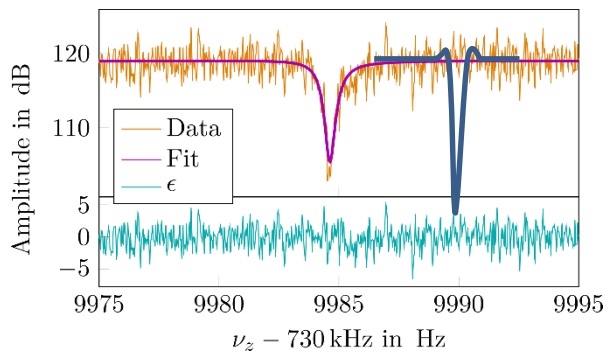
Sideband  
Coupling  $\omega_-$  to  $\omega_z$



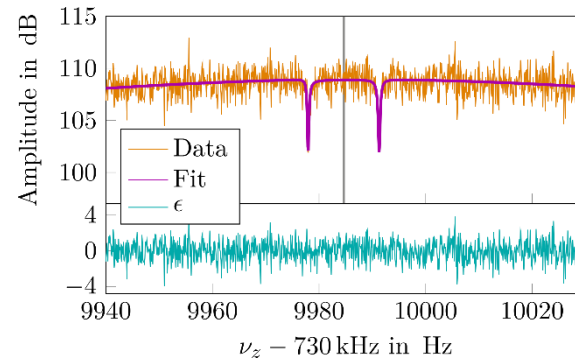
# Fourier transform ion cyclotron resonance – FT-ICR



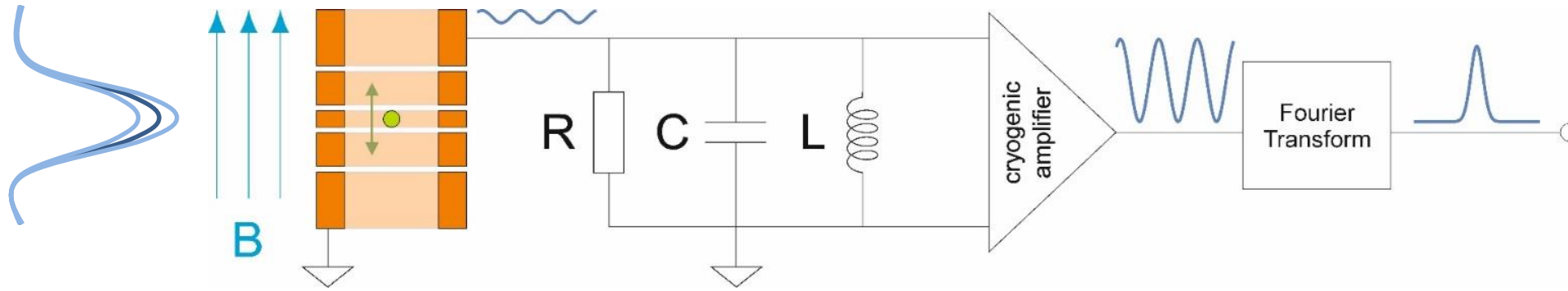
Direct measurement  
of  $\omega_z$  by dip method



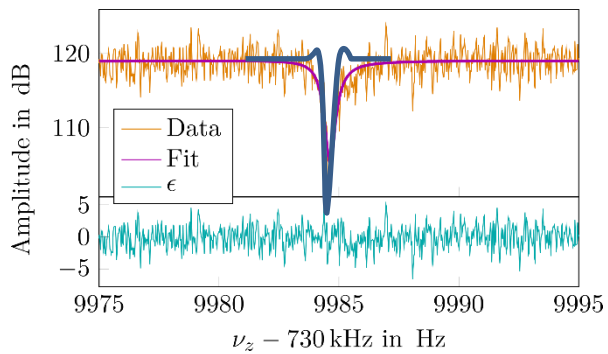
Sideband  
Coupling  $\omega_-$  to  $\omega_z$



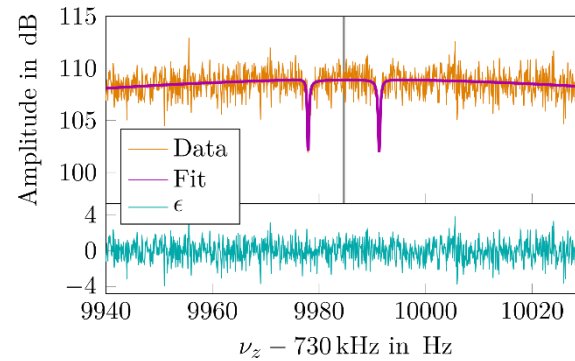
# Fourier transform ion cyclotron resonance – FT-ICR



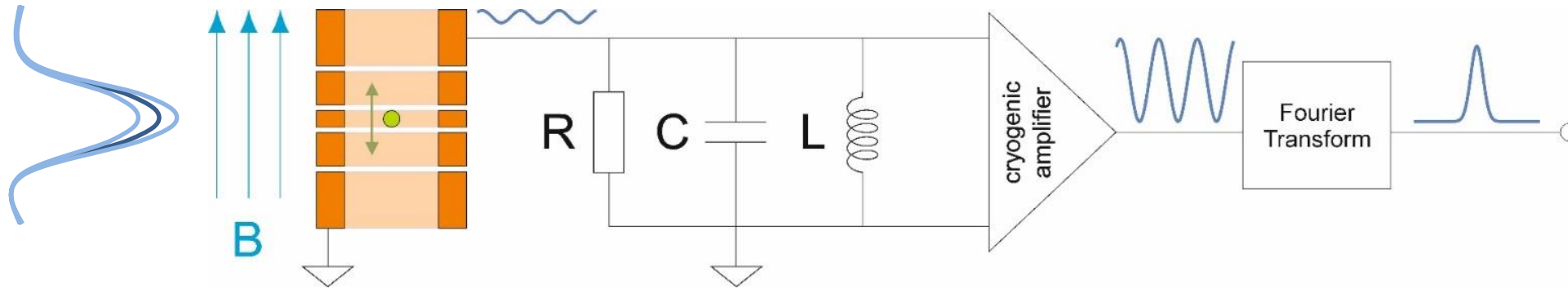
Direct measurement  
of  $\omega_z$  by dip method



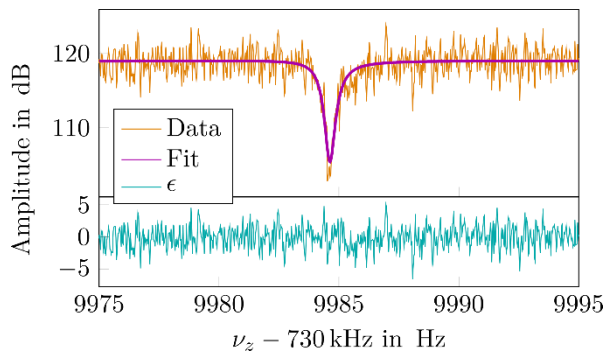
Sideband  
Coupling  $\omega_-$  to  $\omega_z$



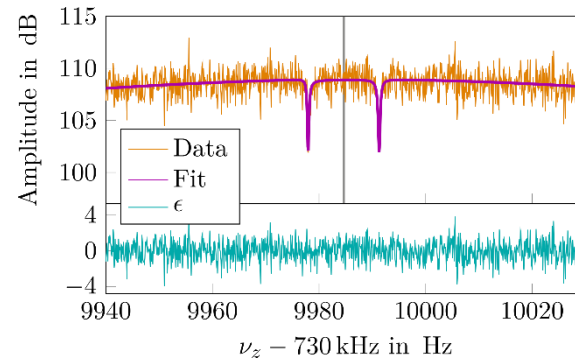
# Fourier transform ion cyclotron resonance – FT-ICR



Direct measurement of  $\omega_z$  by dip method

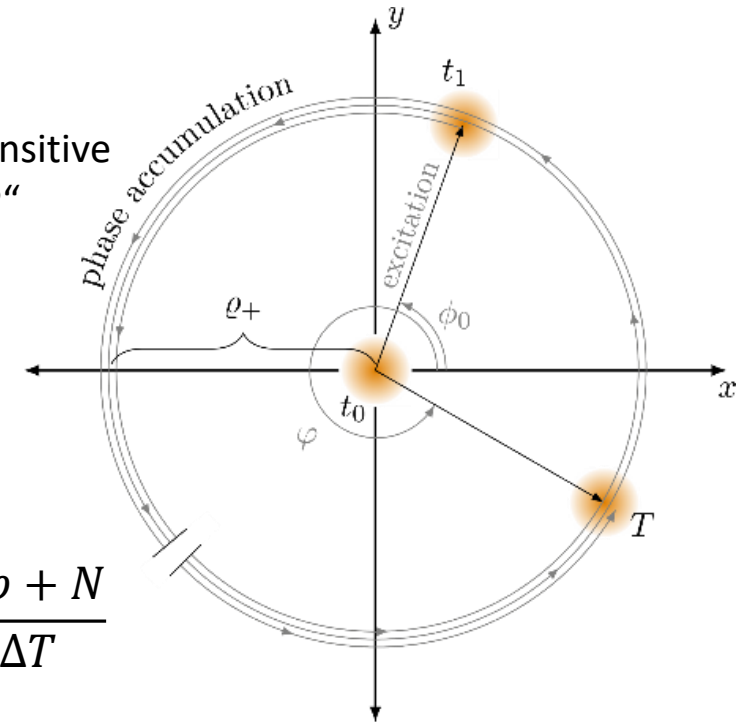


Sideband Coupling  $\omega_-$  to  $\omega_z$



$\omega_+$ : phase sensitive method „PnP“

$$\omega_+ = \frac{1}{2\pi} \frac{\Delta\phi + N}{\Delta T}$$



# Penning-trap mass measurement

$^{172}\text{Yb}^{42+}$

$$\nu_c \approx \nu_+ \approx 26 \text{ MHz}$$

$$\nu_z \approx 500 \text{ kHz}$$

$$\nu_- \approx 4 \text{ kHz}$$

$$\nu_c^2 = \nu_+^2 + \nu_-^2 + \nu_z^2$$

L.S. Brown, G. Gabrielse, Phys. Rev. A 25 (1982) 2423.

$$\delta\nu_c = \sqrt{(\delta\nu_+)^2 + (2 \cdot 10^{-2} \delta\nu_z)^2 + (1.5 \cdot 10^{-4} \delta\nu_-)^2}$$

$$\frac{\delta\nu_c}{\nu_c} = 10^{-12} :$$

$$\delta\nu_+ < 0.015 \text{ mHz}$$

PnP technique

$$\delta\nu_z < 1 \text{ mHz}$$

dip technique

$$\delta\nu_- < 100 \text{ mHz}$$

double-dip technique

# Penning-trap mass measurement

## non-mass doublets

( $^{174}\text{Yb}^{42+}/^{172}\text{Yb}^{42+}$ ):

$$\delta\nu_+ < 0.015 \text{ mHz}$$

$$\delta\nu_z < 1 \text{ mHz}$$

$$\delta\nu_- < 100 \text{ mHz}$$

## “ordinary” mass doublets

( $^{187}\text{Re}^{29+}/^{187}\text{Os}^{29+}$ ):

$$M(^{187}\text{Re}^{29+}) - M(^{187}\text{Os}^{29+}) \approx 2.5 \text{ keV}/c^2$$

$$\delta\nu_+ < 0.015 \text{ mHz}$$

$$\delta\nu_z < 1 \text{ mHz}$$

~~$$\nu_-(^{187}\text{Re}^{29+}) \equiv \nu_-(^{187}\text{Os}^{29+})$$~~

## “excellent” mass doublets

( $^{208\text{m}}\text{Pb}^{41+}/^{208\text{g}}\text{Pb}^{41+}$ ):

$$M(^{208\text{m}}\text{Pb}^{41+}) - M(^{208\text{g}}\text{Pb}^{41+}) \approx 31 \text{ eV}/c^2$$

$$\delta\nu_+ < 0.015 \text{ mHz}$$

~~$$\nu_z(^{208\text{m}}\text{Pb}^{41+}) \equiv \nu_z(^{208\text{g}}\text{Pb}^{41+})$$~~

~~$$\nu_-(^{208\text{m}}\text{Pb}^{41+}) \equiv \nu_-(^{208\text{g}}\text{Pb}^{41+})$$~~

# Penning-trap mass measurement

**non-mass doublets**  
( $^{174}\text{Yb}^{42+}/^{172}\text{Yb}^{42+}$ ):

$$\delta\nu_+ < 0.015 \text{ mHz}$$

$$\delta\nu_z < 1 \text{ mHz}$$

$$\delta\nu_- < 100 \text{ mHz}$$

**“ordinary” mass doublets**  
( $^{187}\text{Re}^{29+}/^{187}\text{Os}^{29+}$ ):

$$M(^{187}\text{Re}^{29+}) - M(^{187}\text{Os}^{29+}) \approx 2.5 \text{ keV}/c^2$$

$$\delta\nu_+ < 0.015 \text{ mHz}$$

$$\delta\nu_z < 1 \text{ mHz}$$

$$\nu_-(^{187}\text{Re}^{29+}) \equiv \nu_-(^{187}\text{Os}^{29+})$$

**“excellent” mass doublets**  
( $^{208\text{m}}\text{Pb}^{41+}/^{208\text{g}}\text{Pb}^{41+}$ ):

$$M(^{208\text{m}}\text{Pb}^{41+}) - M(^{208\text{g}}\text{Pb}^{41+}) \approx 31 \text{ eV}/c^2$$

$$\delta\nu_+ < 0.015 \text{ mHz}$$

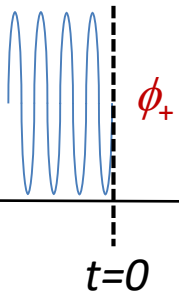
$$\nu_z(^{208\text{m}}\text{Pb}^{41+}) \equiv \nu_z(^{208\text{g}}\text{Pb}^{41+})$$

$$\nu_-(^{208\text{m}}\text{Pb}^{41+}) \equiv \nu_-(^{208\text{g}}\text{Pb}^{41+})$$

**simultaneous** measurement of  $\nu_+$  and  $\nu_z$

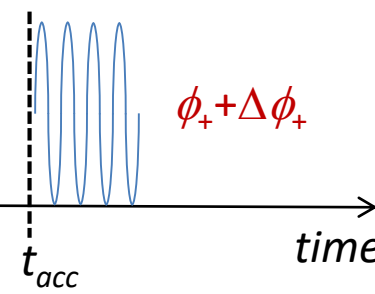
## *simultaneous* measurement of $\nu_+$ (PnP) and $\nu_z$ (dip)

excitation of  $\nu_+$  motion  
(from 1  $\mu\text{m}$  to 10  $\mu\text{m}$ )



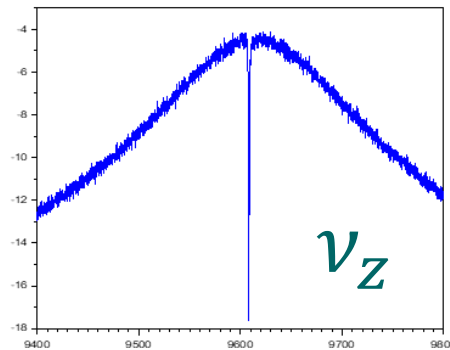
phase-accumulation time (up to 70 s)

measurement of  
accumulated  $\Delta\phi_+$



$$\nu_+ = \frac{\Delta\phi_+ + 2\pi N}{2\pi t_{acc}}$$

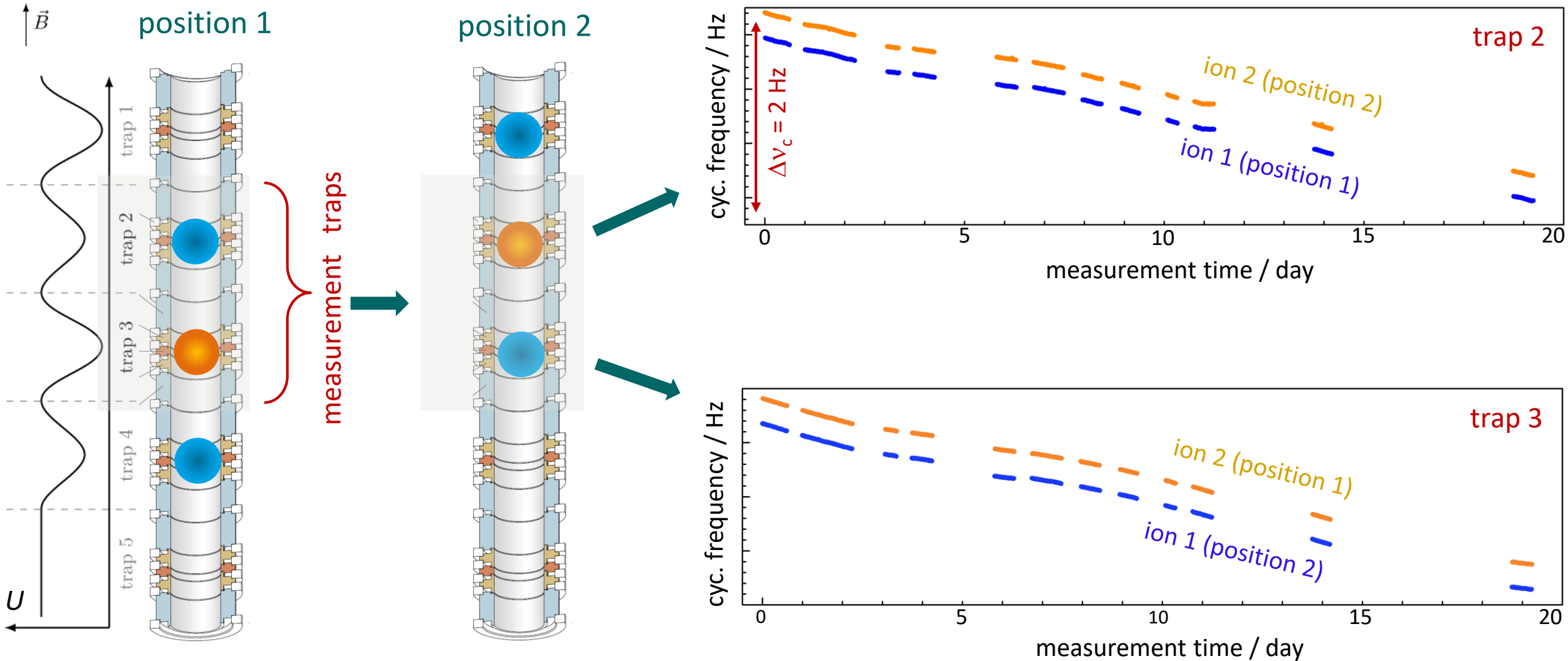
measurement of  $\nu_z$  with dip



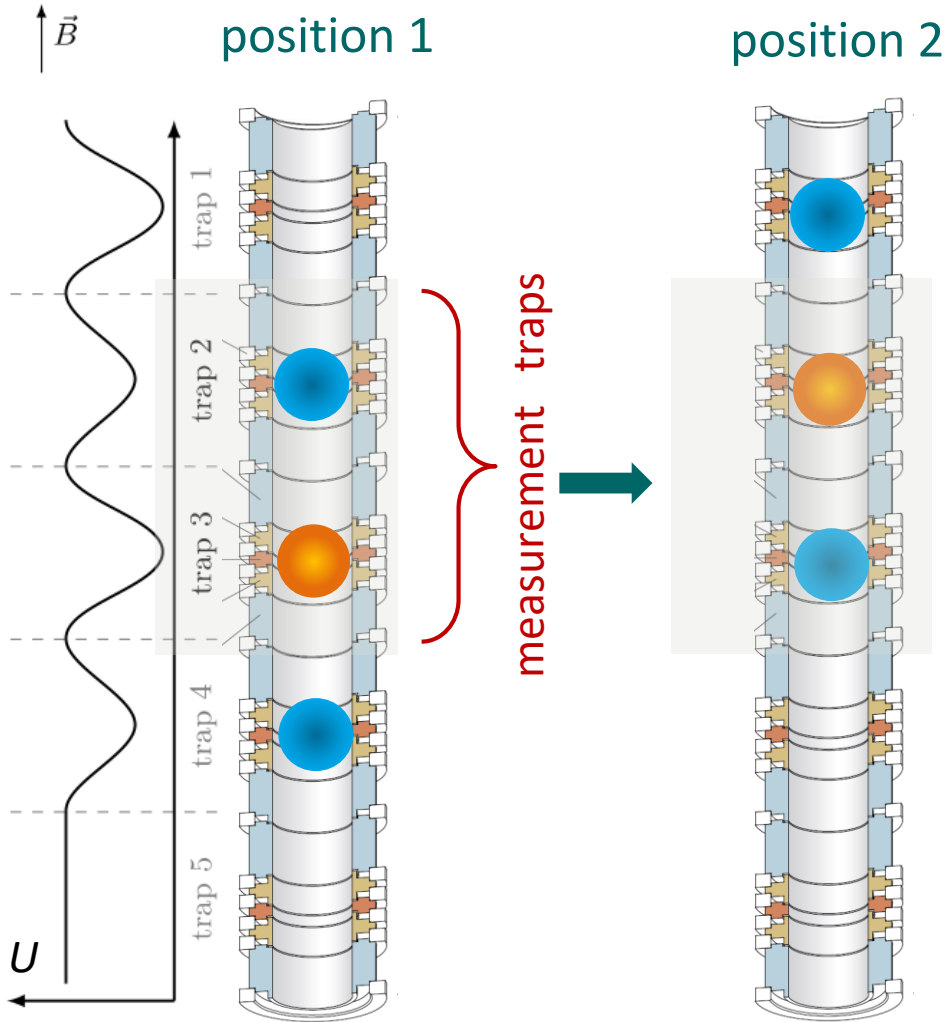
E. A. Cornell *et al.*, Phys. Rev. Letter 63 (1989) 1674

D. J. Wineland and H. G. Dehmelt, J. of Appl. Phys. 46 (1975) 919

# Simultaneous measurements in two traps



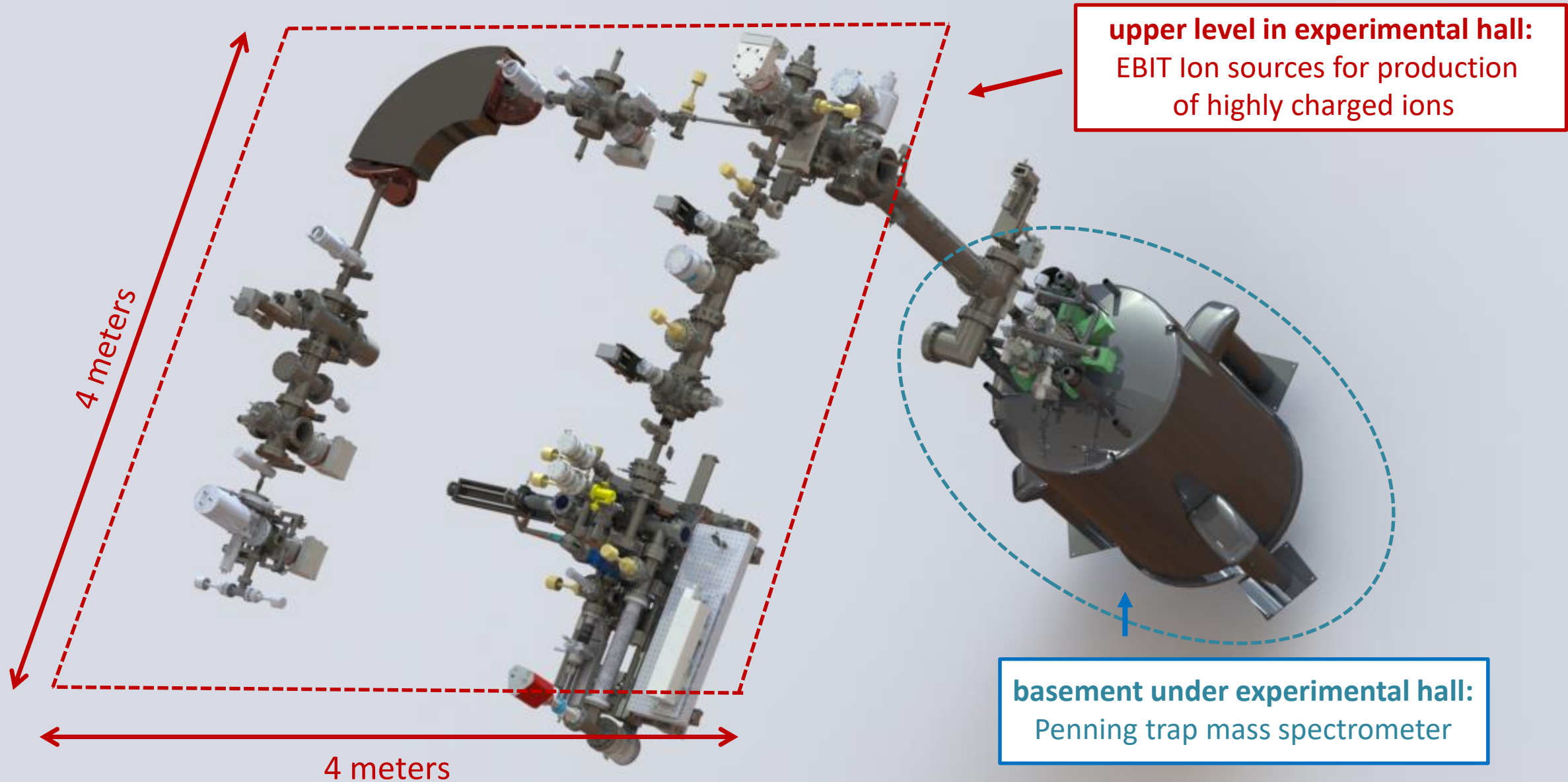
# Independent analysis methods



## various data analysis methods:

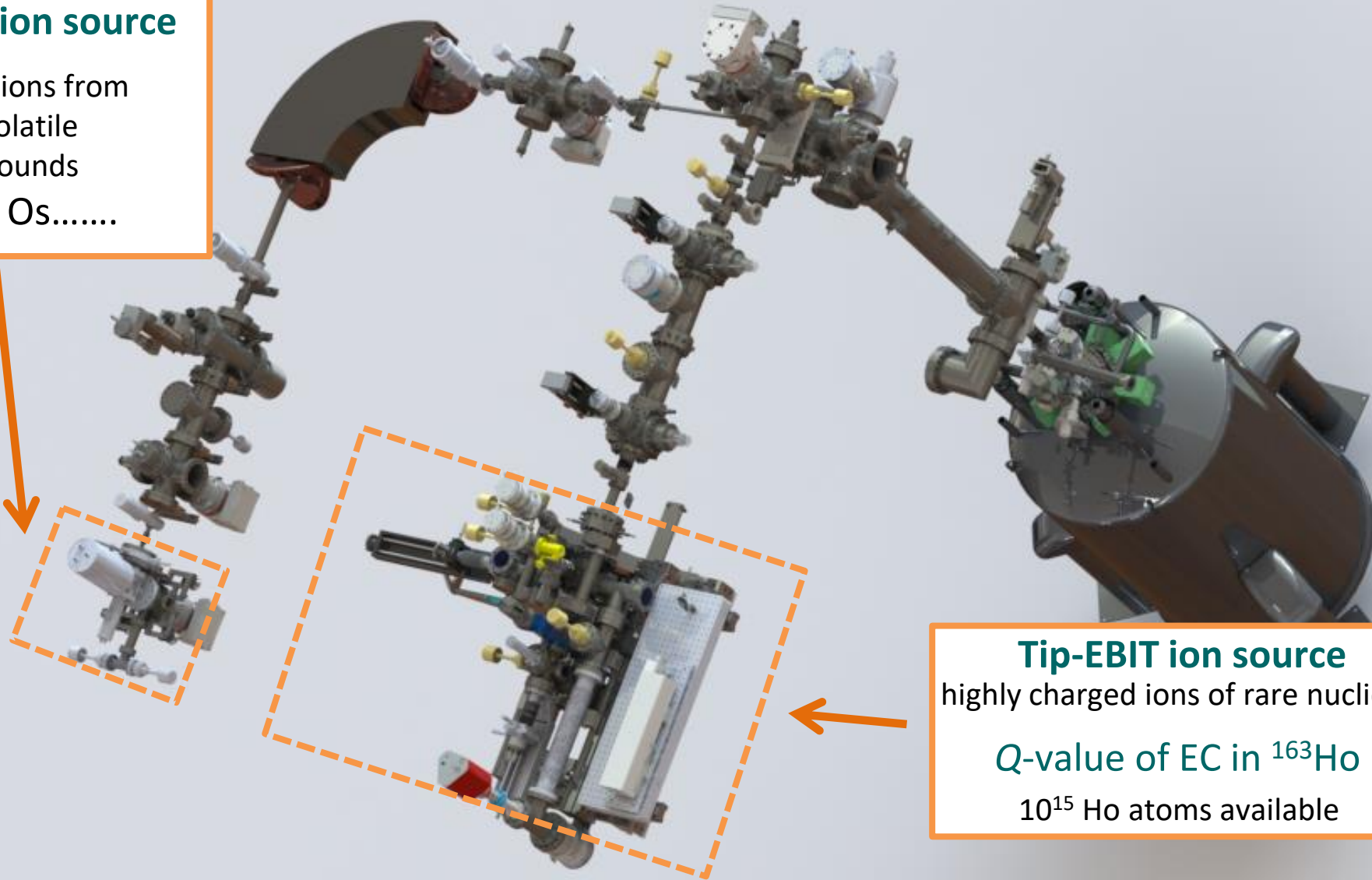
- interpolation
- polynomial
- cancelation
- polycancel

↓  
**reliability of results**



## Dresden-EBIT ion source

highly charged ions from  
gaseous & volatile  
chem. compounds  
Ar, Xe, Re, Os.....



## Tip-EBIT ion source

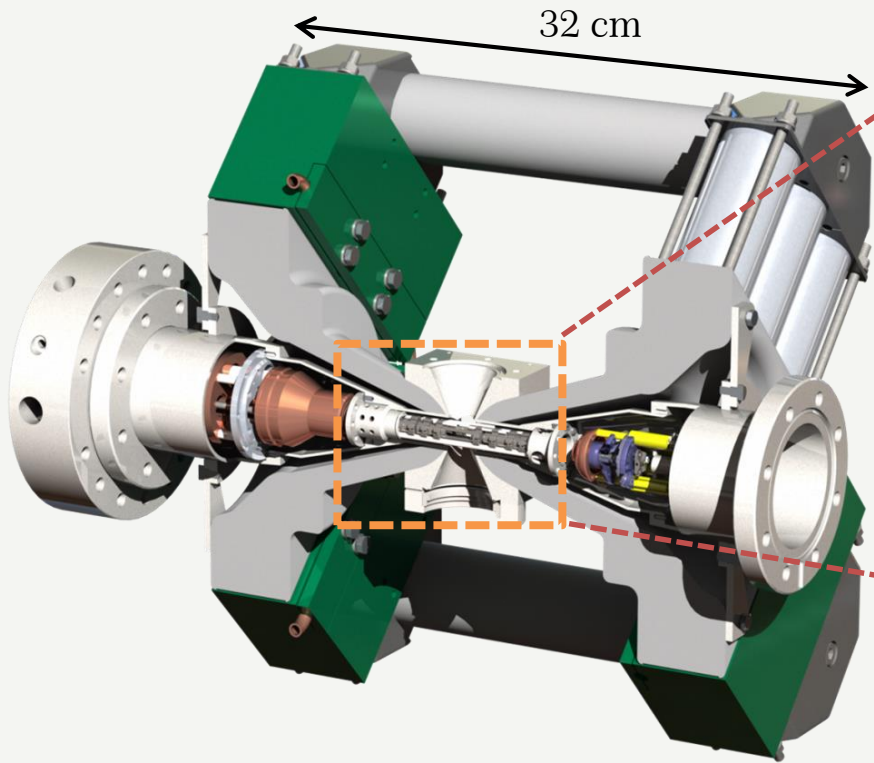
highly charged ions of rare nuclides

$Q$ -value of EC in  $^{163}\text{Ho}$

$10^{15}$  Ho atoms available

## Mini-EBIT developed in J.R. Crespo's group

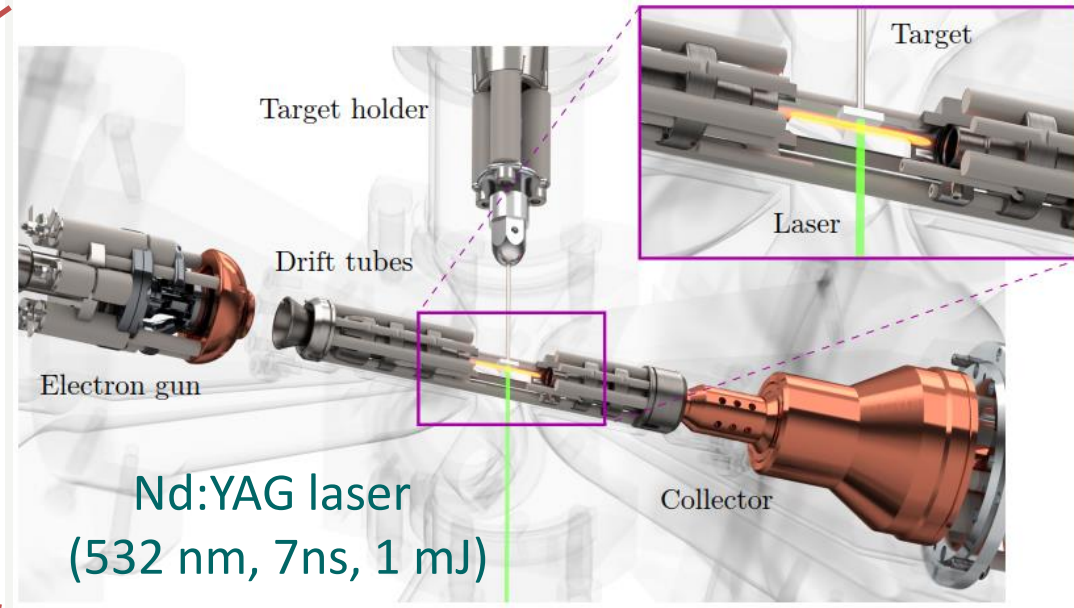
Micke, P. et al., Rev. Sci. Instr. 89, 063109 (2018)



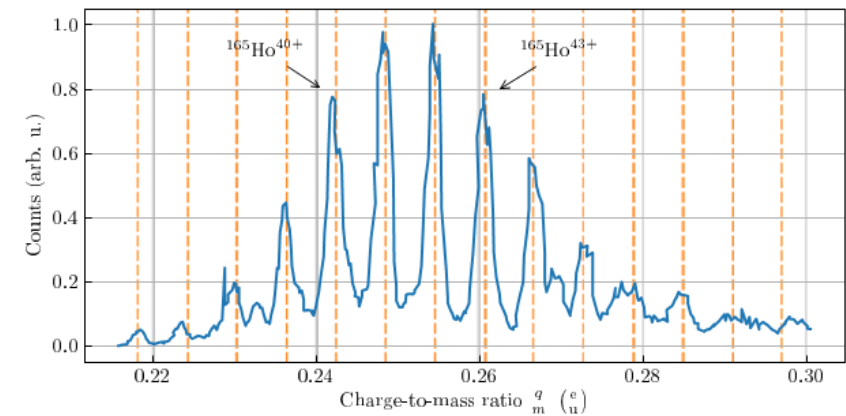
compact room temperature  
permanent magnet, 0.85 T  
max. electron current = 80 mA  
max. electron energy = 10 keV

## in-trap laser desorption

Schweiger, Ch. et al., Rev. Sci. Instr. 90, 123201 (2019)



$^{165}\text{Ho}$  sample:  $10^{12}$  atoms  
life time: 20000 laser shots



90° dipole magnet

90° electrostatic benders

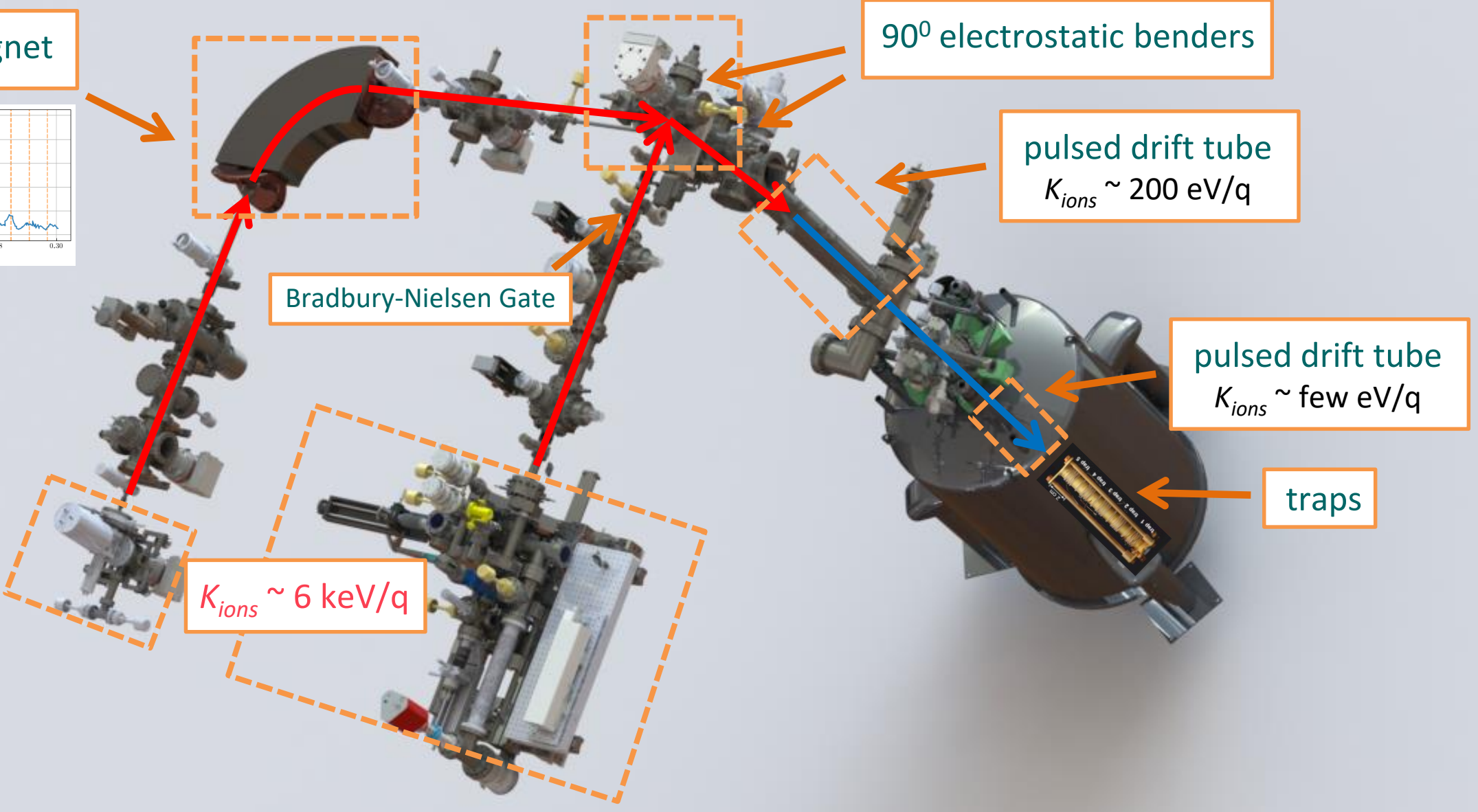
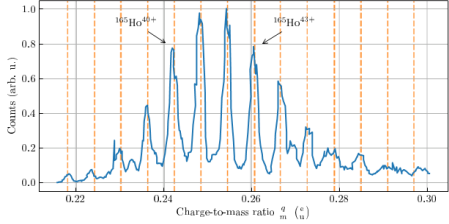
pulsed drift tube  
 $K_{ions} \sim 200 \text{ eV/q}$

pulsed drift tube  
 $K_{ions} \sim \text{few eV/q}$

traps

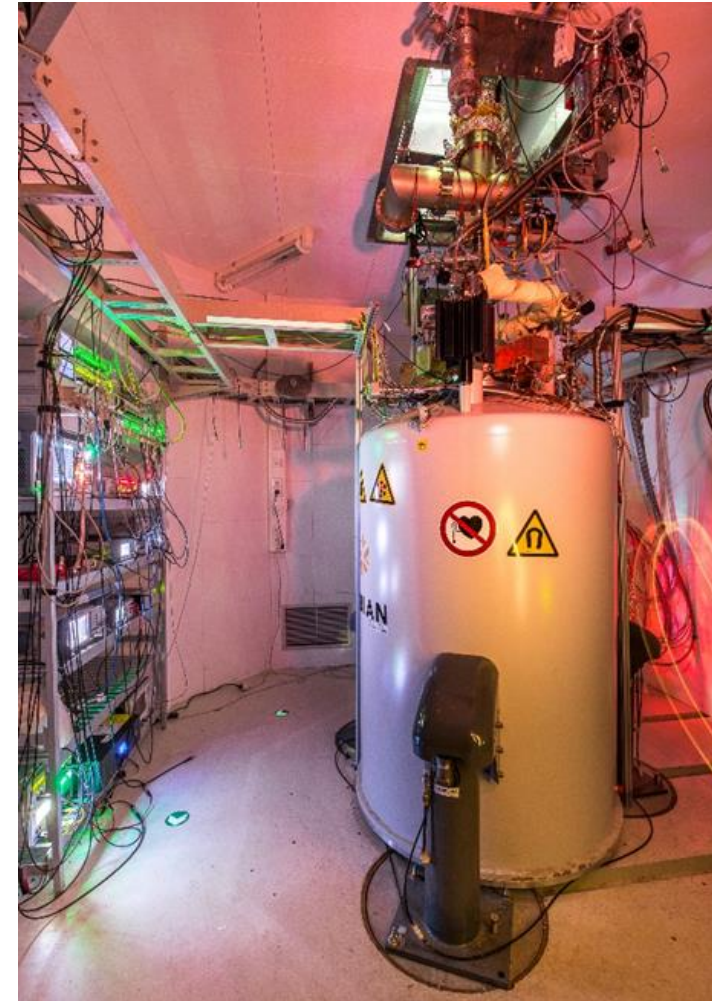
Bradbury-Nielsen Gate

$K_{ions} \sim 6 \text{ keV/q}$



## unique features of PENTATRAP:

- Stack of five Penning traps
- Cryogenic environment (4.2 K)
- 7 T superconducting magnet with vertical **cold** bore
- Temperature in the lab is stabilized:  $\pm 0.05$  K/day
- LHe-level in the bore is stabilized:  $\pm 50$   $\mu\text{m}$
- He-pressure in the bore is stabilized:  $\pm 2$   $\mu\text{bar}$
- Relative stability of  $B$ -field:  $10^{-10}$  / hour
- Ultra-stable voltage source:  $\Delta U/U < 10^{-7}$  / 100 s
- Highly charged ions

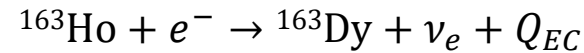
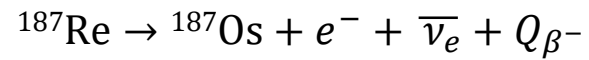


Repp, J. et al., Appl. Phys. B 107, 983 (2012)  
Roux, C. et al., Appl. Phys. B 107, 997 (2012)  
Böhm, C. et al., Nucl. Instrum. Meth. A 828, 125 (2016)

## Applications of relative mass measurements at a level of $\frac{\delta m}{m} \leq 10^{-11}$

### Neutrino physics

Gastaldo, L. et al., Eur. Phys. J. ST 226, 1623 (2017)



Filianin, P. et al.,  $\delta Q = 1.3 \text{ eV}$   
Phys. Rev. Lett. 127, 072502 (2021)

In review, Schweiger, Ch.  
Nature (2022)  $\delta Q = 0.8 \text{ eV}$

### Meta-stable states for HCl clocks

Kozlov, M. G. et al., Rev. Mod. Phys. 90, 045005 (2018)

$$\Delta m(^{208}\text{Pb}^{41+} - ^{208}\text{Pb}^{*41+})$$

$$\Delta m(^{187}\text{Re}^{29+} - ^{187}\text{Re}^{*29+})$$

In preparation, Kromer, K. (2022)

Schuessler, R. X. et al.,  
Nature 581, 42 (2020)

### Test of QED

Binding energies:  $E_B(\text{Xe}^{17+}) = \Delta m(\text{Xe}^{17+} - \text{Xe}^{18+})c^2 - m_e c^2$

g-factor: 
$$g = 2 \frac{v_L}{v_c} \frac{m_e}{m(^{20}\text{Ne})} \frac{q}{e}$$

Shabaev, V. M. et al., Int. J. of Mass Spec. 251, 109, (2006)

Rischka, A. et al.,  
Phys. Rev. Lett. 124, 113001 (2020)

In preparation, Sailer, T. (2022)

### Dark Matter search: Isotope shift

Flambaum, V. V. et al., Phys. Rev. A 79, 032510 (2018)

$$\nu_i^{AA'} = K_i \mu_{AA'} + F_i \delta \langle r^2 \rangle_{AA'} + \alpha_{NP} X_i \gamma_{AA'}$$

Current measurement campaign  
of Yb isotope mass-ratios

### Test of $E = mc^2$

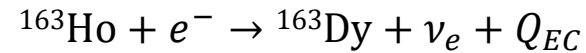
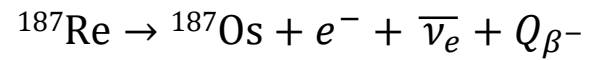
Rainville, S. et al., Nature 438, 1096 (2005)

$$E = \frac{hc}{\lambda} = \Delta m(^{36}\text{Cl} - ^{35}\text{Cl} - n)c^2$$

## Applications of relative mass measurements at a level of $\frac{\delta m}{m} \leq 10^{-11}$

### Neutrino physics

Gastaldo, L. et al., Eur. Phys. J. ST 226, 1623 (2017)



Filianin, P. et al.,  $\delta Q = 1.3 \text{ eV}$   
Phys. Rev. Lett. 127, 072502 (2021)

In review, Schweiger, Ch.  
Nature (2022)  $\delta Q = 0.8 \text{ eV}$

### Meta-stable states for HCl clocks

Kozlov, M. G. et al., Rev. Mod. Phys. 90, 045005 (2018)

$$\Delta m(^{208}\text{Pb}^{41+} - ^{208}\text{Pb}^{*41+})$$

$$\Delta m(^{187}\text{Re}^{29+} - ^{187}\text{Re}^{*29+})$$

In preparation, Kromer, K. (2022)

Schuessler, R. X. et al.,  
Nature 581, 42 (2020)

### Test of QED

Binding energies:  $E_B(\text{Xe}^{17+}) = \Delta m(\text{Xe}^{17+} - \text{Xe}^{18+})c^2 - m_e c^2$

g-factor: 
$$g = 2 \frac{v_L}{v_c} \frac{m_e}{m(^{20}\text{Ne})} \frac{q}{e}$$

Shabaev, V. M. et al., Int. J. of Mass Spec. 251, 109, (2006)

Rischka, A. et al.,  
Phys. Rev. Lett. 124, 113001 (2020)

In preparation, Sailer, T. (2022)

### Dark Matter search: Isotope shift

Flambaum, V. V. et al., Phys. Rev. A 79, 032510 (2018)

$$\nu_i^{AA'} = K_i \mu_{AA'} + F_i \delta \langle r^2 \rangle_{AA'} + \alpha_{NP} X_i \gamma_{AA'}$$

Current measurement campaign  
of Yb isotope mass-ratios

### Test of $E = mc^2$

Rainville, S. et al., Nature 438, 1096 (2005)

$$E = \frac{hc}{\lambda} = \Delta m(^{36}\text{Cl} - ^{35}\text{Cl} - n)c^2$$

# Neutrino Mass



**PROJECT 8**

## $\beta^-$ -decay of tritium

$$m_{\bar{\nu}_e} < 0.9 \frac{eV}{c^2} \text{ (90\% C.L.)}$$

$$Q_\beta = 18\,592.01(7) \text{ eV}$$

### KATRIN experiment

The KATRIN Collaboration., Nature Phys. 18 (2022) 160.

### FSU trap

E. G. Myers *et al.*, PRL 114 (2015) 013003.

**MINEBA & MANU**

**MARE**

## $\beta^-$ -decay of $^{187}\text{Re}$

$$m_{\bar{\nu}_e} < 15 \frac{eV}{c^2} \text{ (90\% C.L.)}$$

$$Q_\beta = 2466.7(1.6) \text{ eV}$$

$$Q_\beta = 2492(33) \text{ eV}$$

M. Sisti *et al.*, Nucl. Inst. Meth. A520, 125 (2004).

C. Arnaboldi *et al.*, PRL 91, 161802 (2003).

**SHIPTRAP** D. Nesterenko *et al.*, PRC 90, 042501 (R) (2014).



**HOLMES**

## electron capture (EC) in $^{163}\text{Ho}$

$$m_{\nu_e} < 225 \frac{eV}{c^2} \text{ (95\% C.L.)}$$

$$Q_{EC} = 2858 (51) \text{ eV}$$

$$Q_{EC} = 2833 (33) \text{ eV}$$

P. Springer *et al.*, Phys. Rev. A 35, 679 (1987).

**ECHO**

P. Ranitzsch *et al.*, PRL 119, 122501 (2017).

**SHIPTRAP**

S. Eliseev *et al.*, PRL 115, 062501 (2015).

# Determination of $Q$ -value of $\beta^-$ -decay of $^{187}\text{Re}$

$^{187}\text{Re}$ :  $T_{1/2} \approx 4 \cdot 10^{10}$  years; abundance  $\approx 63\%$ ; a few mg of volatile  $\text{C}_8\text{H}_5\text{O}_3\text{Re}$

$^{187}\text{Os}$ : stable; abundance = 1.6%; a few mg of volatile  $\text{C}_{10}\text{H}_{10}\text{Os}$

$$\frac{M[^{187}\text{Re}] - M[^{187}\text{Os}]}{M[^{187}\text{Re}]} \approx 10^{-8} !!!$$

**we measure:**

$$R = \frac{\nu_c[^{187}\text{Os}^{29+}]}{\nu_c[^{187}\text{Re}^{29+}]}$$

**we want to determine:**

$$Q = M[^{187}\text{Re}] - M[^{187}\text{Os}] = M[^{187}\text{Os}^{29+}] \cdot [R-1] + \Delta B$$

**optimal charge state for Re/Os ions is 29+:**

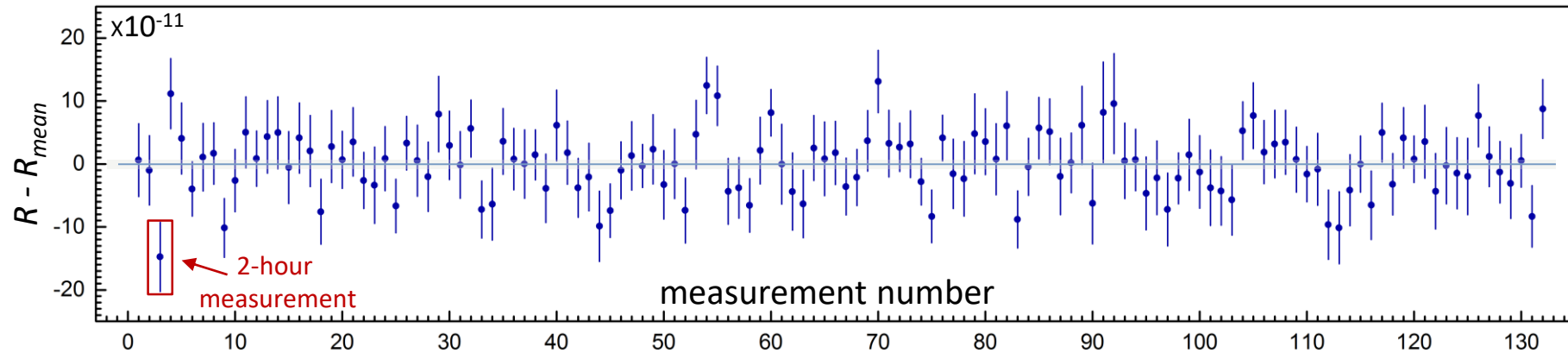
- easy to achieve an uncertainty  $< 10^{-11}$  in  $R$ -measurement
- easy to produce 29+ Re/Os ions with our EBIT
- “easy” electron configurations:  $^{187}\text{Re}^{29+} - [\text{Kr}]^4\text{d}^{10}$ ;  $^{187}\text{Os}^{29+} - [\text{Kr}]^4\text{d}^{10}4\text{f}^1$

Maurits Haverkort  
Heidelberg University Institute for Theoretical Physics

Zoltan Harman  
Max-Planck Institute for Nuclear Physics

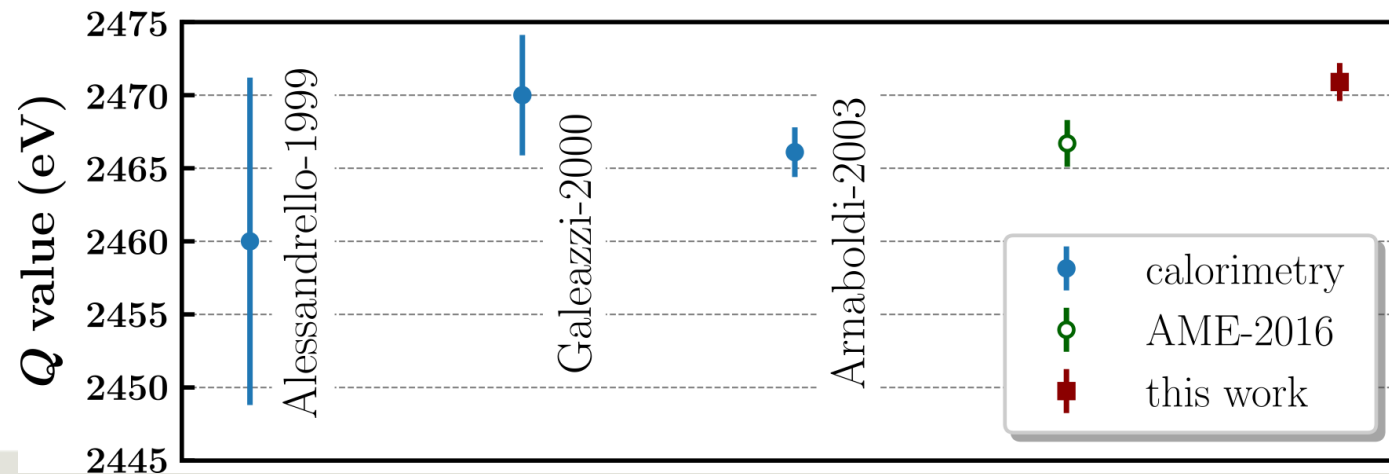
Paul Indelicato  
Directeur de Recherche au CNRS

# Determination of $Q$ -value of $\beta^-$ -decay of $^{187}\text{Re}$



uncertainty in  
determination of  $R$   
 **$5 \cdot 10^{-12}$**

$$Q = M[^{187}\text{Re}] - M[^{187}\text{Os}] = M[^{187}\text{Os}^{29+}] \cdot [R-1] + \Delta B = \mathbf{2470.9(1.3) \text{ eV}}$$



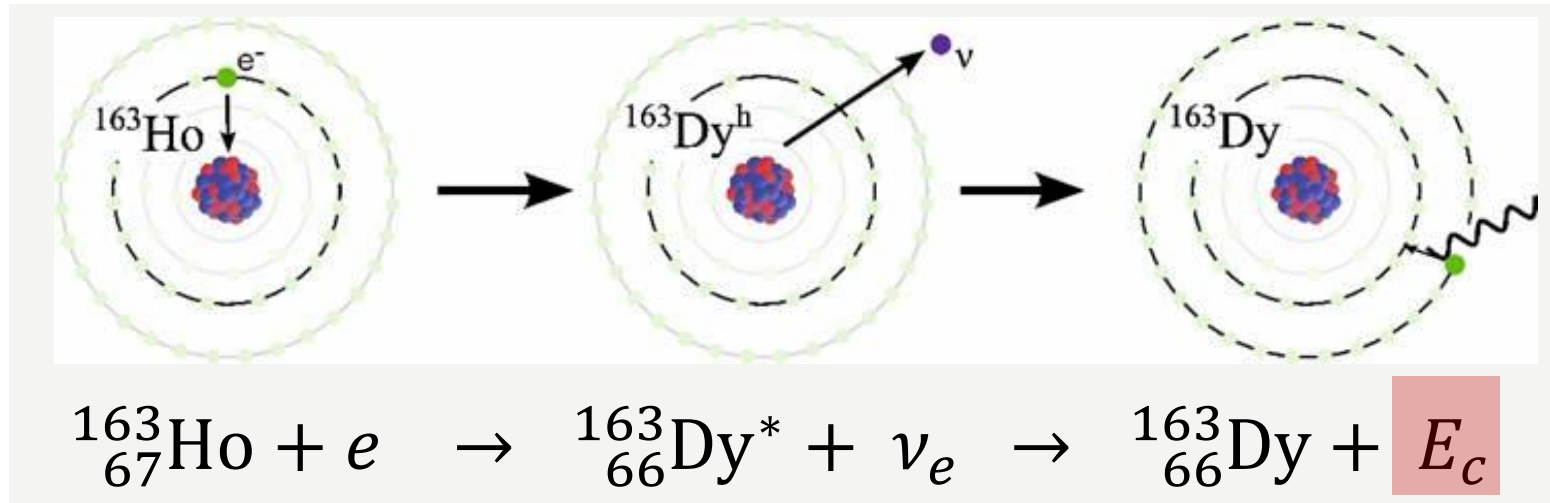
**$53.5(1.0) \text{ eV}$**

Maurits Haverkort  
Heidelberg University Institute for Theoretical Physics

Zoltan Harman  
Max-Planck Institute for Nuclear Physics

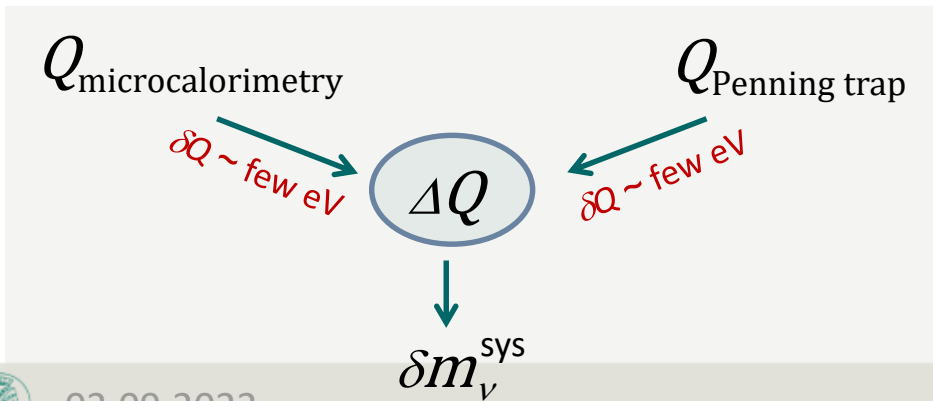
Paul Indelicato  
Directeur de Recherche au CNRS

# The Electron Capture in Holmium experiment

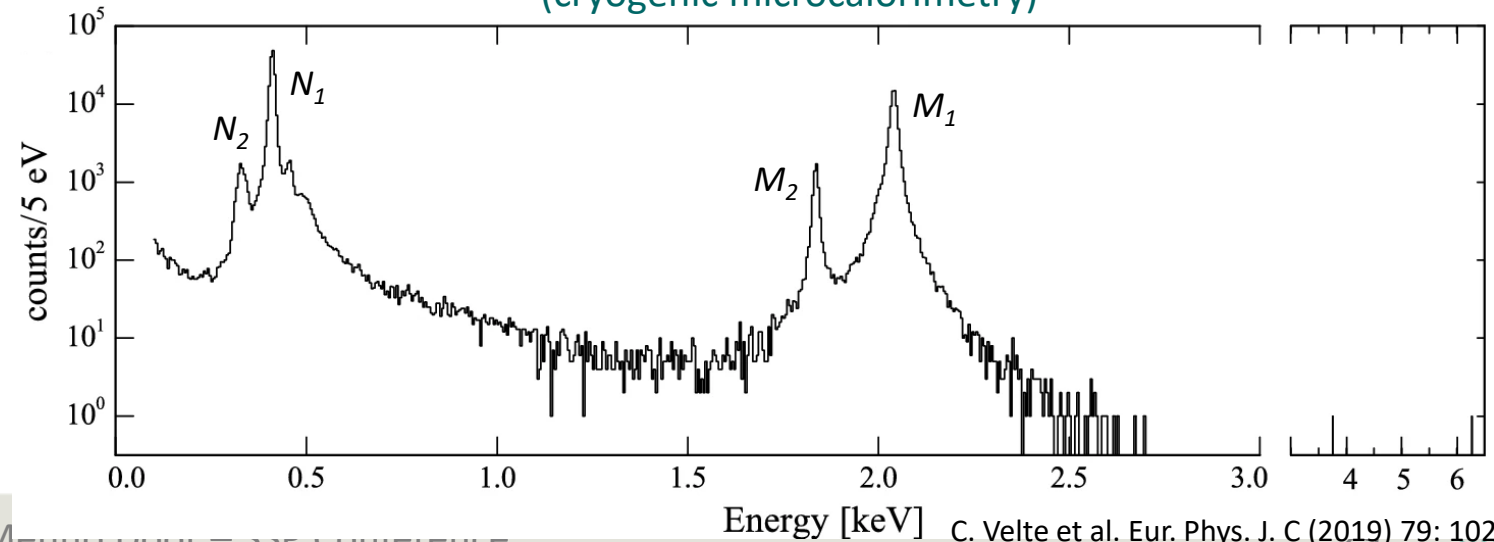


$$\frac{dN}{dE} = F(Q, m_\nu)$$

M. Braß and M. W. Haverkort, arXiv: 2002.05989v1



atomic de-excitation spectrum  
(cryogenic microcalorimetry)



# Determination of Q-value of EC in $^{163}\text{Ho}$

$$Q = M[^{163}\text{Ho}] - M[^{163}\text{Dy}] = M[^{163}\text{Dy}^{n+}] \cdot [R-1] + \Delta B \leftarrow$$

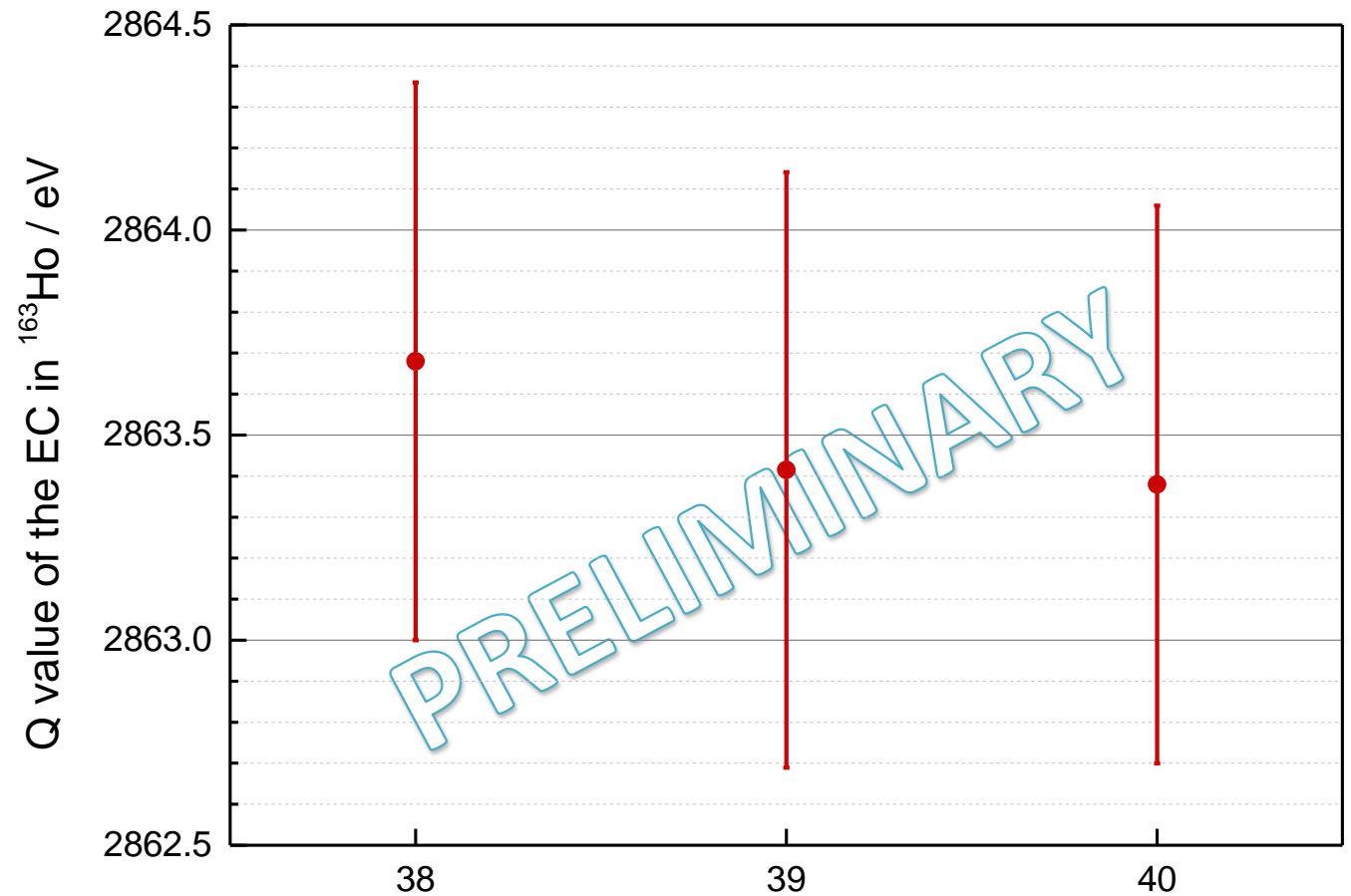
Maurits Haverkort  
Zoltan Harman  
Paul Indelicato

We have measured cyc-freq ratios of Dy and Ho in 3 charge states: 38+, 39+ and 40+

| charge state | cyc freq ratio, $R$                      |
|--------------|--|
| 38+          | $1.0000000186233 \pm 3.0 \cdot 10^{-12}$ |
| 39+          | $1.0000000113075 \pm 4.0 \cdot 10^{-12}$ |
| 40+          | $1.0000000115156 \pm 3.5 \cdot 10^{-12}$ |

preliminary final uncertainty:

$$\delta Q < 0.8 \text{ eV}$$



## Applications of relative mass measurements at a level of $\frac{\delta m}{m} \leq 10^{-11}$

### Neutrino physics

Gastaldo, L. et al., Eur. Phys. J. ST 226, 1623 (2017)



Filianin, P. et al.,  $\delta Q = 1.3 \text{ eV}$   
Phys. Rev. Lett. 127, 072502 (2021)

In review, Schweiger, Ch.  
Nature (2022)  $\delta Q = 0.8 \text{ eV}$

### Meta-stable states for HCl clocks

Kozlov, M. G. et al., Rev. Mod. Phys. 90, 045005 (2018)

$$\Delta m(^{208}\text{Pb}^{41+} - ^{208}\text{Pb}^{*41+})$$

$$\Delta m(^{187}\text{Re}^{29+} - ^{187}\text{Re}^{*29+})$$

In preparation, Kromer, K. (2022)

Schuessler, R. X. et al.,  
Nature 581, 42 (2020)

### Test of QED

Binding energies:  $E_B(\text{Xe}^{17+}) = \Delta m(\text{Xe}^{17+} - \text{Xe}^{18+})c^2 - m_e c^2$

g-factor:  $g = 2 \frac{v_L}{v_c} \frac{m_e}{m(^{20}\text{Ne})} \frac{q}{e}$

Shabaev, V. M. et al., Int. J. of Mass Spec. 251, 109, (2006)

Rischka, A. et al.,  
Phys. Rev. Lett. 124, 113001 (2020)

In preparation, Sailer, T. (2022)

### Dark Matter search: Isotope shift

Flambaum, V. V. et al., Phys. Rev. A 79, 032510 (2018)

$$\nu_i^{AA'} = K_i \mu_{AA'} + F_i \delta \langle r^2 \rangle_{AA'} + \alpha_{NP} X_i \gamma_{AA'}$$

Current measurement campaign  
of Yb isotope mass-ratios

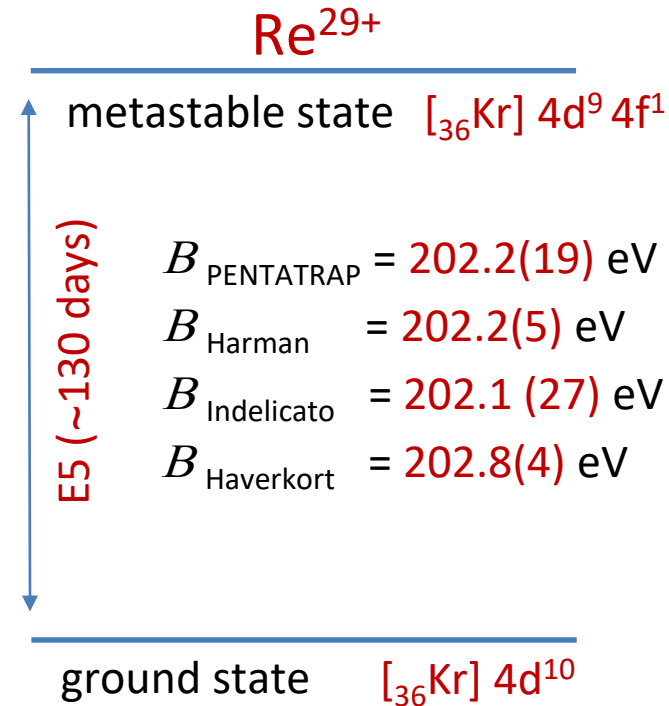
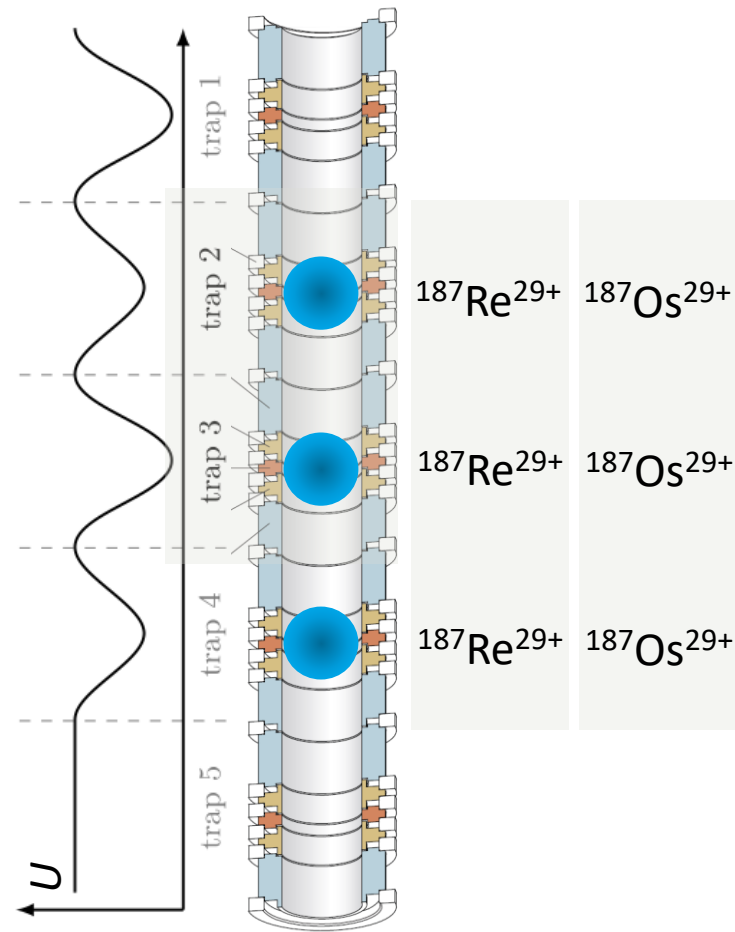
### Test of $E = mc^2$

Rainville, S. et al., Nature 438, 1096 (2005)

$$E = \frac{hc}{\lambda} = \Delta m(^{36}\text{Cl} - ^{35}\text{Cl} - n)c^2$$

# excitation energies of atomic metastable states

- $Os^{29+}$  vs.  $Os^{29+}$  measurements yield always unity.
- $Re^{29+}$  vs.  $Re^{29+}$  measurements yield either unity or  $1+1.14 \cdot 10^{-9}$ .



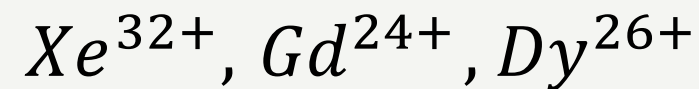
Possible application: search for suitable clock transitions

# excitation energies of atomic metastable states

Table 1. Summary of metastable state in highly charged ions.

| isoelectron | ion               | metastable state                                   | energy (eV) | lifetime   |
|-------------|-------------------|--|-------------|------------|
| 23V-like    | U <sup>69+</sup>  | [Ar]3d <sup>5</sup> <sup>2</sup> H <sub>11/2</sub> | 197.0       | 12.6 hours |
| 23V-like    | Th <sup>67+</sup> | [Ar]3d <sup>5</sup> <sup>2</sup> H <sub>11/2</sub> | 176.3       | 25.3 hours |
| 41Nb-like   | U <sup>51+</sup>  | [Kr]4d <sup>5</sup> <sup>2</sup> H <sub>11/2</sub> | 57.5        | 8.3 days   |
| 22Ti-like   | U <sup>70+</sup>  | [Ar]3d <sup>4</sup> <sup>3</sup> H <sub>4</sub>    | 205.9       | 46.3 days  |
| 22Ti-like   | Xe <sup>32+</sup> | [Ar]3d <sup>4</sup> <sup>5</sup> D <sub>4</sub>    | 17.9        | 3.0 hours  |
| 22Ti-like   | Ba <sup>34+</sup> | [Ar]3d <sup>4</sup> <sup>5</sup> D <sub>4</sub>    | 21.1        | 10.3 hours |
| 22Ti-like   | Ce <sup>36+</sup> | [Ar]3d <sup>4</sup> <sup>5</sup> D <sub>4</sub>    | 24.8        | 54.5 hours |
| 40Zr-like   | U <sup>52+</sup>  | [Kr]4d <sup>5</sup> <sup>2</sup> H <sub>11/2</sub> | 59.8        | 10.9 years |
| 40Zr-like   | Gd <sup>24+</sup> | [Kr]3d <sup>4</sup> <sup>5</sup> D <sub>4</sub>    | 9.0         | 5.3 hours  |
| 40Zr-like   | Dy <sup>26+</sup> | [Kr]3d <sup>4</sup> <sup>3</sup> F <sub>4</sub>    | 10.6        | 16.3 hours |

next goal:



## Applications of relative mass measurements at a level of $\frac{\delta m}{m} \leq 10^{-11}$

### Neutrino physics

Gastaldo, L. et al., Eur. Phys. J. ST 226, 1623 (2017)



Filianin, P. et al.,  $\delta Q = 1.3 \text{ eV}$   
Phys. Rev. Lett. 127, 072502 (2021)

In review, Schweiger, Ch.  
Nature (2022)  $\delta Q = 0.8 \text{ eV}$

### Meta-stable states for HCl clocks

Kozlov, M. G. et al., Rev. Mod. Phys. 90, 045005 (2018)

$$\Delta m(^{208}\text{Pb}^{41+} - ^{208}\text{Pb}^{*41+})$$

$$\Delta m(^{187}\text{Re}^{29+} - ^{187}\text{Re}^{*29+})$$

In preparation, Kromer, K. (2022)

Schuessler, R. X. et al.,  
Nature 581, 42 (2020)

### Test of QED

**Binding energies:**  $E_B(\text{Xe}^{17+}) = \Delta m(\text{Xe}^{17+} - \text{Xe}^{18+})c^2 - m_e c^2$

**g-factor:** 
$$g = 2 \frac{v_L}{v_c} \frac{m_e}{m(^{20}\text{Ne})} \frac{q}{e}$$

Shabaev, V. M. et al., Int. J. of Mass Spec. 251, 109, (2006)

Rischka, A. et al.,  
Phys. Rev. Lett. 124, 113001 (2020)

In preparation, Sailer, T. (2022)

### Dark Matter search: Isotope shift

Flambaum, V. V. et al., Phys. Rev. A 79, 032510 (2018)

$$\nu_i^{AA'} = K_i \mu_{AA'} + F_i \delta \langle r^2 \rangle_{AA'} + \alpha_{NP} X_i \gamma_{AA'}$$

Current measurement campaign  
of Yb isotope mass-ratios

### Test of $E = mc^2$

Rainville, S. et al., Nature 438, 1096 (2005)

$$E = \frac{hc}{\lambda} = \Delta m(^{36}\text{Cl} - ^{35}\text{Cl} - n)c^2$$

Measurement with Alphatrap of the g-factor of an electron in  $^{20}\text{Ne}^{9+}$

$$g_{\text{exp}} = 2 \frac{\nu_L}{\nu_C} \frac{m_e}{m(^{20}_{10}\text{Ne})} \frac{q}{e}$$

Alphatrap

from Atomic Mass Evaluation (AME)

Measurement with Alphatrap of the g-factor of an electron in  $^{20}\text{Ne}^{9+}$

$$g_{\text{exp}} = 2 \frac{\nu_L}{\nu_c} \frac{m_e}{m(^{20}_{10}\text{Ne})} \frac{q}{e}$$

Alphatrap

from Atomic Mass Evaluation (AME)

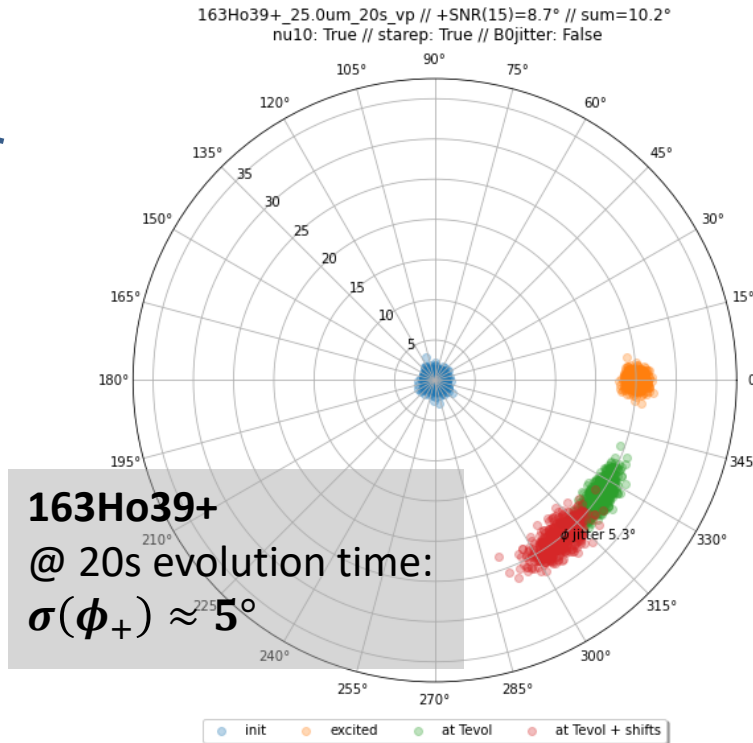
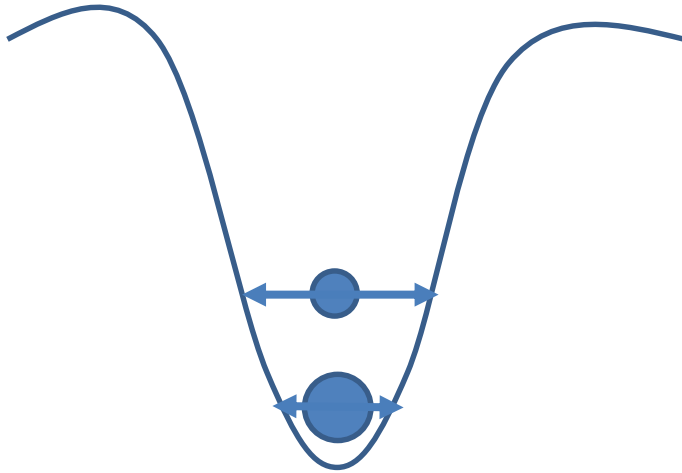
$g_{\text{exp}} \neq g_{\text{theory}}$   
(discrepancy of about  $3\sigma$ ) 

# $^{20}\text{Ne}$ mass measurement – smaller masses

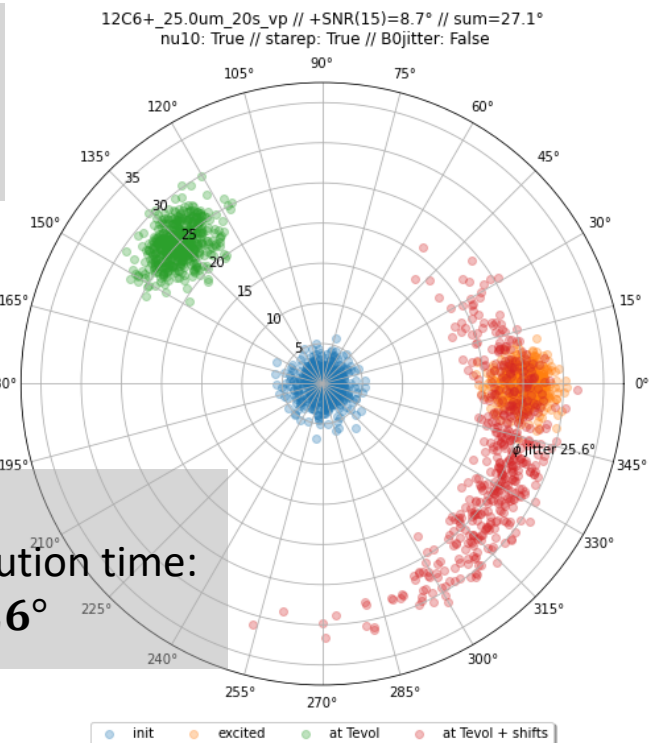
Mass ratio measurement of  $R = m(^{20}\text{Ne}^{10+}) / m(^{12}\text{C}^{6+})$

First direct mass measurement with Pentatrap, what is different to higher masses?

Lower masses  $\rightarrow$  higher “thermal” radii  $\rightarrow$  higher PnP phase jitter  $\rightarrow$  **more statistics needed**  
 $\rightarrow$  **& higher uncertainty on relativistic shift**



**Simulation:**  
 $T(\text{trap2}) = 6\text{ K}$   
 $\rho_{\text{exc,+}} = 25\ \mu\text{m}$   
 Without SNR jitter



## light non-mass doublet



$$R \equiv \frac{\nu_c(\text{Ne})}{\nu_c(\text{C})} = \text{Function} \left( \frac{\rho_+(\text{Ne}) - \rho_+(\text{C})}{\rho_+} \right)$$



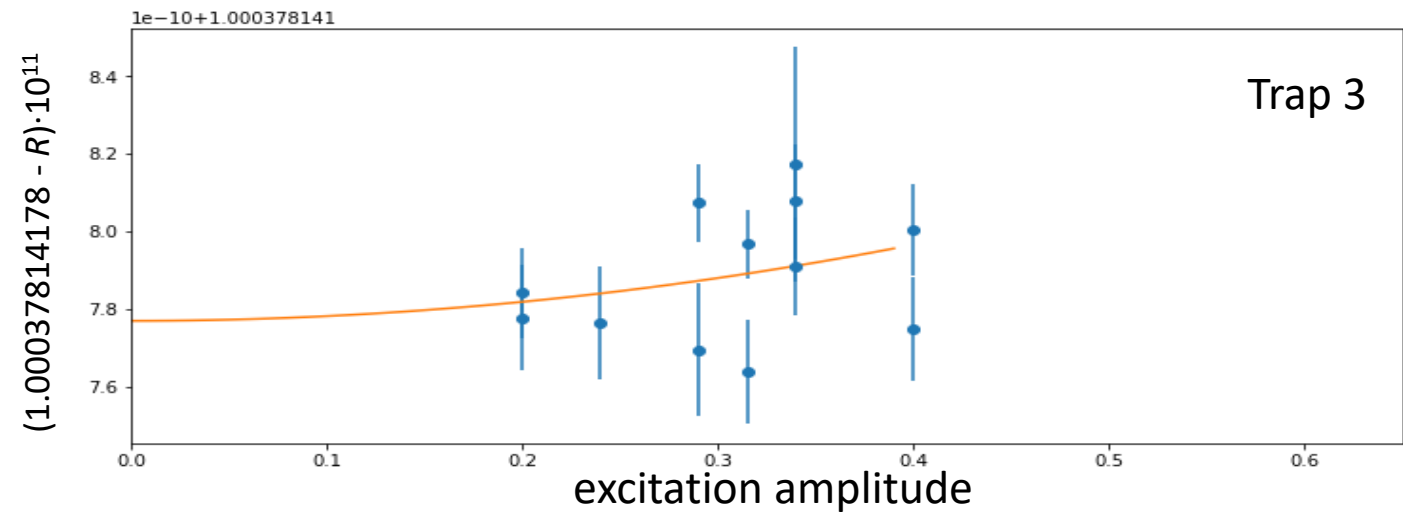
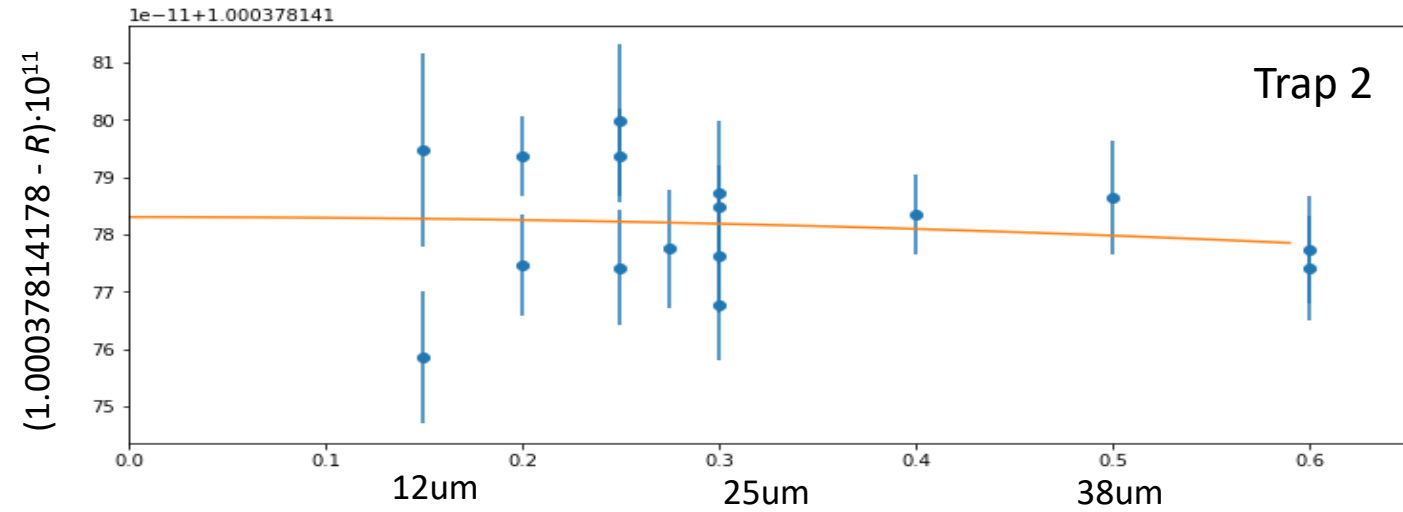
$R$  was measured at several  $\rho_+$  values



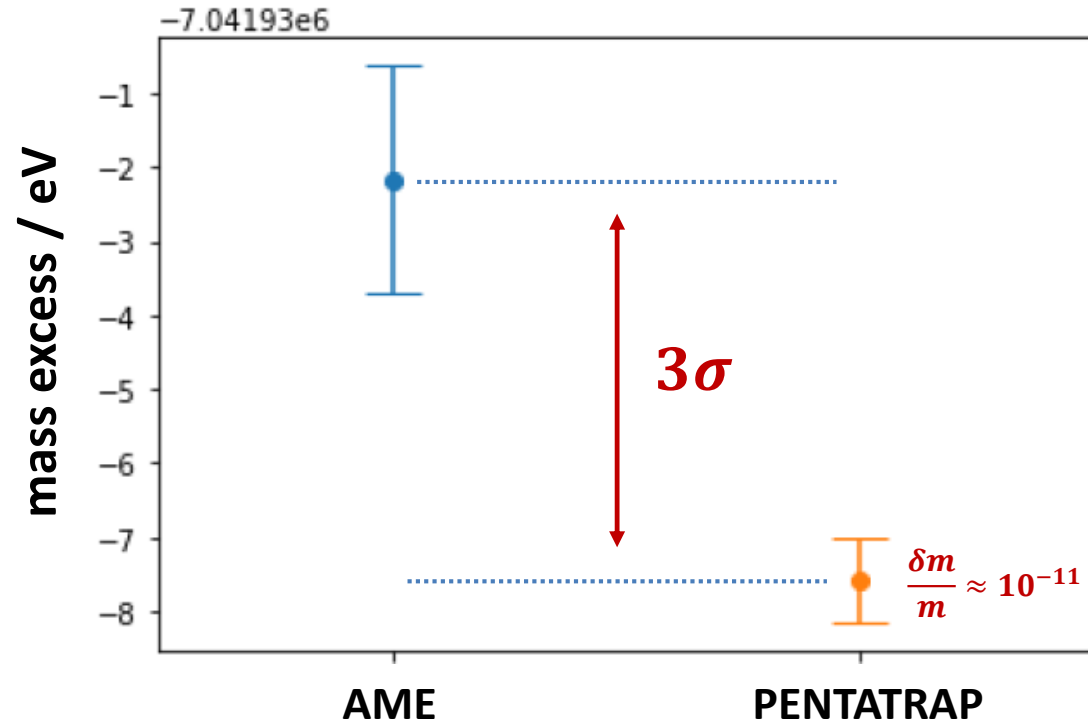
extrapolation to  $\rho_+ = 0$



$$\delta R_{\rho_+ = 0} \approx 10^{-11}$$



# $^{20}\text{Ne}$ mass measurement – smaller masses



$$g_{\text{exp}} = g_{\text{theory}} \quad \text{😊}$$

## $^{20}\text{Ne}$ mass measurement – smaller masses

|   |                  | $\delta m / m$ | Penning-trap Group          | Year |
|---|------------------|----------------|-----------------------------|------|
| ✓ | $^{20}\text{Ne}$ | 7.5E-11        | MIT / DiFilippo / Pritchard | 1995 |
|   | $^{14}\text{N}$  | 1.7E-11        | MIT / DiFilippo / Pritchard | 1995 |
|   | $^{16}\text{O}$  | 2.0E-11        | UW / van Dyke               | 2006 |
|   | $^{28}\text{Si}$ | 2.0E-11        | FSU / Redshaw / Myers       | 2008 |



We are planning to measure other low masses sooner or later

## Applications of relative mass measurements at a level of $\frac{\delta m}{m} \leq 10^{-11}$

### Neutrino physics

Gastaldo, L. et al., Eur. Phys. J. ST 226, 1623 (2017)



Filianin, P. et al.,  $\delta Q = 1.3 \text{ eV}$   
Phys. Rev. Lett. 127, 072502 (2021)

In review, Schweiger, Ch.  
Nature (2022)  $\delta Q = 0.8 \text{ eV}$

### Meta-stable states for HCl clocks

Kozlov, M. G. et al., Rev. Mod. Phys. 90, 045005 (2018)

$$\Delta m(^{208}\text{Pb}^{41+} - ^{208}\text{Pb}^{*41+})$$

$$\Delta m(^{187}\text{Re}^{29+} - ^{187}\text{Re}^{*29+})$$

In preparation, Kromer, K. (2022)

Schuessler, R. X. et al.,  
Nature 581, 42 (2020)

### Test of QED

Binding energies:  $E_B(\text{Xe}^{17+}) = \Delta m(\text{Xe}^{17+} - \text{Xe}^{18+})c^2 - m_e c^2$

g-factor: 
$$g = 2 \frac{v_L}{v_c} \frac{m_e}{m(^{20}\text{Ne})} \frac{q}{e}$$

Shabaev, V. M. et al., Int. J. of Mass Spec. 251, 109, (2006)

Rischka, A. et al.,  
Phys. Rev. Lett. 124, 113001 (2020)

In preparation, Sailer, T. (2022)

### Dark Matter search: Isotope shift

Flambaum, V. V. et al., Phys. Rev. A 79, 032510 (2018)

$$\nu_i^{AA'} = K_i \mu_{AA'} + F_i \delta \langle r^2 \rangle_{AA'} + \alpha_{NP} X_i \gamma_{AA'}$$

**Current measurement campaign  
of Yb isotope mass-ratios**

### Test of $E = mc^2$

Rainville, S. et al., Nature 438, 1096 (2005)

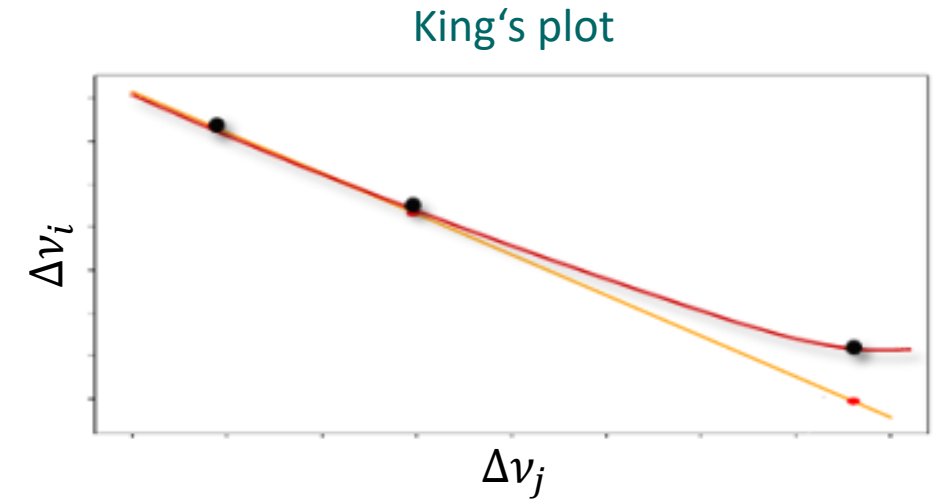
$$E = \frac{hc}{\lambda} = \Delta m(^{36}\text{Cl} - ^{35}\text{Cl} - n)c^2$$



# dark matter and 5<sup>th</sup> force

$$\Delta\nu_i = C_1 \cdot \frac{m_1 - m_2}{m_1 m_2} + C_2 \cdot \Delta\nu_j + [\text{higher-order SM effects} + \text{LDM bosons}]$$

$$\nu_i(\text{isotope}_1) - \nu_i(\text{isotope}_2) \equiv \Delta\nu_i$$

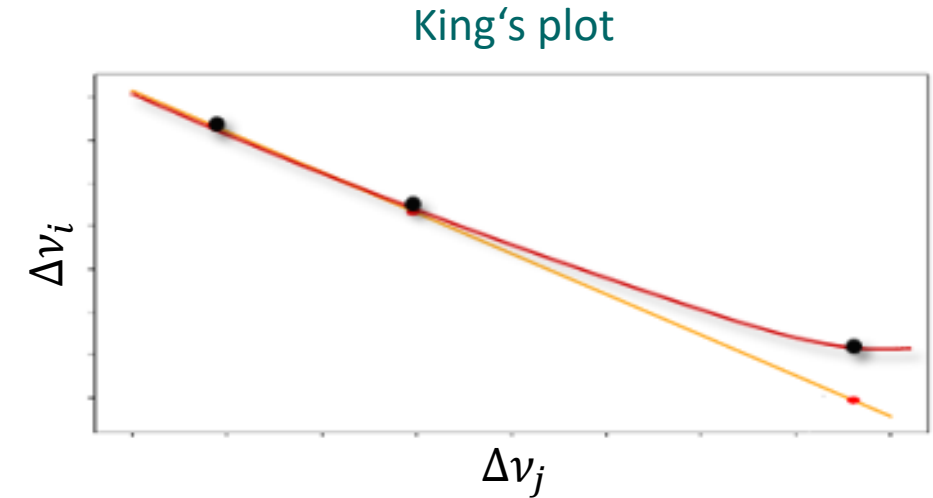


# dark matter and 5<sup>th</sup> force

$$\Delta\nu_i = C_1 \cdot \frac{m_1 - m_2}{m_1 m_2} + C_2 \cdot \Delta\nu_j + [\text{higher-order SM effects} + \text{LDM bosons}]$$

$$\nu_i(\text{isotope}_1) - \nu_i(\text{isotope}_2) \equiv \Delta\nu_i$$

one needs elements with many even-even isotopes  
and quadrupole (narrow optical) transitions:



168,170,172,174,176Yb  ${}^2S_{1/2} \leftrightarrow {}^2D_{5/2}$  (411 nm) I. Counts et al., PRL 125, 123002 (2020)  
 ${}^2S_{1/2} \leftrightarrow {}^2D_{3/2}$  (436 nm)

40,42,44,46,48Ca  $4s^2S_{1/2} \leftrightarrow 3d^2D_{5/2}$  (729 nm) C. Solaro et al., PRL 125, 123003 (2020)  
 $4s^2S_{1/2} \leftrightarrow 3d^2D_{3/2}$  (732 nm) F.W. Knollmann et al., PRA 100, 022514 (2019)

84,86,88,90Sr  $5S_{1/2} - 4D_{5/2}$  T. Manowitz et al., PRL 123, 203001 (2019)  
 $1S_0 - 3P_1, 1S_0 - 3P_0$  H. Miyake et al., PRR 1, 033113 (2019)

142,144,146,148,150Nd

N. Bhatt et al., ArXiv 2002.08290

130,132,134,136,138Ba

P. Imgram et al., PRA 99, 012511 (2019)

# dark matter and 5<sup>th</sup> force

$$\Delta\nu_i = C_1 \cdot \frac{m_1 - m_2}{m_1 m_2} + C_2 \cdot \Delta\nu_j + [\text{higher-order SM effects} + \text{LDM bosons}]$$

$$\nu_i(\text{isotope}_1) - \nu_i(\text{isotope}_2) \equiv \Delta\nu_i$$

one needs elements with many even-even isotopes  
and quadrupole (narrow optical) transitions:

168,170,172,174,176 **Yb**       $^2S_{1/2} \leftrightarrow ^2D_{5/2}$  (411 nm)  
 $^2S_{1/2} \leftrightarrow ^2D_{3/2}$  (436 nm)      I. Counts et al., PRL 125, 123002 (2020)

40,42,44,46,48 **Ca**       $4s^2S_{1/2} \leftrightarrow 3d^2D_{5/2}$  (729 nm)      C. Solaro et al., PRL 125, 123003 (2020)  
 $4s^2S_{1/2} \leftrightarrow 3d^2D_{3/2}$  (732 nm)      F.W. Knollmann et al., PRA 100, 022514 (2019)

84,86,88,90 **Sr**       $5S_{1/2} - 4D_{5/2}$       T. Manowitz et al., PRL 123, 203001 (2019)  
 $1S_0 - 3P_1, 1S_0 - 3P_0$       H. Miyake et al., PRR 1, 033113 (2019)

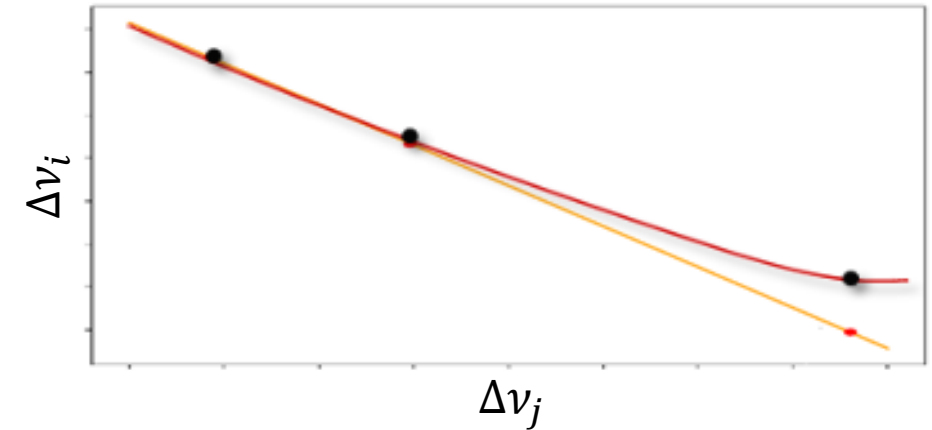
142,144,146,148,150 **Nd**

N. Bhatt et al., ArXiv 2002.08290

130,132,134,136,138 **Ba**

P. Imgram et al., PRA 99, 012511 (2019)

King's plot



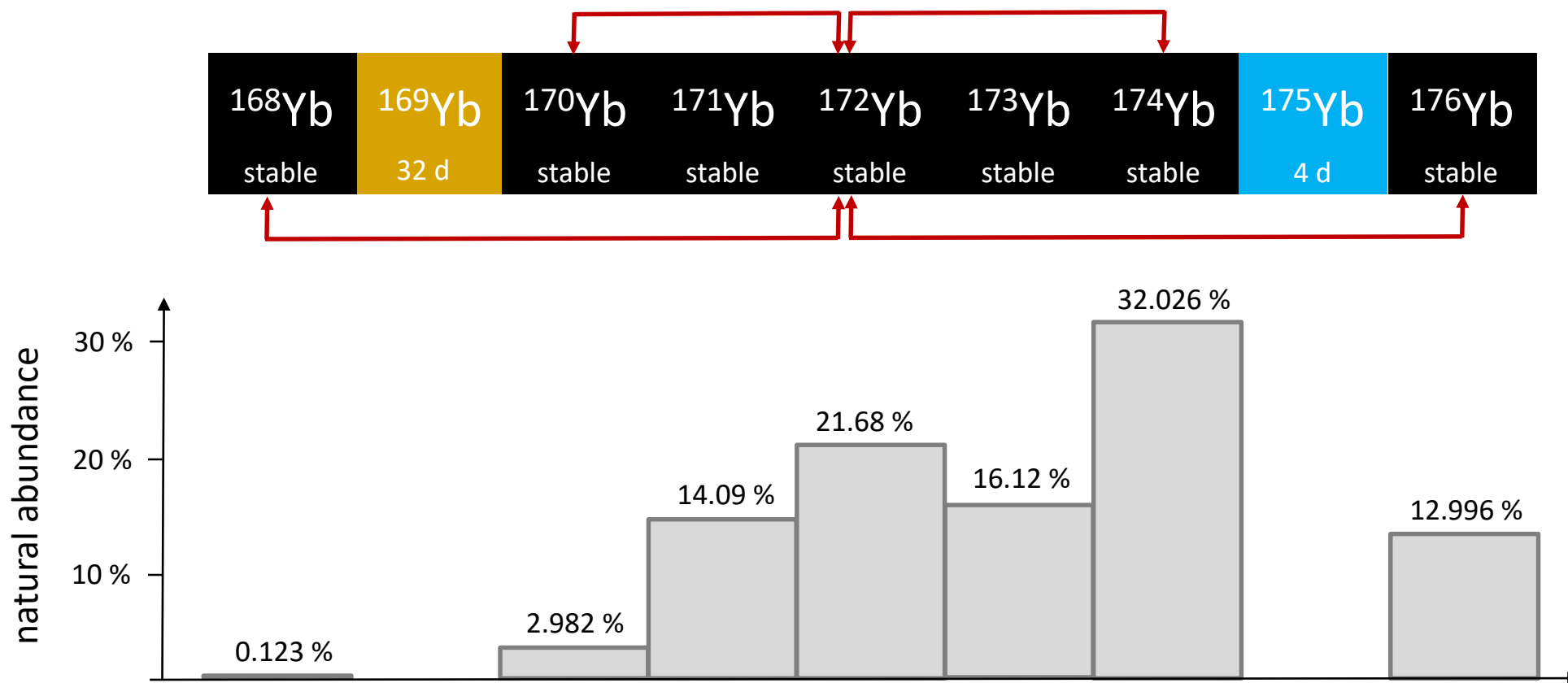
## FUTURE of Yb:

$$\delta(\Delta\nu_i) \approx 10 \text{ mHz}$$

$$\delta\left(\frac{m_1}{m_2}\right) \approx 5 \cdot 10^{-12}$$

# Yb mass-ratio measurements – ongoing !

$^{187}\text{Re}/^{187}\text{Os}$ ,  $^{187\text{m}}\text{Re}/^{187\text{g}}\text{Re}$ ,  $^{187\text{m}}\text{Os}/^{187\text{g}}\text{Os}$ ,  $^{163}\text{Ho}/^{163}\text{Dy}$ ,  $^{12}\text{C}/^{20}\text{Ne}$  – mass or  $m/q$  doublets !!!



# Yb mass-ratio measurements – ongoing !

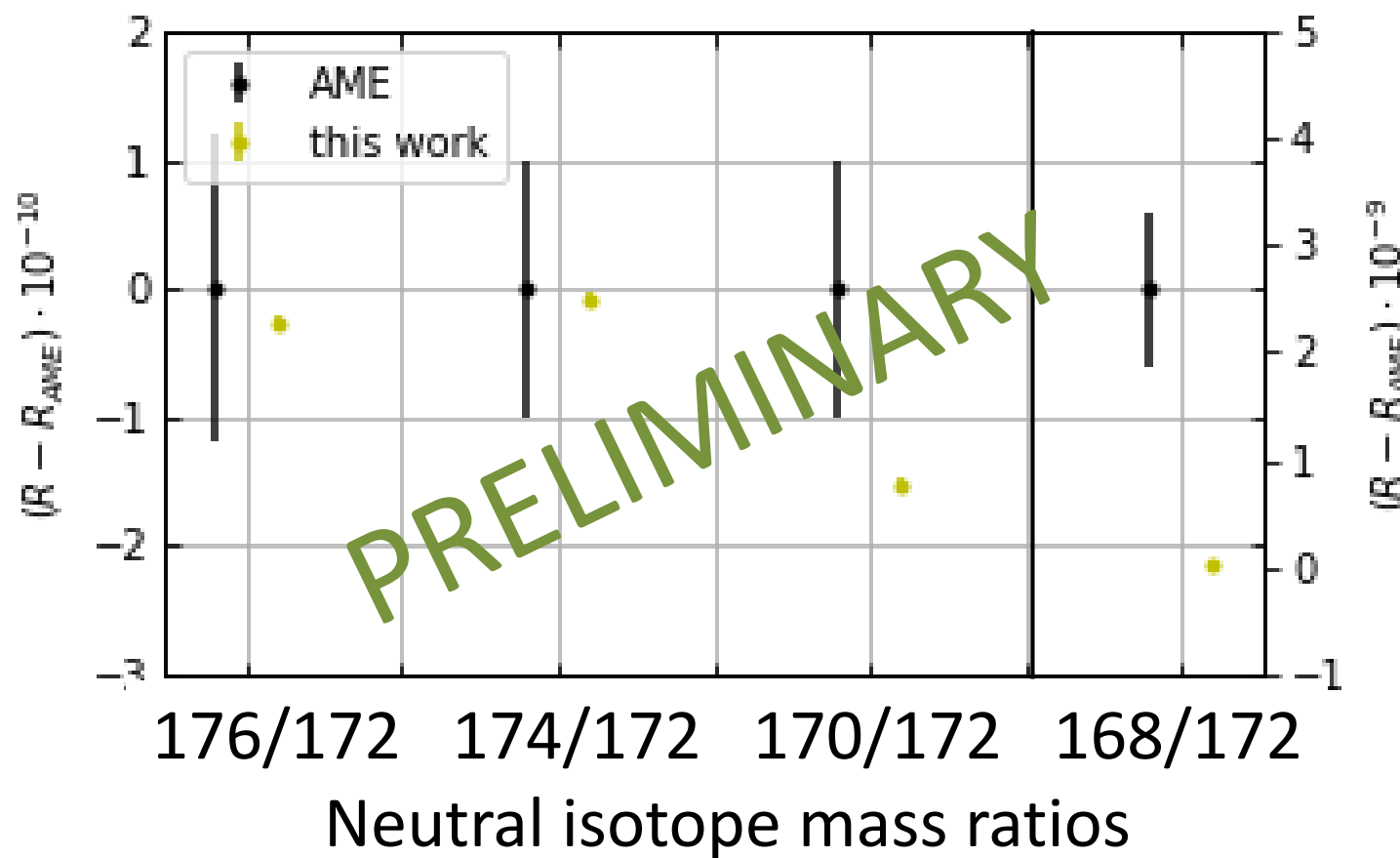
$$\delta R \approx 5 * 10^{-12}$$

strongest systematic  
uncertainties:

- 1) dip line shape / fit
- 2) relativistic shifts

Measured as non-doublets:

*Varactor diodes are used to tune  
detection system instead of the ions axial  
frequencies to keep trap depth constant  
and thereby drastically reduce  
systematic uncertainties*



# Summary & Outlook

- Pentatrap can perform few ppt mass-ratio measurements on wide range of stable nuclides
- Current limitations are
  - the axial dip lineshape and “on-resonance tuning”
  - ion temperature & relativistic shifts
  - Voltage stability (statistics)

Next measurements:

- 1) Yb odd stable isotopes  
& absolute mass measurement vs  $^{12}\text{C}$   
& Yb binding energies as crosscheck
- 2) Other chains of isotopes
- 3) Meta stable states for HCl clocks

Next Upgrades:

- 1) Josephson Junction for more stable voltages
- 2) Feedback cooling to reduce radial amplitudes
- 3) Phase sensitive axial frequency measurement



# Thank you for your attention!



DFG FOR 2202



DFG SFB 1225



European Research Council  
Established by the European Commission

ERC AdG 832848 - FunI

## Present and former PENTATRAP members:

Christine Böhm, Menno Door, Andreas Dörr, Sergey Eliseev, Pavel Filianin, Jost Herkenhoff, Daniel Lange, Kathrin Kromer, Marius Müller, Yuri N. Novikov, Julia Repp, Alexander Rischka, Christian Roux, Christoph Schweiger, Rima X. Schüssler and Klaus Blaum

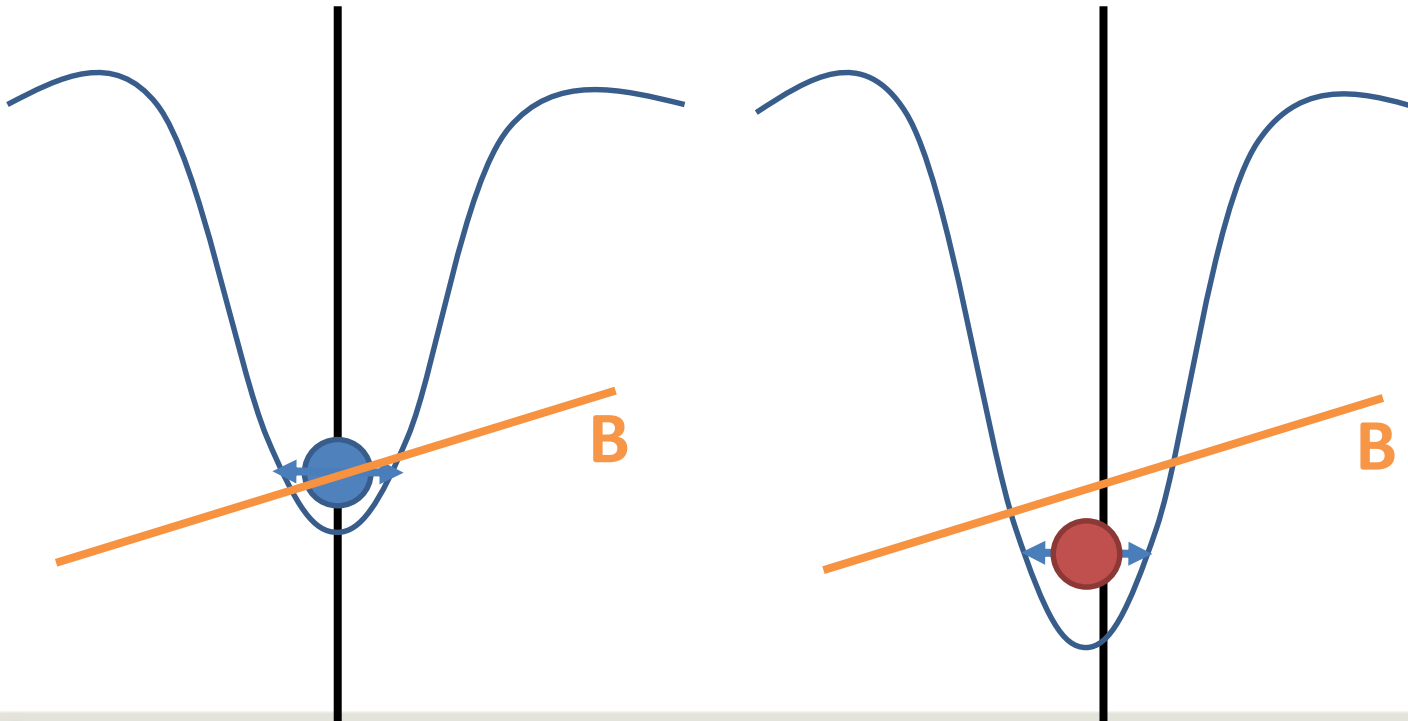
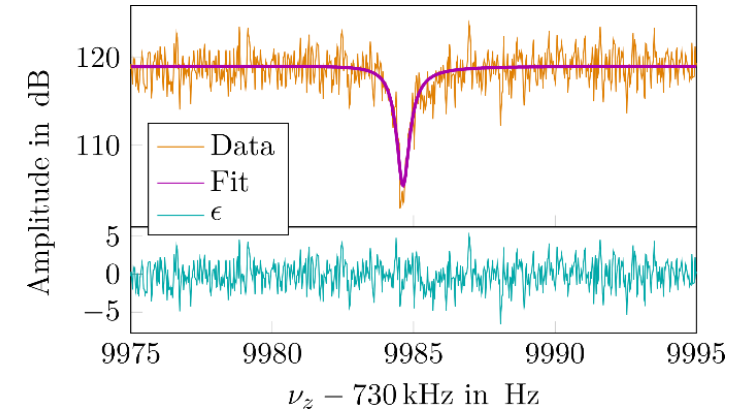


# BACKUP SLIDES



# $^A\text{Yb} / ^{A'}\text{Yb}$ issues with same-charge state measurements:

- Difference in axial frequency is huge! Up to 8 kHz! But axial frequency has to match detection system  
 → trap depth has to be adjusted for each ion



**Problem:**

Potential not perfectly symmetric  
 → depth change = ion mean position changes

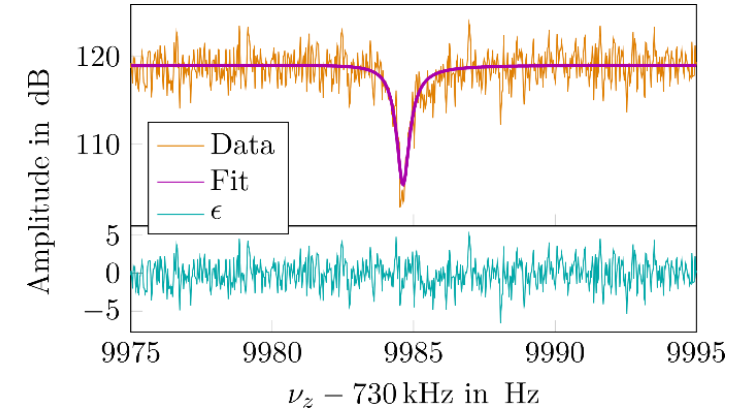
Magnetic field not perfectly homogeneous:  
 effective magnetic field changes

$$R = \frac{\omega_c^A}{\omega_c^B} = \frac{q^A m^B B^A}{q^B m^A B^B}$$



# ${}^A\text{Yb} / {}^{A'}\text{Yb}$ issues with same-charge state measurements:

- Difference in axial frequency is huge! Up to 8 kHz! But axial frequency has to match detection system  
 → trap depth has to be



Huge systematic effect on the mass ratio result...  
Not feasible

### Problem:

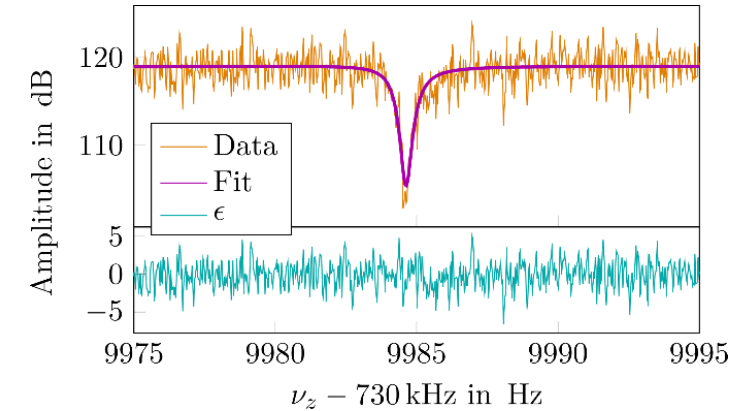
Potential not perfectly symmetric  
 → depth change = ion mean position changes

Magnetic field not perfectly homogeneous:  
 effective magnetic field changes

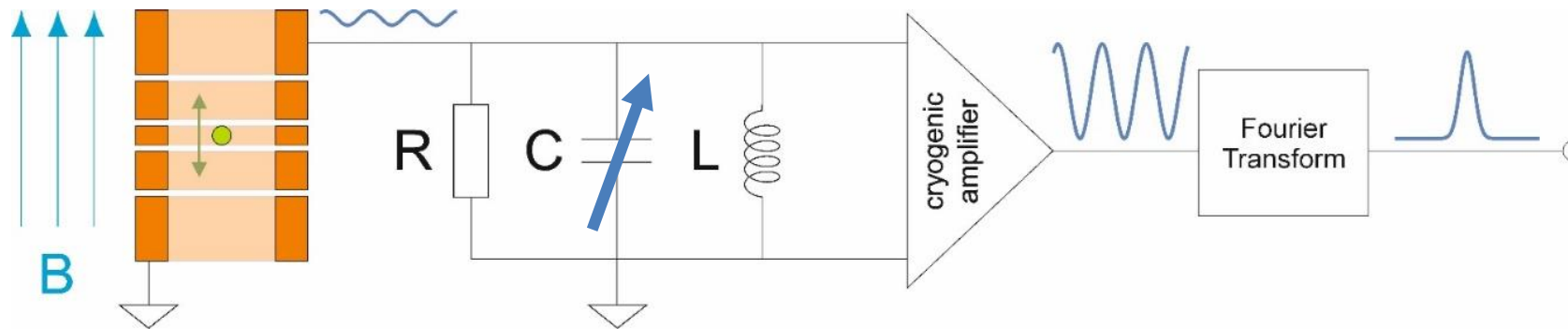
$$R = \frac{\omega_C^A}{\omega_C^B} = \frac{q^A m^B B^A}{q^B m^A B^B}$$

# $^A\text{Yb} / ^{A'}\text{Yb}$ issues with same-charge state measurements:

- Difference in axial frequency is huge! Up to 8 kHz! But axial frequency has to match detection system  
→ trap depth has to be adjusted for each ion



- Solution: VariCap (variable capacitance) to tune detection system instead of trap potential



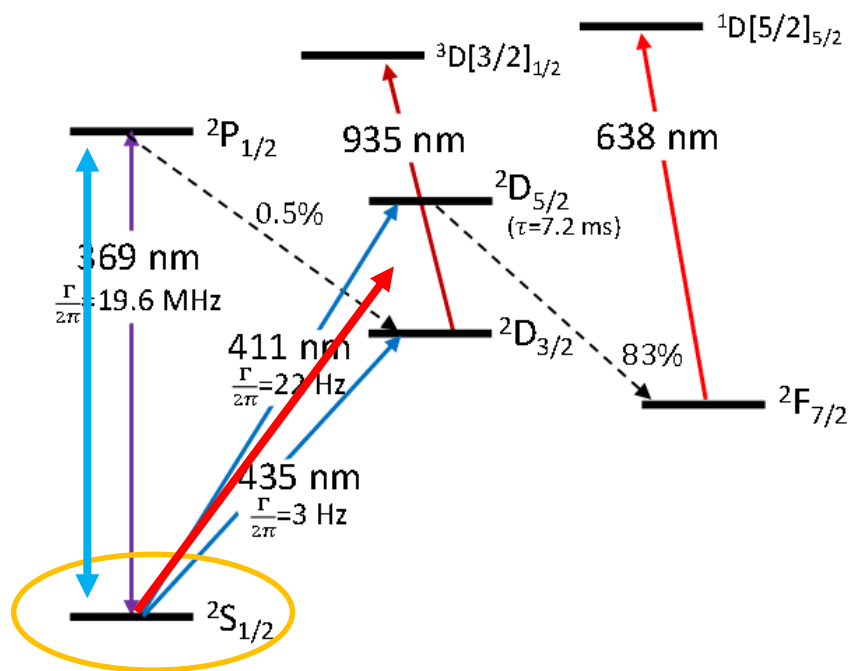
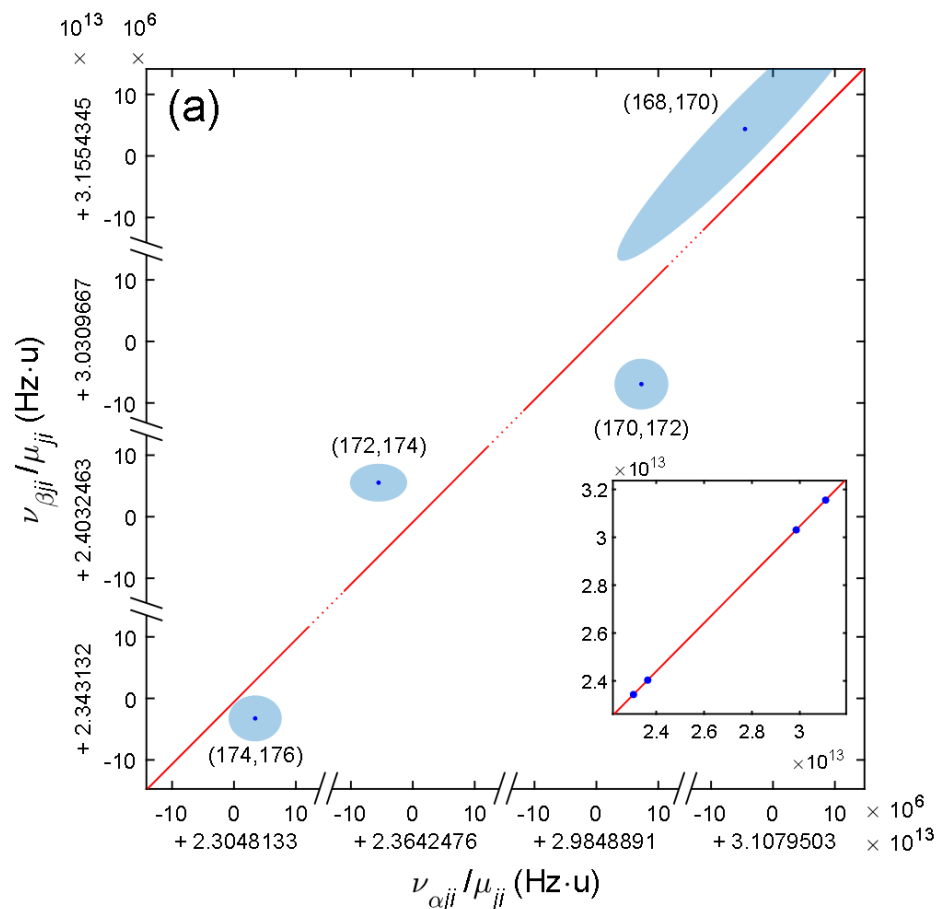


FIG. S1. Partial  $\text{Yb}^+$  level diagram.

- single  $\text{Yb}^+$  ion trapped 135 $\mu\text{m}$  above the a lithographic microchip surface Paul trap
- The transitions at 411 nm ( $6s^2 S_{1/2} \rightarrow 5d^2 D_{5/2}$ ;  $\Gamma/(2\pi) = 22$  Hz) and 436 nm ( $6s^2 S_{1/2} \rightarrow 5d^2 D_{3/2}$ ;  $\Gamma/(2\pi) = 3$  Hz) are probed with a Ti:Sapphire laser, tuned to 822 nm and 871 nm, respectively
- The readout of the state is carried out via an electron-shelving scheme (dark state detection) – we covered this not long ago in the Journal Club, here a small recap:

1. Ions in the **ground state  $S_{1/2}$**  are detected via fluorescence during the cooling with 369 nm light.
2. If the ion is **fluorescing** before a **probe pulse** and no longer fluorescing afterwards, the ion is said to have completed a quantum jump.
3. Otherwise, the ion failed to quantum jump (or, if there was no fluorescence before the probe pulse, the ion failed to be initialized).
4. By dividing the number of quantum jumps by the total number of successful initialization, we can measure a probability of excitation as a function of frequency.

~ 400 Hz precision on the measured transitions  
 @ 2 GHz IS, relative ~  $2e-7$



- single Yb+ ion trapped 135μm above the a lithographic microchip surface Paul trap
- The transitions at 411 nm ( $6s^2 S_{1/2} \rightarrow 5d^2 D_{5/2}$ ;  $\Gamma/(2\pi) = 22$  Hz) and 436 nm ( $6s^2 S_{1/2} \rightarrow 5d^2 D_{3/2}$ ;  $\Gamma/(2\pi) = 3$  Hz) are probed with a Ti:Sapphire laser, tuned to 822 nm and 871 nm, respectively
- The readout of the state is carried out via an electron-shelving scheme (dark state detection) – we covered this not long ago in the Journal Club, here a small recap:
  1. Ions in the **ground state S1/2** are detected via fluorescence during the cooling with 369 nm light.
  2. If the ion is **fluorescing** before a **probe pulse** and no longer fluorescing afterwards, the ion is said to have completed a quantum jump.
  3. Otherwise, the ion failed to quantum jump (or, if there was no fluorescence before the probe pulse, the ion failed to be initialized).
  4. By dividing the number of quantum jumps by the total number of successful initialization, we can measure a probability of excitation as a function of frequency.

~ 400 Hz precision on the measured transitions  
 @ 2 GHz IS, relative ~ 2e-7

# IS spectroscopy (future)

Manovitz, T. et al. Phys. Rev. Lett. **123** (2019) 203001

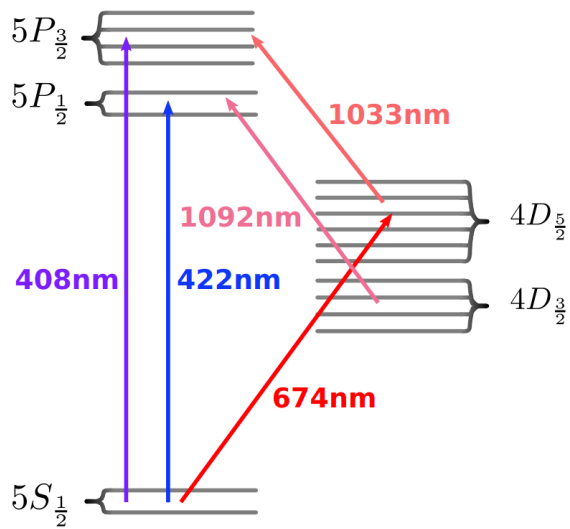


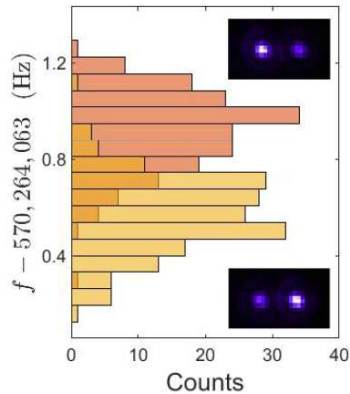
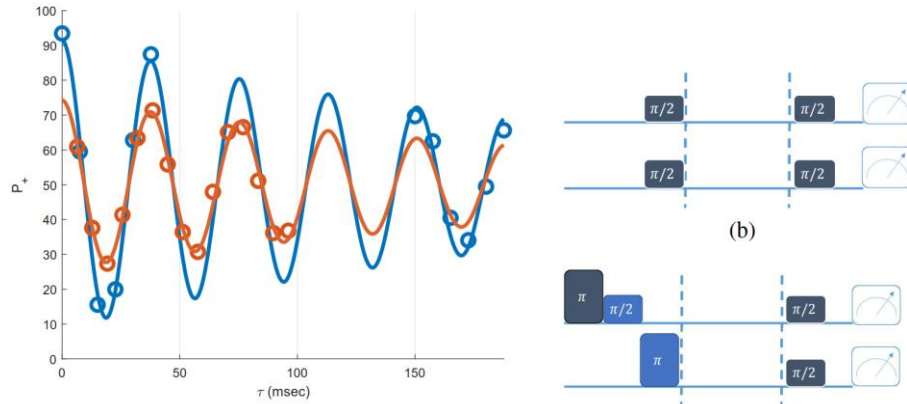
Figure 6.1:  $^{88}\text{Sr}^+$  energy levels diagram

- Two isotope ion crystal of Sr86 and Sr88 in Paul trap
- Also state read out (fluorescence, state preparation, cooling) via an electron-shelving scheme (dark state detection) but using bichromatic laser fields resonant to the relevant transitions in both isotopes.
- The  $5S_{1/2} \rightarrow 4D_{5/2}$  transition is driven by a narrow ( $\sim 20$  Hz) linewidth laser, splitted into different **AO frequency shifters that bridge the  $\sim 570$  MHz IS gap**. The two beams are recombined and sent through another AO frequency shifter for common frequency control
- Ions are prepared in entangled state  $|\psi_i\rangle = \frac{1}{\sqrt{2}} (|g_m e_n\rangle + e^{i\phi_0} |e_m g_n\rangle)$ .
- The energy difference between the two states in this superposition is exactly the isotope shift times the Planck constant. Therefore, during free evolution for time  $\tau$ , these states will acquire a relative

$$|\psi_\tau\rangle = \frac{1}{\sqrt{2}} \left( |g_m e_n\rangle + e^{i\phi_0 - i\delta\nu_{nm}^i \tau} |e_m g_n\rangle \right)$$

# IS spectroscopy (future)

Manovitz, T. et al. Phys. Rev. Lett. **123** (2019) 203001



Reaching ~ 10 mHz precision directly on IS(!)  
@ 570 MHz, relative ~ 1E-11

- Ions are prepared in entangled state  $|\psi_i\rangle = \frac{1}{\sqrt{2}} (|g_m e_n\rangle + e^{i\phi_0} |e_m g_n\rangle)$ .
- The energy difference between the two states in this superposition is exactly the isotope shift times the Planck constant. Therefore, during free evolution for time  $\tau$ , these states will acquire a relative

$$|\psi_\tau\rangle = \frac{1}{\sqrt{2}} (|g_m e_n\rangle + e^{i\phi_0 - i\delta\nu_{nm}^i \tau} |e_m g_n\rangle)$$

- The superposition phase is estimated by performing a parity measurement. Two  $\pi/2$  pulses are applied, each at the carrier frequency of one of the isotopes. The resulting populations will obey the relation

$$\begin{aligned} p_{ee} + p_{gg} - (p_{eg} + p_{ge}) &= \cos(\phi_0 + \delta\nu_{nm}^i \tau - (\varphi_m - \varphi_n)) \\ &= \cos(\phi_0 + (\delta\nu_{nm}^i - \delta f_{nm})\tau - (\phi_m - \phi_n)) \end{aligned}$$

- The parity signal will oscillate in time at the detuning of the two fields' frequency difference, which can be dictated by an RF source, with respect to the isotope shift. Laser phase-noise is cancelled since it is common to both addressing fields.

# Mass situation

| Nuclide | Current mass precision (AME2016) $\delta m/m$ | Labs performing spectroscopy measurements of the IS                            |
|---------|---|--|
| Ca40    | 5.51e-10                                      | PTB (Germany)<br>IQOQI (Austria)   |
| Ca42    | 3.79e-09                                      |  |
| Ca44    | 7.92e-09                                      |  |
| Ca46    | 5.22e-08                                      |  |
| Ca48    | 2.15e-09                                      |  |
| Sr84    | 1.59e-08                                      | Weizmann Institute (Israel)<br>RIKEN (Japan)                                   |
| Sr86    | 6.53e-11                                      |  |
| Sr88    | 6.81e-11                                      |  |
| Sr90    | 2.54e-08                                      |  |
| Yb168   | 7.63e-09                                      | Weizmann Institute (Israel)<br>NIST (USA)<br><i>Better value JYFLTRAP 2020</i> |
| Yb170   | 6.47e-11                                      |  |
| Yb172   | 8.14e-11                                      |  |
| Yb174   | 6.32e-11                                      |  |
| Yb176   | 8.53e-11                                      |  |

Needed relative precision compared to IS precision, a factor of roughly:

$$\frac{m_A}{m_{A_0} - m_A}$$

48/8 = 6

88/4 = 22

176/8 = 22

Current IS precision

~ 1e-08

~ /

~ 1e-07

Needed mass precision

~ 2e-09

~ 5e-09



# King Plot – vector space

## I. VISUALIZING THE VECTOR SPACE

In the main text we define the following vectors in the  $A'$  vector space

$$\vec{m}\nu_i \equiv (m\nu_i^{AA'_1}, m\nu_i^{AA'_2}, m\nu_i^{AA'_3}), \quad (S1)$$

$$\vec{m}\delta\langle r^2 \rangle \equiv (\langle r^2 \rangle_{AA'_1}/\mu_{AA'_1}, \langle r^2 \rangle_{AA'_2}/\mu_{AA'_2}, \langle r^2 \rangle_{AA'_3}/\mu_{AA'_3}), \quad (S2)$$

$$\vec{m}\mu \equiv (1, 1, 1). \quad (S3)$$

As long as  $\vec{m}\nu_{1,2}$  are spanned by  $\vec{m}\mu$  and  $\vec{m}\delta\langle r^2 \rangle$ , the resulting King plot will be linear. In Fig. S1, we illustrate the vector space of the various components related to isotope shifts that leads to the nonlinearities. The NP contribution to IS,  $\alpha_{\text{NP}}X_i\vec{h}$ , may lift the IS vectors from the  $(\vec{m}\mu, \vec{m}\delta\langle r^2 \rangle)$  plane, resulting in a nonlinear King plot. Fig. S2 illustrates a nonlinear King plot, where the area of the triangle corresponds to the NL of Eq. (6).

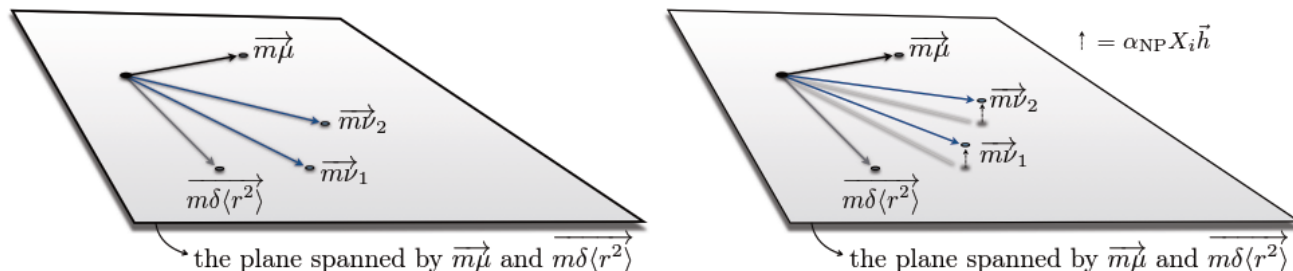


FIG. S1: Left: A cartoon of the prediction of factorization, Eq. (5) in vector language. All of the isotope shift measurements (which are here three dimensional vectors  $\vec{m}\nu_{1,2}$ ) lie in the plane that is spanned by  $\vec{m}\mu$  and  $\vec{m}\delta\langle r^2 \rangle$ . This coplanarity can be tested by measuring whether  $\vec{m}\nu_1$ ,  $\vec{m}\nu_2$  and  $\vec{m}\mu$  are coplanar. Right: In the presence of new physics the isotope shift get a contribution which can point out of the plane. A new long range force can spoil the coplanarity of  $\vec{m}\nu_1$ ,  $\vec{m}\nu_2$  and  $\vec{m}\mu$ .

## Reminder...

$$m\nu_i^{A_0A} = \frac{v_i^{A_0A}}{\mu_{A_0A}} = K_i + \frac{F_i}{\mu_{A_0A}} \delta\langle r^2 \rangle_{A_0A}$$

$$m\nu_2^{A_0A} = K_{21} + F_{21}m\nu_1^{A_0A}$$

with  $F_{21} = F_2/F_1$ , and  $K_{21} = K_2 - F_{21}K_1$

$$\vec{m}\nu_i = K_i \vec{m}\mu + F_i \vec{m}\delta\langle r^2 \rangle.$$

$$\vec{m}\nu_2 = K_{21} \vec{m}\mu + F_{21} \vec{m}\nu_1$$

## Nonlinearity?

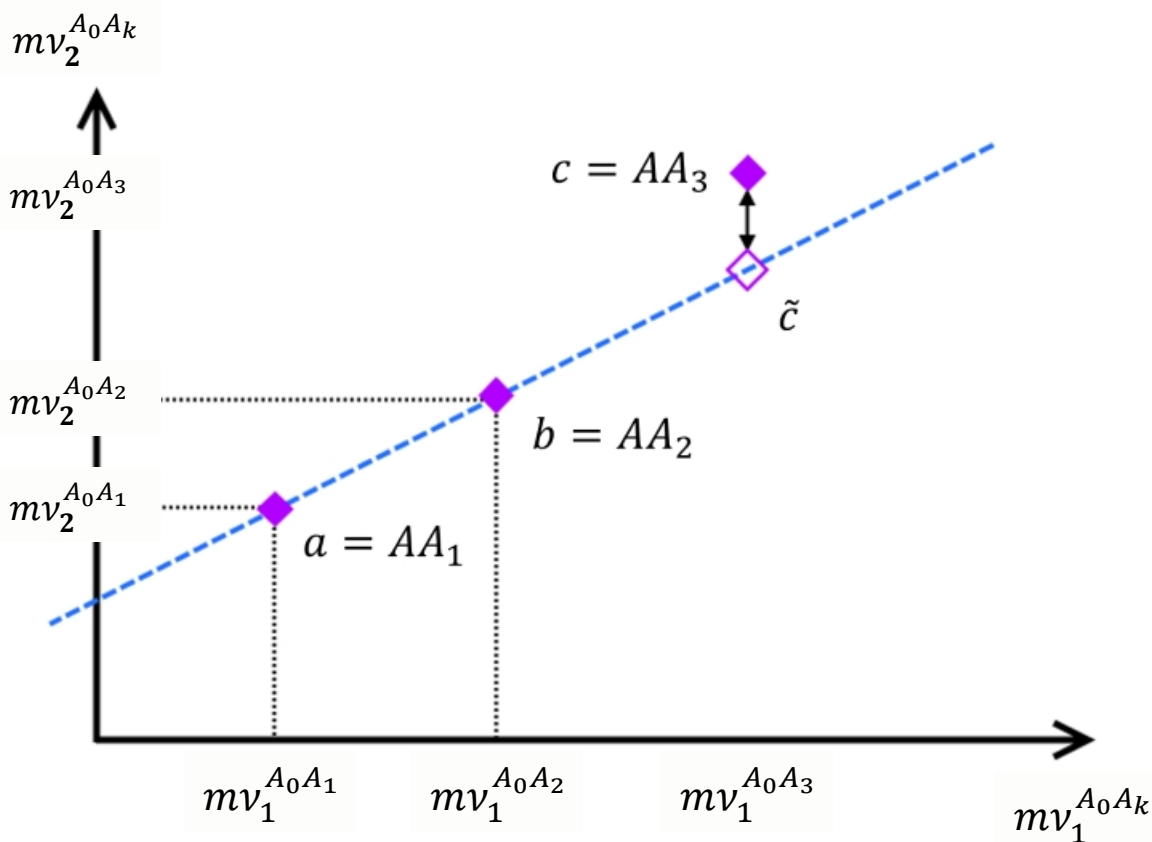
$$\text{NL} = \frac{1}{2} |(\vec{m}\nu_1 \times \vec{m}\nu_2) \cdot \vec{m}\mu| . \quad >$$

$$\sigma_{\text{NL}} = \sqrt{\sum_k (\partial \text{NL} / \partial \mathcal{O}_k)^2 \sigma_k^2}$$

(squared error of all measured values)



# Non-linearities



Other sources than new physics: The formular for the IS is an approximation:

$$v_i^{AA'} = K_i \mu_{AA'} + F_i \delta \langle r^2 \rangle_{AA'} + \alpha_{NP} X_i \gamma_{AA'}$$

Only valid at leading order of variation of the nuclear mass and charge distribution, expansion needed:

$$K_i \rightarrow K_i^{A_0 A} \text{ and } F_i \rightarrow F_i^{A_0 A}$$

This breaks linearity (now isotope depended)!

Calculating these nuclear effects theoretically is challenging... and with higher precision in the experimental input data, these effect will dominate the linearity test.... more later...

Effects can be parametrized:

$$v_i^{AA'} = K_i \mu_{AA'} + F_i \delta \langle r^2 \rangle_{AA'} + \sum_{l=2}^{inf} F_{il} \lambda_{l,A_0 A}$$

$\lambda_{l,A_0 A}$ : independ. nuclear param.,  $F_{il}$ : electronic const.

## No-mass King analysis

Two transitions, e.g.  $i=\{1,2\}$ , are used to extract the mass and field shift **nuclear parameters**

Third transition uses nuclear parameters in theory predictions

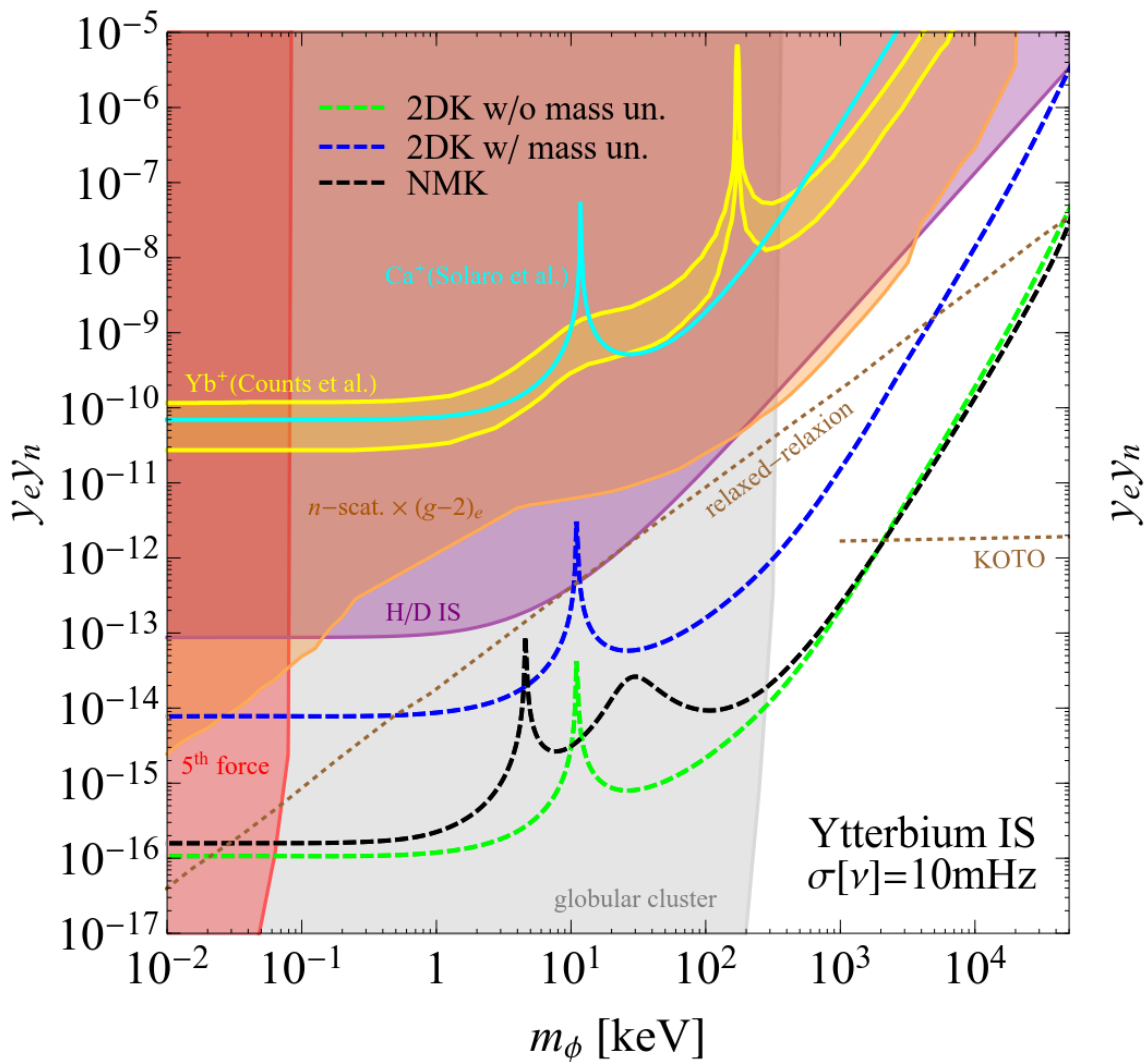
Also this linearity by itself can be tested without theory input

Uses third transition to remove the mass shift parameters

$$v_i^{A_0A} = K_i \mu_{A_0A} + F_i \delta\langle r^2 \rangle_{A_0A} + \alpha_{NP} X_i \gamma_{A_0A}$$

$$v_3^{A_0A} = f_3^\alpha v_\alpha^{A_0A} + \alpha_{NP} (X_3 - f_3^\alpha X_\alpha) \gamma_{A_0A}$$

# No-mass King analysis



Uses third transition to remove the mass shift parameters

$$v_i^{A_0A} = K_i \mu_{A_0A} + F_i \delta \langle r^2 \rangle_{A_0A} + \alpha_{NP} X_i \gamma_{A_0A}$$

$$v_3^{A_0A} = f_3^\alpha v_\alpha^{A_0A} + \alpha_{NP} (X_3 - f_3^\alpha X_\alpha) \gamma_{A_0A}$$



# Generalized King analysis (GK)

Basically the same as the no-mass analysis: using additional transitions to exchange additional electronic and nuclear parameters by IS measurement data

At least  $m-1$  transitions needed to fix parameters...  
Reaching this relation:

(Apparently) this generalized King analysis method allows to probe for new physics even though the typical King linearity is broken. It needs however  $m+2$  isotopes and  $m-1$  transitions...

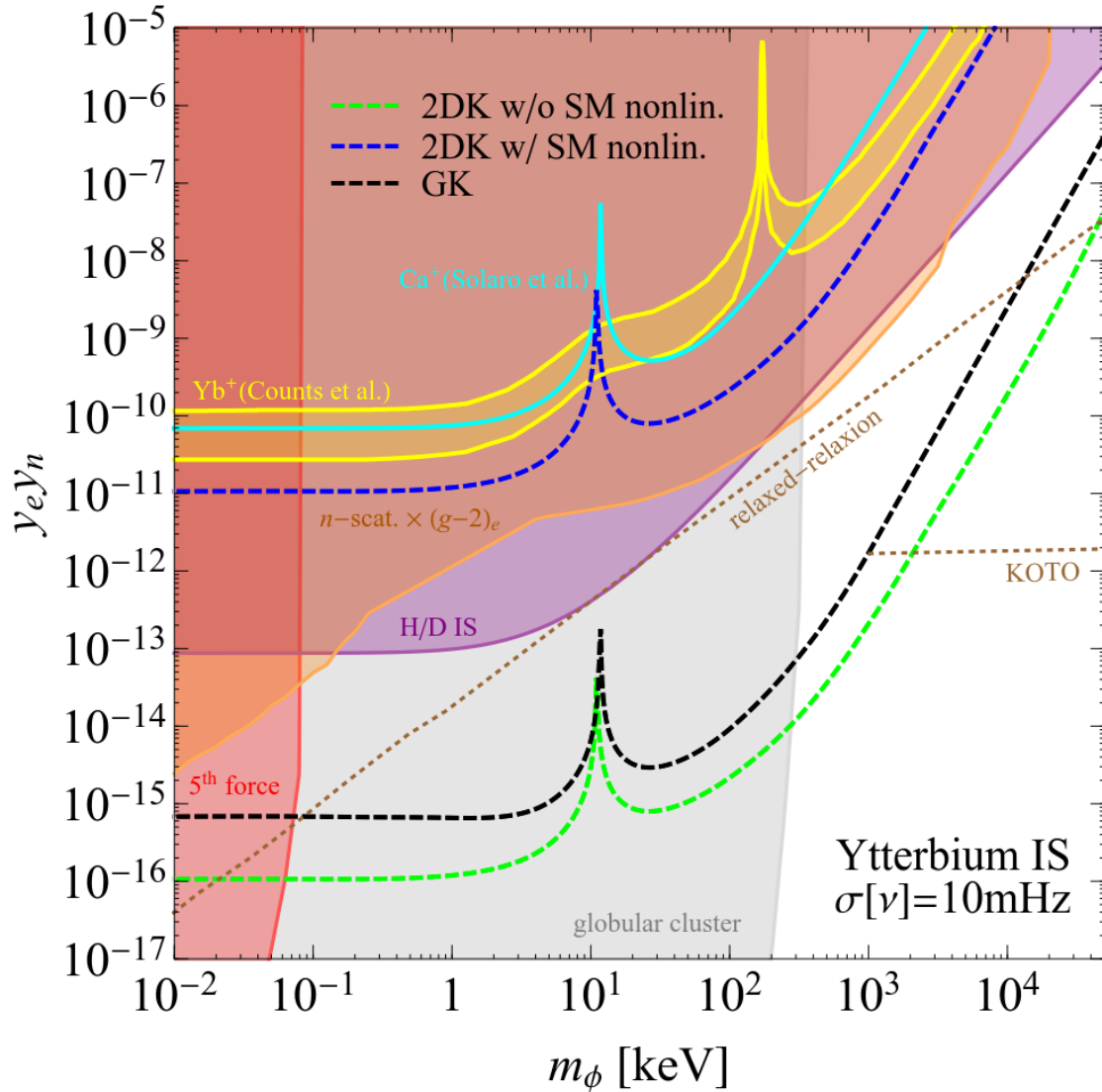
This is possible for Ytterbium (5 isotopes, 3 transitions)

$$m\nu_i^{AA'} = K_i + \sum_{l=1}^{m-1} F_{il} m \lambda_{l,A_0A} + \alpha_{NP} X_i h_{A_0A}$$

$\lambda_{l,A_0A}$ : independ. nuclear param.,  $F_{il}$ : electronic const.

$$m\nu_k^a = [K_k - f_{ki}K_i] + f_{ki}m\nu_i^a + \alpha_{NP}[X_k - f_{ki}X_i]h_a, \quad (11)$$

# Generalized King analysis (GK)



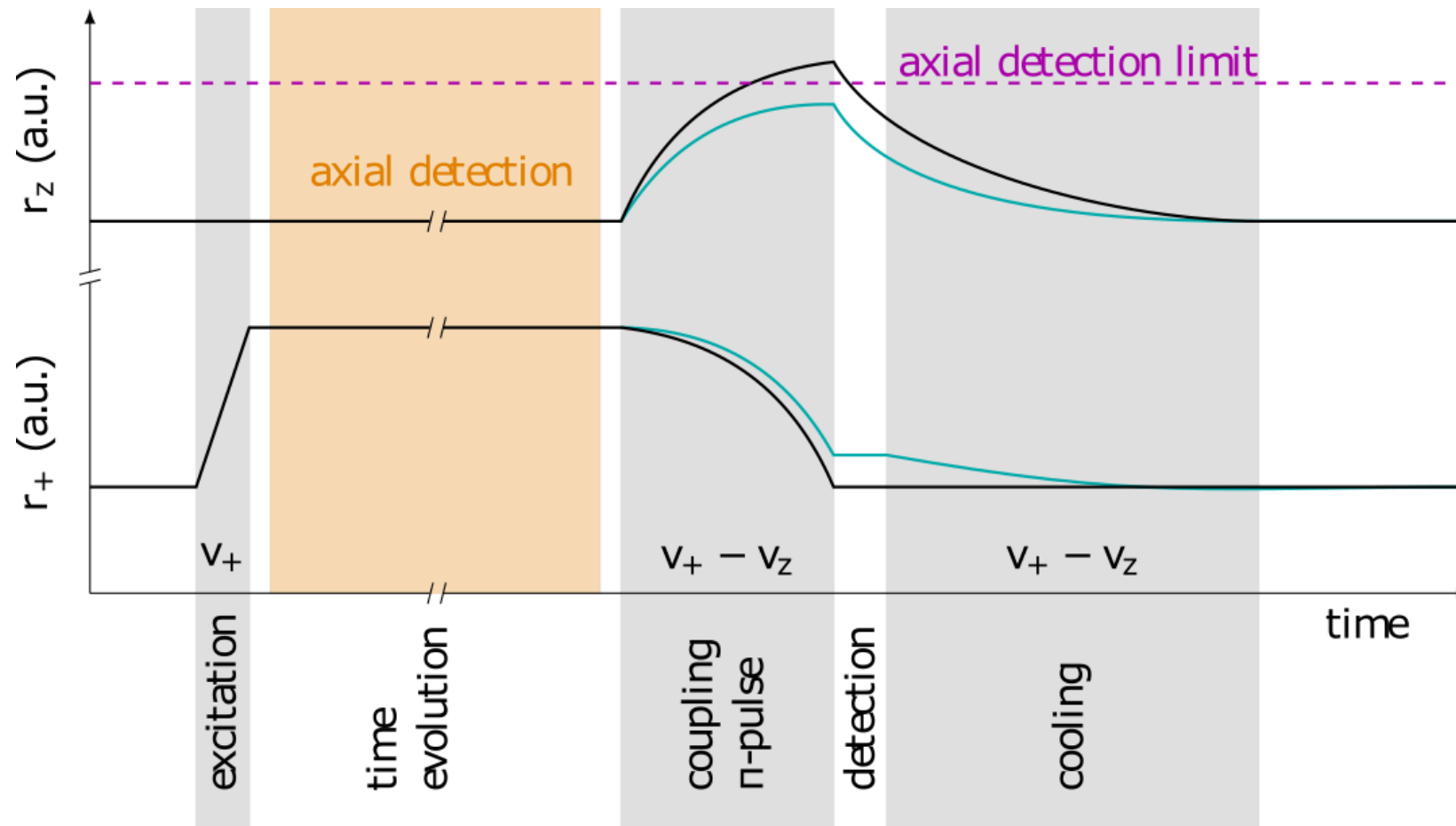
$$m\nu_i^{AA'} = K_i + \sum_{l=1}^{m-1} F_{il} m \lambda_{l,A_0A} + \alpha_{NP} X_i h_{A_0A}$$

$\lambda_{l,A_0A}$ : independ. nuclear param.,  $F_{il}$ : electronic const.

$$m\nu_k^a = [K_k - f_{ki}K_i] + f_{ki}m\nu_i^a + \alpha_{NP}[X_k - f_{ki}X_i]h_a, \quad (11)$$



# Phase sensitive measurement PnP: the sequence



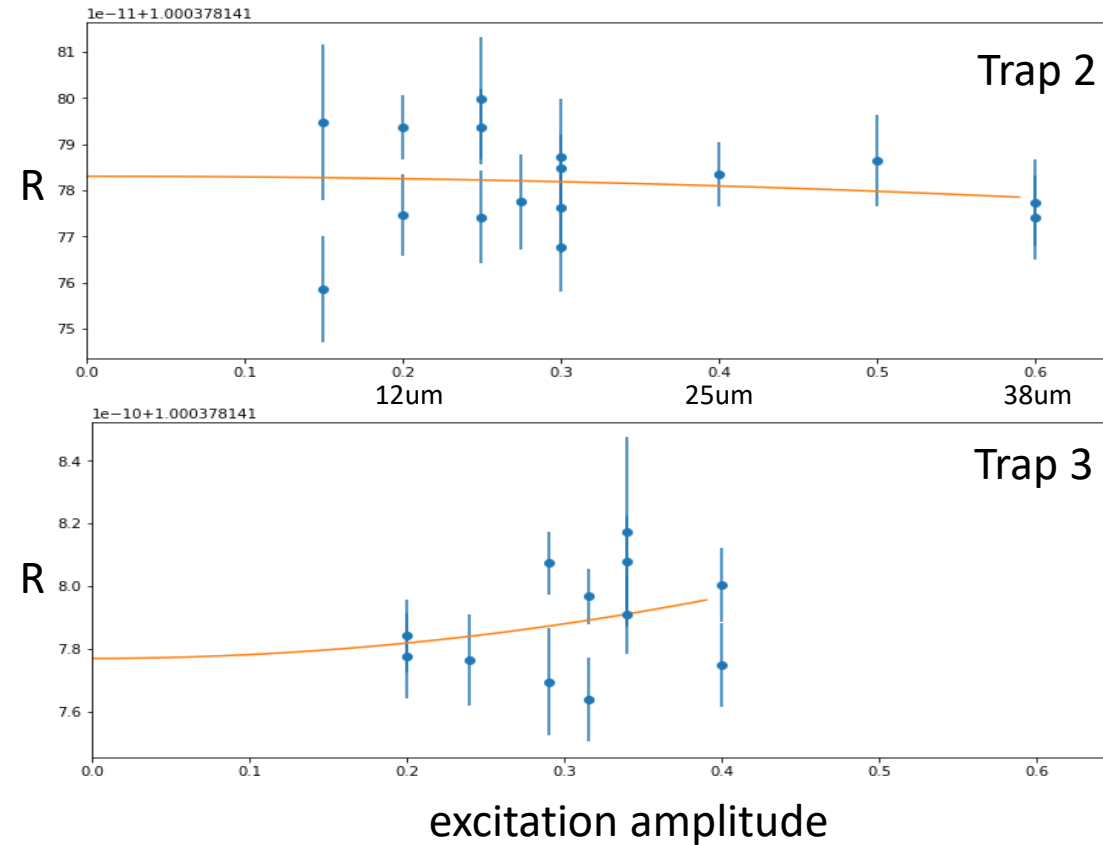
# $^{20}\text{Ne}$ mass measurement - Systematics

Ratio measurements were done at multiple excitation amplitudes:

No significantly measurable dependence on excitation amplitude

With extrapolation to zero excitation amplitude:

$$dR \sim 1e-11$$



Final measured ratio uncertainty  $dR \sim 1e-11$

## 20-Ne mass measurement

---

We measure  $^{20}\text{Ne}^{10+}$  against  $^{12}\text{C}^{6+}$ . First direct mass measurement with Pentatrap, what is different to higher masses?

Lower masses -> **mass-to-charge-“doubletivity” is often less good**, frequency differences are bigger (in HoDy or for metastables there is no difference in axial frequency and sub Hz difference in cyclotron frequency)

|                      | $^{20}\text{Ne}^{10+}$ | $^{12}\text{C}^{6+}$ | $\Delta\nu_i$ (Hz) |
|----------------------|------------------------|----------------------|--------------------|
| $\nu_+$ (Hz)         | 53792993.89            | 53772656.43          | <b>20337.46</b>    |
| $\nu_z$ (tuned) (Hz) | 736080.7               | 736080.7             | 0 (~100 @ same U0) |
| $\nu_-$ (Hz)         | 5036.09                | 5038.38              | 2.29               |

**The difference in  $\nu_+$  might(!) result in different excitation radii** due to a non-constant transfer function from the RF-generator output to the trap electrodes over the needed frequency range, **e.g. by non-linear filters and/or switches or static noise resonances.**

**What would the systematics look like?**

## More low masses as cross check

---

We are planning to measure other low masses sooner or later, e.g.:

|      | $\delta m/m_{AME}$ | Group                      | Year |
|------|--------------------|----------------------------|------|
| 14N  | 1.71E-11           | MIT / DiFilippo /Pritchard | 1995 |
| 16O  | 2.00E-11           | UW / van Dyke              | 2006 |
| 28Si | 1.97E-11           | FSU / Redshaw / Myers      | 2008 |

Neon mass measurement showed:

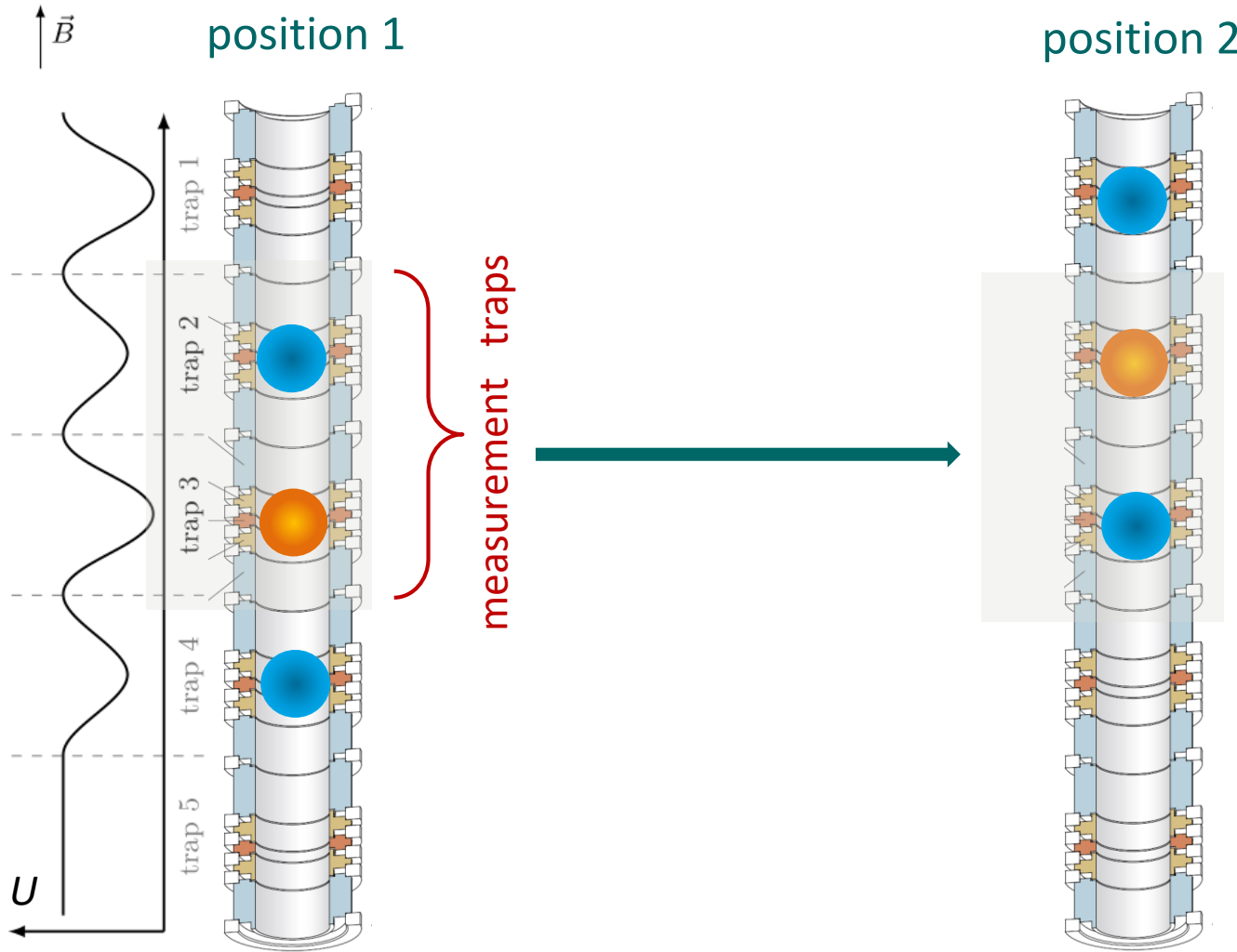
Pentatrap is able to measure low masses.

-> even more candidates to measure!

Systematics are more prominent, better to investigate with low masses.

Discrepancy between AME and our result, more comparisons are needed.

# Data Analysis: Cancel Method



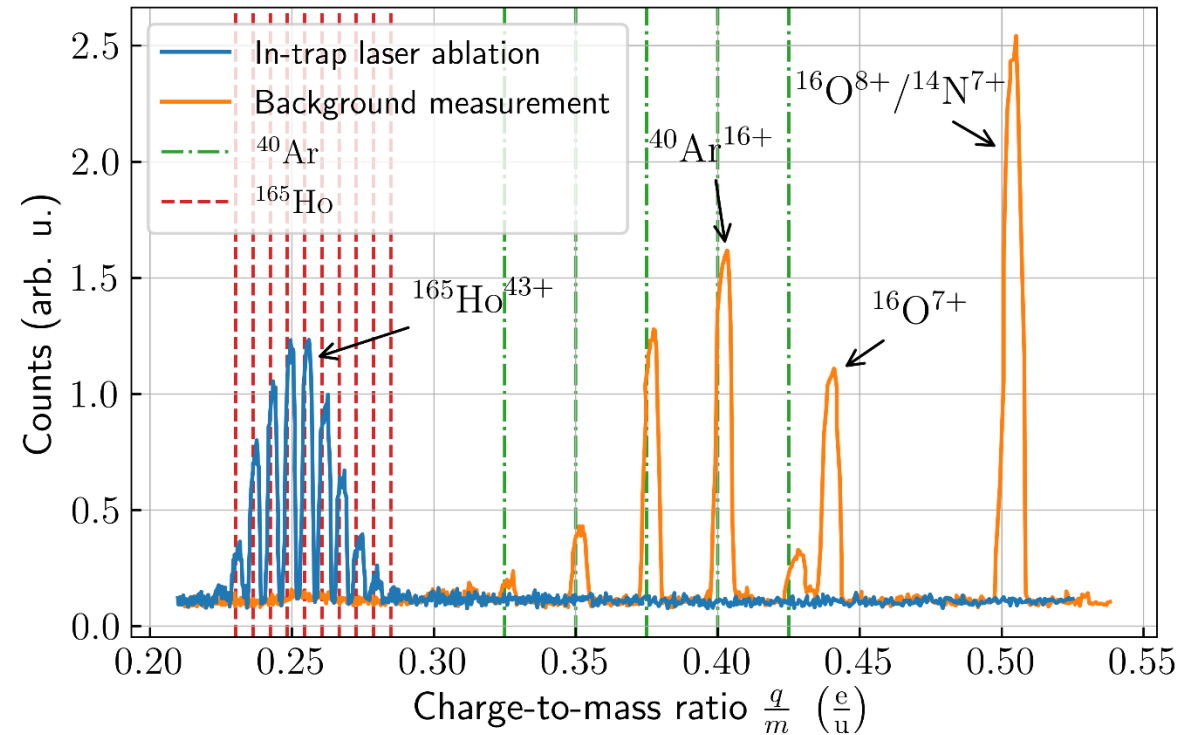
$$R = \sqrt{R(t_1)R(t_2)} = \frac{m_2}{m_1}$$

if  $\frac{B_{trap2}}{B_{trap3}} = const$

$$R(t_1) = \frac{v_{ion1}}{v_{ion2}}(t_1) = \frac{m_2 B_{trap2}}{m_1 B_{trap3}}(t_1)$$

$$R(t_2) = \frac{v_{ion1}}{v_{ion2}}(t_2) = \frac{m_2 B_{trap3}}{m_1 B_{trap2}}(t_2)$$

## Massive $^{165}\text{Ho}$ target

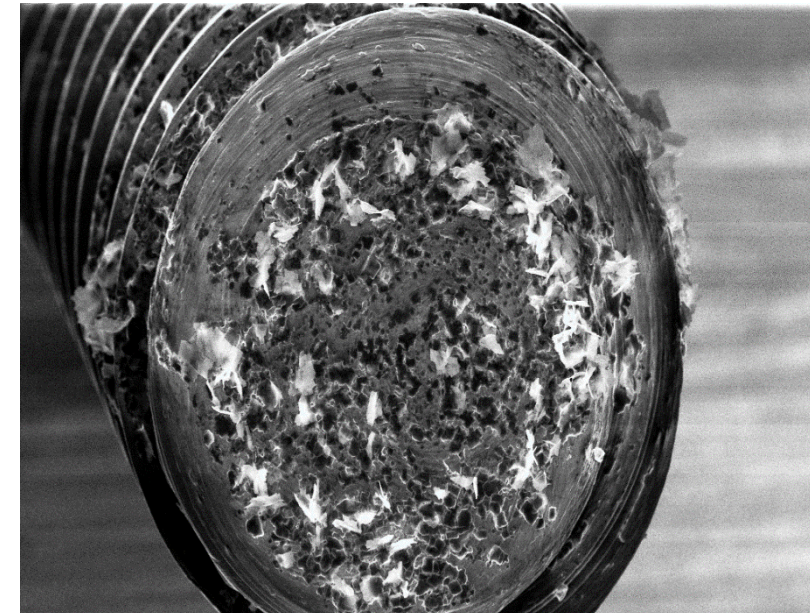
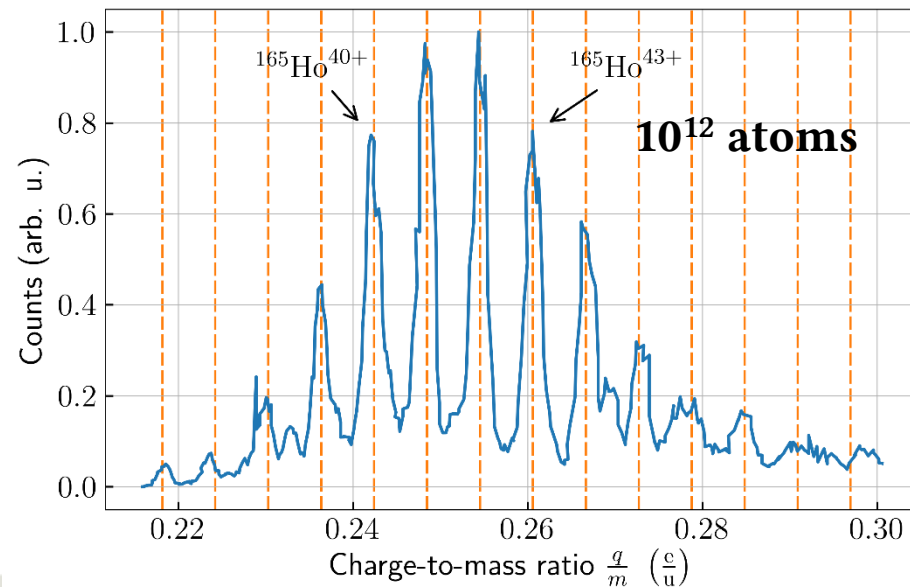


Blue curve: Laser ablation from  $^{165}\text{Ho}$  target

Orange curve: Background measurement without laser

## Small holmium targets

- 1 mm diameter Ti-wire
- Targets with known number of  $^{165}\text{Ho}$  atoms on the surface:  
Drop-on-demand inkjet printing technique  
(group of Ch. Düllmann @ JGU Mainz)



, 30kV, 91x, 14mm, 22.7.19

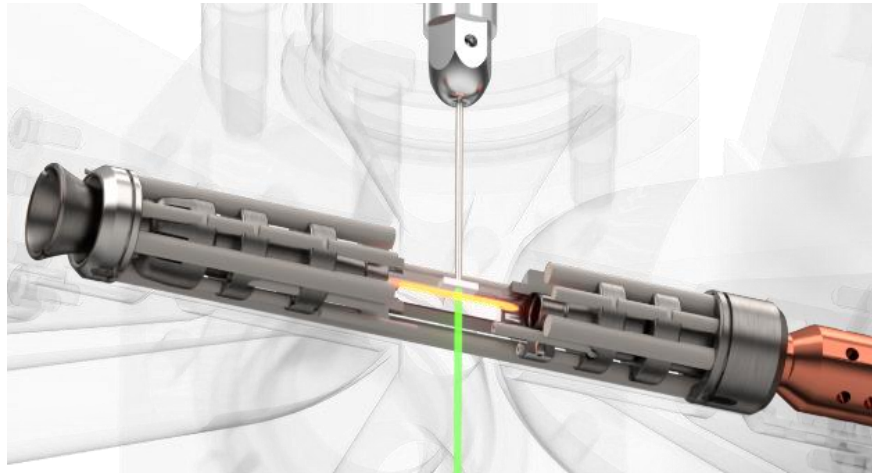
— 200  $\mu\text{m}$  —



Lens: ZS200.X300

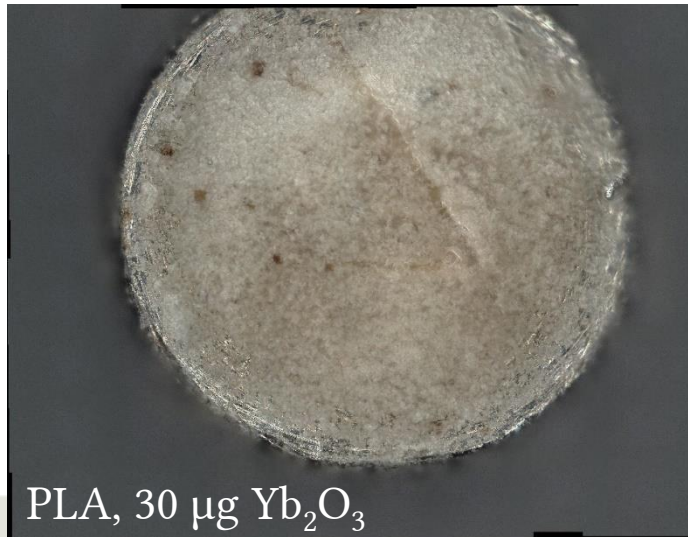
100.00  $\mu\text{m}$

## Targets for in-trap laser desorption

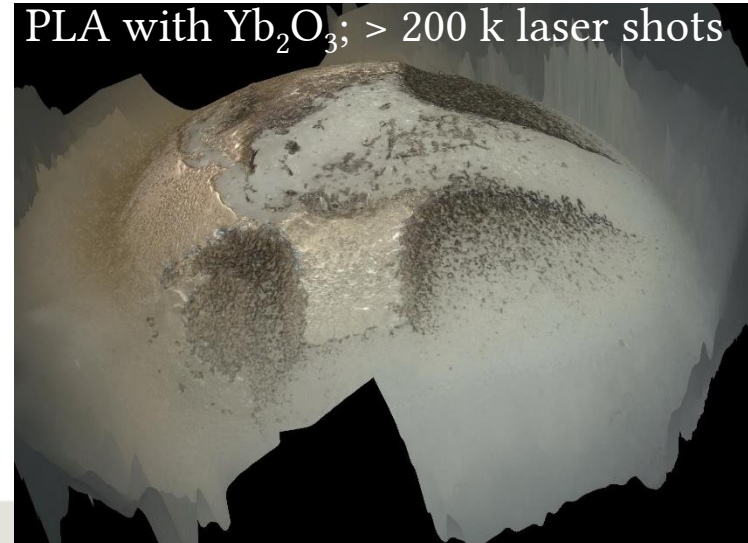


### Target types:

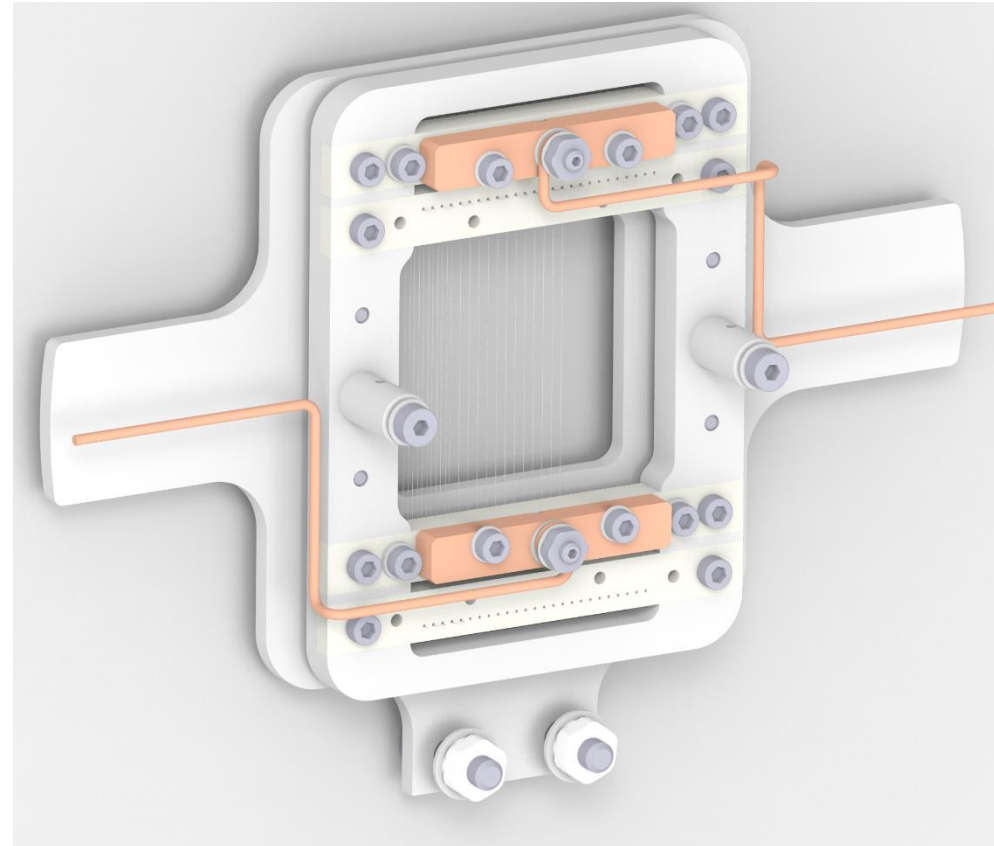
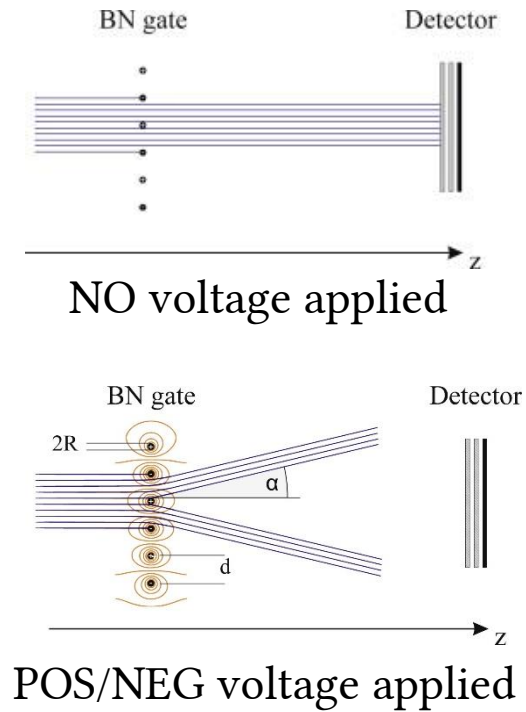
- „Drop-on-demand“ printed targets:  $\mu\text{g}$  to ng samples, smallest target:  $10^{12}$  atoms  $^{165}\text{Ho}$
- PLA-target: tens of  $\mu\text{g}$  to mg
- Massive targets: mg samples, e.g. metallic foil, bulk material



PLA with  $\text{Yb}_2\text{O}_3$ ; > 200 k laser shots



# Bradbury-Nielsen Gate: design

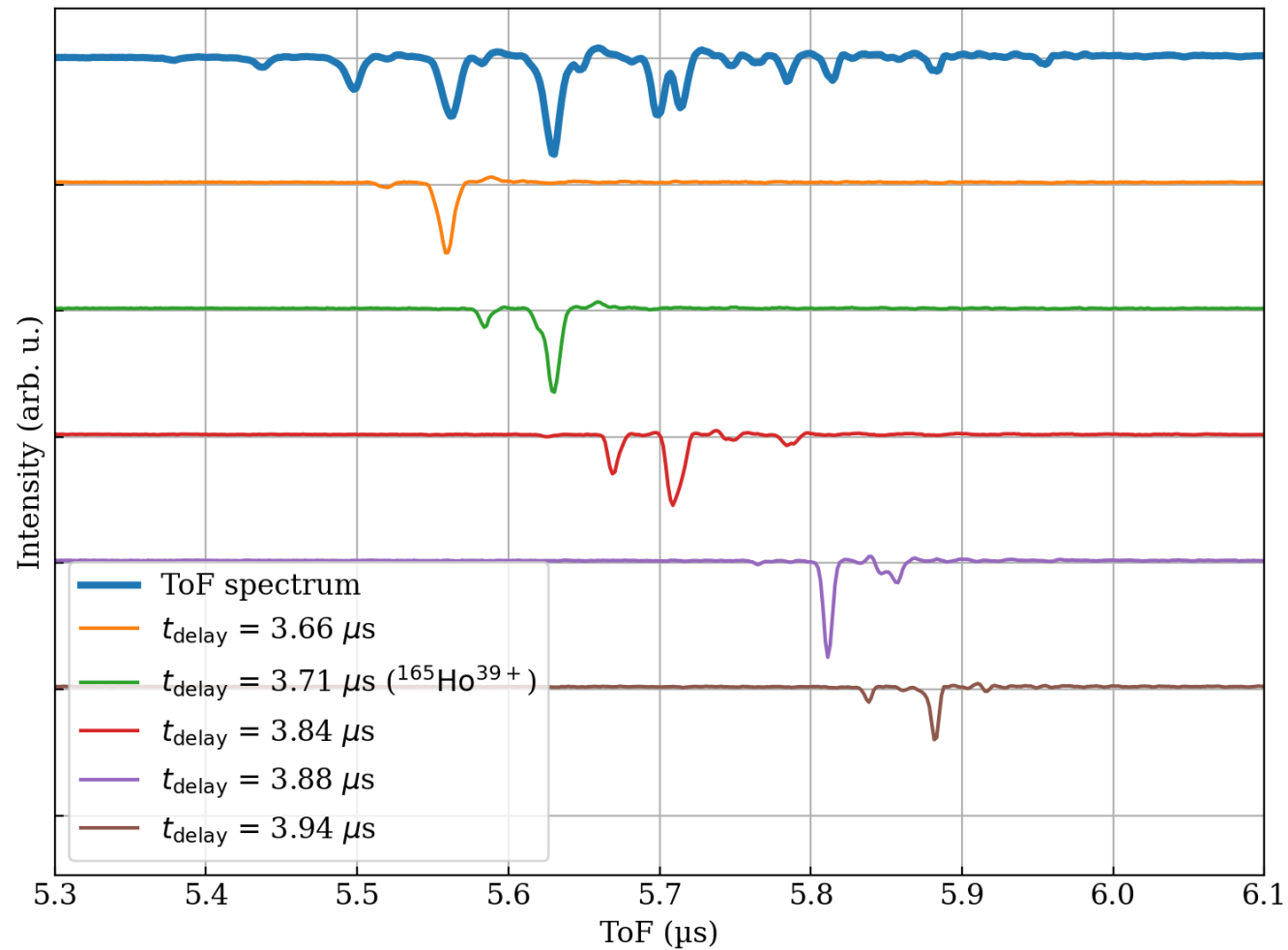


Wolf, R.N. et al., *NIMA* 686, 82 (2012)

Brunner, T. et al., *IJMS* 309, 97 (2012)

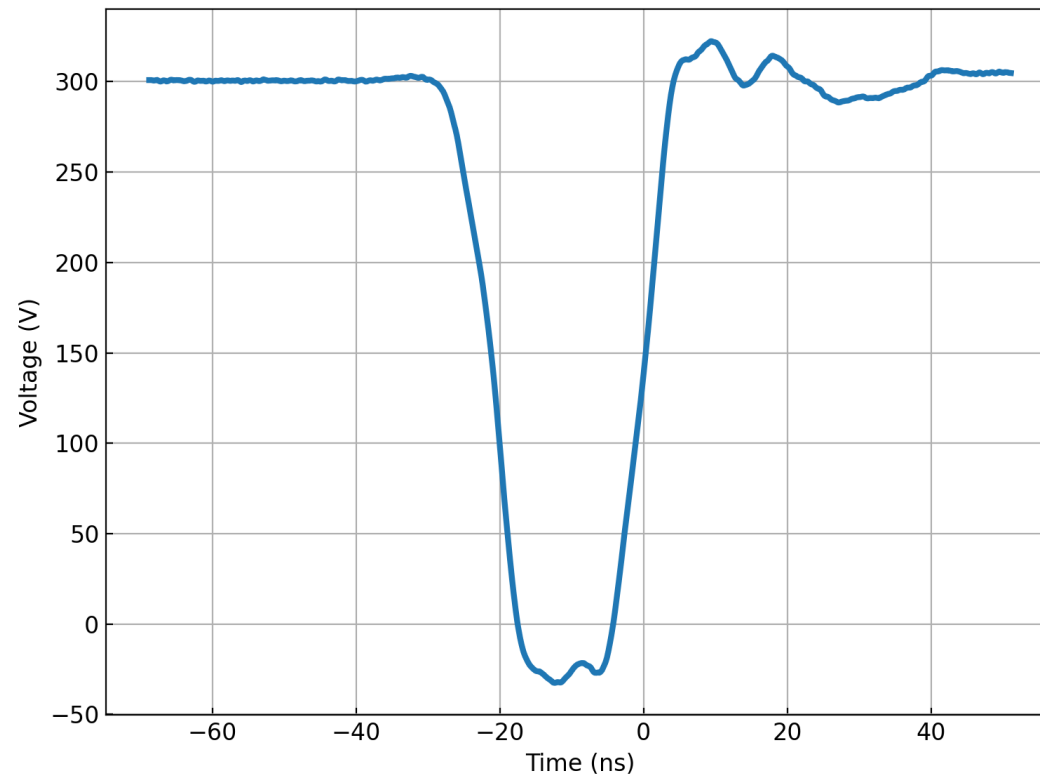
# Bradbury-Nielsen Gate: performance

1st version: 40 ns pulse width/20-30 ns jitter



## MOSFET switch for Bradbury-Nielsen Gate

- Switch based on two N-channel MOSFETs with gate drivers
- Pulse width reduced from 40 to 20 ns
- Near future: Faster MOSFETs placed inside the vacuum chamber



newest design ~20 ns pulse width

# Measurement of trap frequencies with PENTATRAP

$$I_{ion}^{max} = 2\pi\nu_z q \frac{z_{max}}{D} = 15 \text{ fA}$$

$$z_{max} = 10 \text{ }\mu\text{m}$$

$$\nu_z = 500 \text{ kHz}$$

$Re^{29+}$

$$R_{LC} = 2\pi\nu_{LC} LQ = 25 \text{ M}\Omega$$

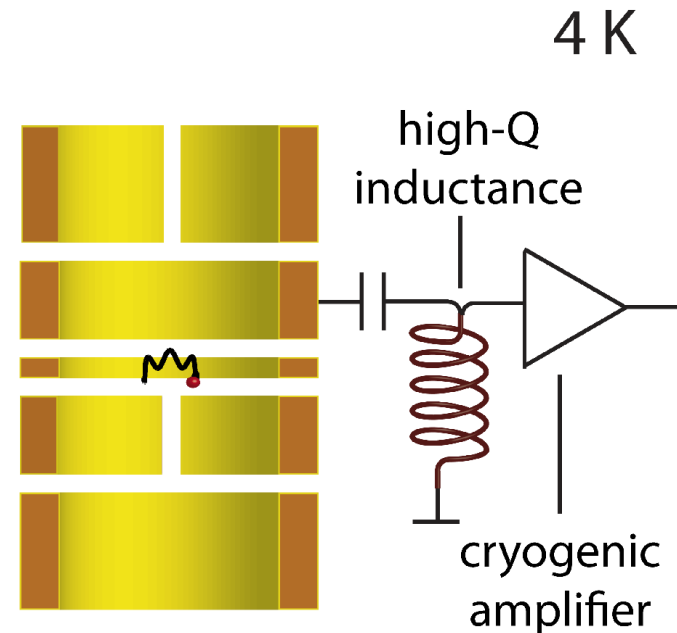
$$L = 1.5 \text{ mH}$$

$$Q = 5000$$

$$U_{ion}^{max} = I_{ion}^{max} R_{LC} = 370 \text{ nV}$$

$$U_{th\_4K} = 70 \text{ nV}$$

$$U_{th\_300K} = 600 \text{ nV}$$



# Determination of $Q$ -value of $\beta^-$ -decay of $^{187}\text{Re}$



$$Q = M[^{187}\text{Re}] - M[^{187}\text{Os}] = M[^{187}\text{Os}^{29+}] \cdot [R-1] + \Delta B$$

Maurits Haverkort  
Heidelberg University Institute for Theoretical Physics

Zoltan Harman  
Max-Planck Institute for Nuclear Physics

Paul Indelicato  
Directeur de Recherche au CNRS

A multiconfiguration Dirac-Hartree-Fock method (MCDHF), a fully relativistic approach, and its combination with Brillouin-Wigner many-body perturbation theory are used.

The ground state of the  $\text{Re}^{29+}$  ion is a simple Pd-like configuration  $[\text{Kr}]4d^{10} 1S_0$ , the neutral Re atom is in the  $[\text{Xe}]4f^{14}5d^56s^2 6S_{5/2}$  electronic state.

The Os ion and atom have an additional electron compared to their Re counterparts, thus their ground states are the Ag-like  $[\text{Kr}]4d^{10}4f^2F_{5/2}$  and  $[\text{Xe}]4f^{14}5d^66s^2 5D_4$  configurations, respectively.

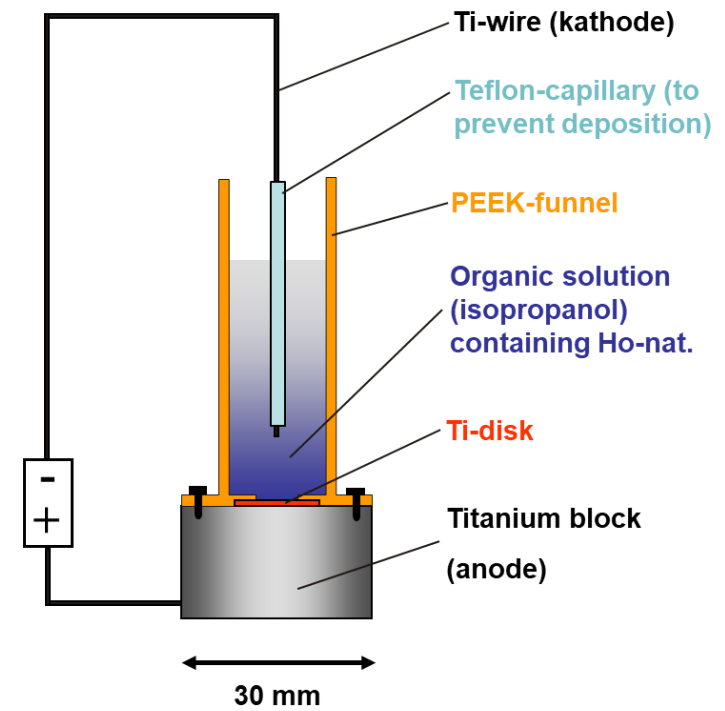
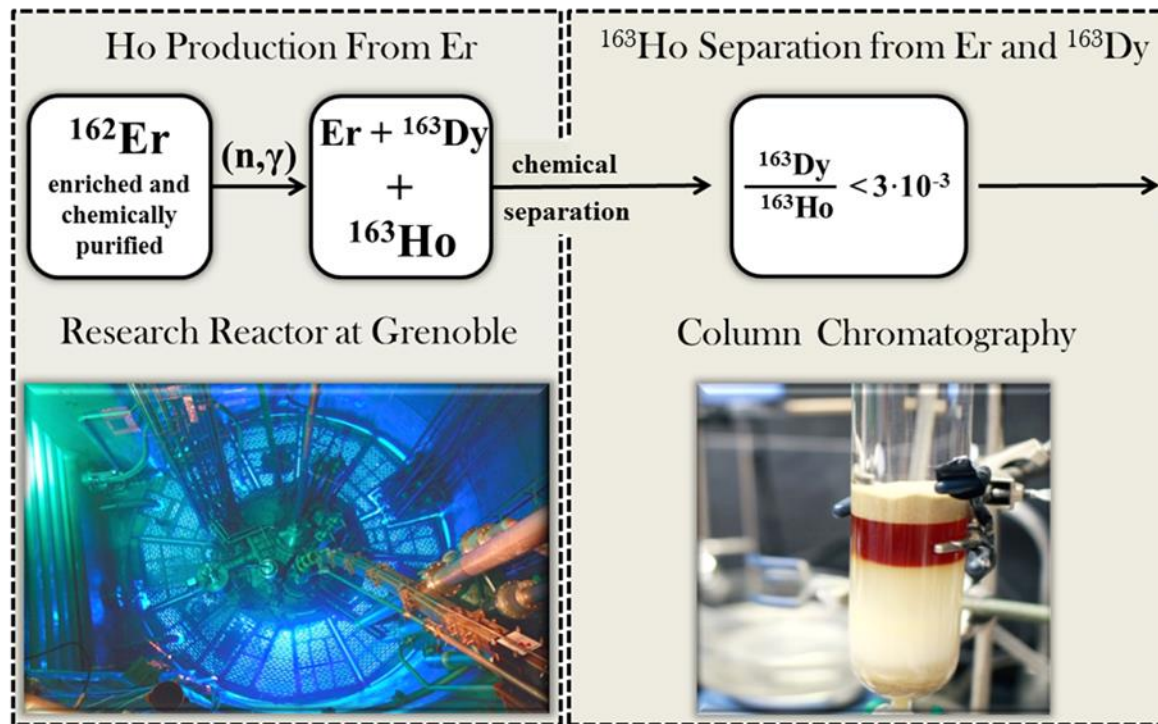
Within the MCDHF scheme, the many-electron atomic state function is given as a linear combination of configuration state functions (CSFs) with a common total angular momentum (J), magnetic (M) and parity (P) quantum numbers:  $|\Gamma PJM\rangle = \sum_k c_k |\gamma k PJM\rangle$ . The CSFs  $|\gamma k PJM\rangle$  are constructed as jj-coupled Slater determinants of one-electron orbitals, and  $\gamma k$  summarizes all the information needed to fully define the CSF, i.e. the orbital occupation and coupling of single-electron angular momenta.  $\Gamma$  collectively denotes all the  $\gamma k$  included in the representation of the ground state.

The GRASP2018 code package [30] is used.



# ECHO Experiment

## $^{163}\text{Ho}$ wire preparation



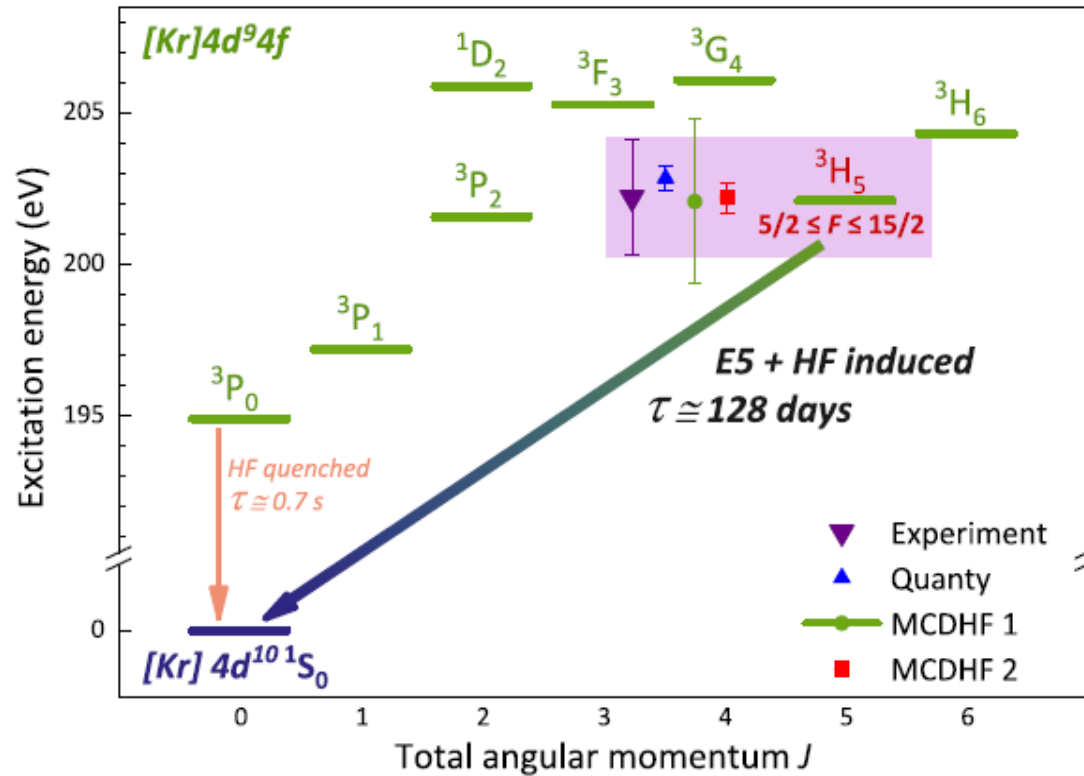


**Figure 2:** The  $4d^{10}$  ground state and relevant  $4d^9 4f$  excited electronic states of the  $^{187}\text{Re}^{29+}$  ion. Comparison of the experimental result and theoretical values obtained using multi-configuration Dirac-Hartree Fock approaches in two different implementations (MCDHF 1 and 2) and by means of a configuration-interaction (Quanty) calculation is shown in the coloured bar.

# dark matter and 5<sup>th</sup> force

168,170,172,174,176Yb

I. Counts et al., PRL 125, 123002 (2020) (MIT, USA)

**Measurement:** two quadrupole transitions in 5 Yb<sup>+</sup> Isotopes,  $6s^2S_{1/2} \leftrightarrow 5d^2D_{5/2}$  (411 nm),  $6s^2S_{1/2} \leftrightarrow 5d^2D_{3/2}$  (436 nm) with an uncertainty of **300 Hz** (limited by laser drift).

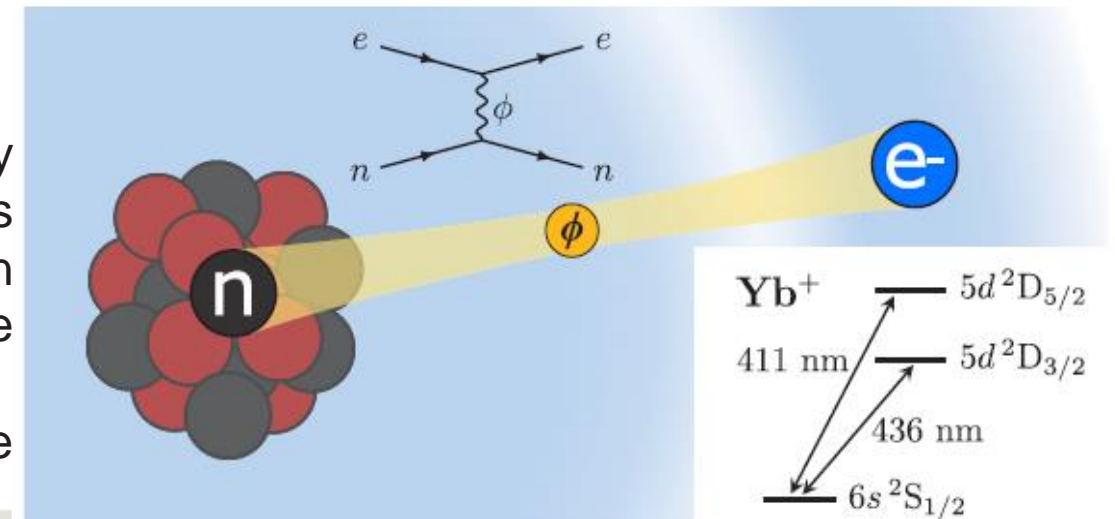
**Method:** ion in Paul trap; Doppler cooled on  $6s^2S_{1/2} \rightarrow 6p^2P_{1/2}$  to 0.5 mK; coherent Ramsey spect./electron-shelving scheme.

**Results:** King plot shows a  $3 \cdot 10^{-7}$  deviation from linearity at  $3\sigma$  uncertainty level.

Indication of the fifth force or higher order nuclear effects within the SM.

## Outlook: (statement in the paper)

In the future, the measurement precision can be increased by several orders of magnitude by cotrapping two isotopes. This improvement, also in combination with measurements on additional transitions, such as the  $^2S_{1/2} \rightarrow ^2F_{7/2}$  octupole transition in Yb<sup>+</sup> or clock transitions in neutral Yb, will allow one to discriminate between nonlinearities of different origin.



# dark matter and 5<sup>th</sup> force

168,170,172,174,176 $\gamma$ b

I. Counts et al., PRL 125, 123002 (2020) (MIT, USA)

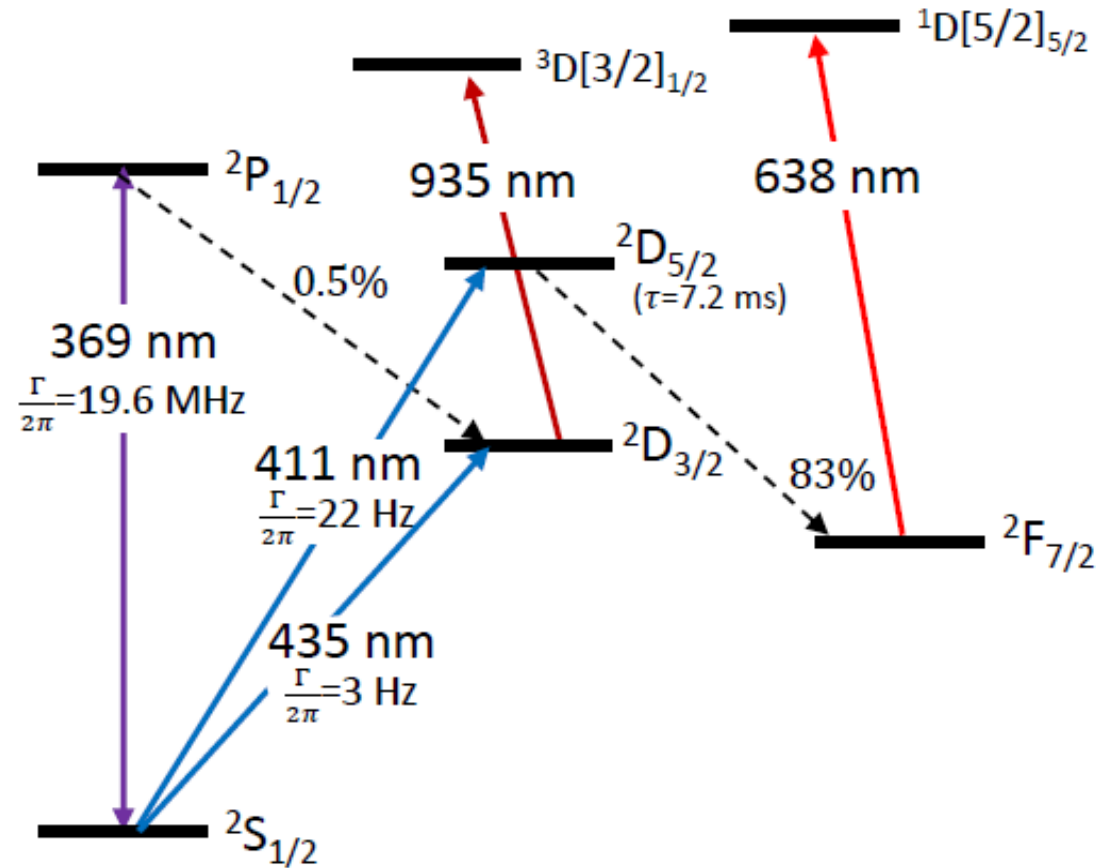


FIG. S1. Partial  $\text{Yb}^+$  level diagram.

# dark matter and 5<sup>th</sup> force

40,42,44,46,48Ca

C. Solaro et al., PRL 125, 123003 (2020) (Aarhus University, Denmark)

F.W. Knollmann et al., PRA 100, 022514 (2019) (Williams College, USA)

**Measurement:** two quadrupole transitions in 5 Ca<sup>+</sup> Isotopes,  $4s^2S_{1/2} \leftrightarrow 3d^2D_{5/2}$  (729 nm),  $4s^2S_{1/2} \leftrightarrow 3d^2D_{3/2}$  (732 nm) with an uncertainty of **20 Hz**.

**Method:** (1) frequency-comb Raman spectroscopy on  $3d^2D_{3/2} \leftrightarrow 3d^2D_{5/2}$  (C. Solaro et al.)  
(2) co-trapped ions in a Paul trap, laser spectroscopy on  $4s^2S_{1/2} \leftrightarrow 3d^2D_{5/2}$  (729 nm) (F.W. Knollmann et al.)

**Results:** no non-linearity of the King's plot is observed.

## Outlook:

D-D transitions with 10 mHz accuracy, S-D with 1 Hz.

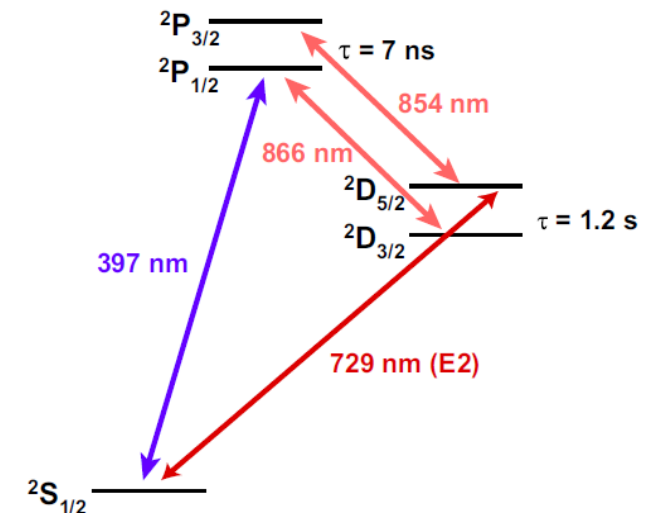


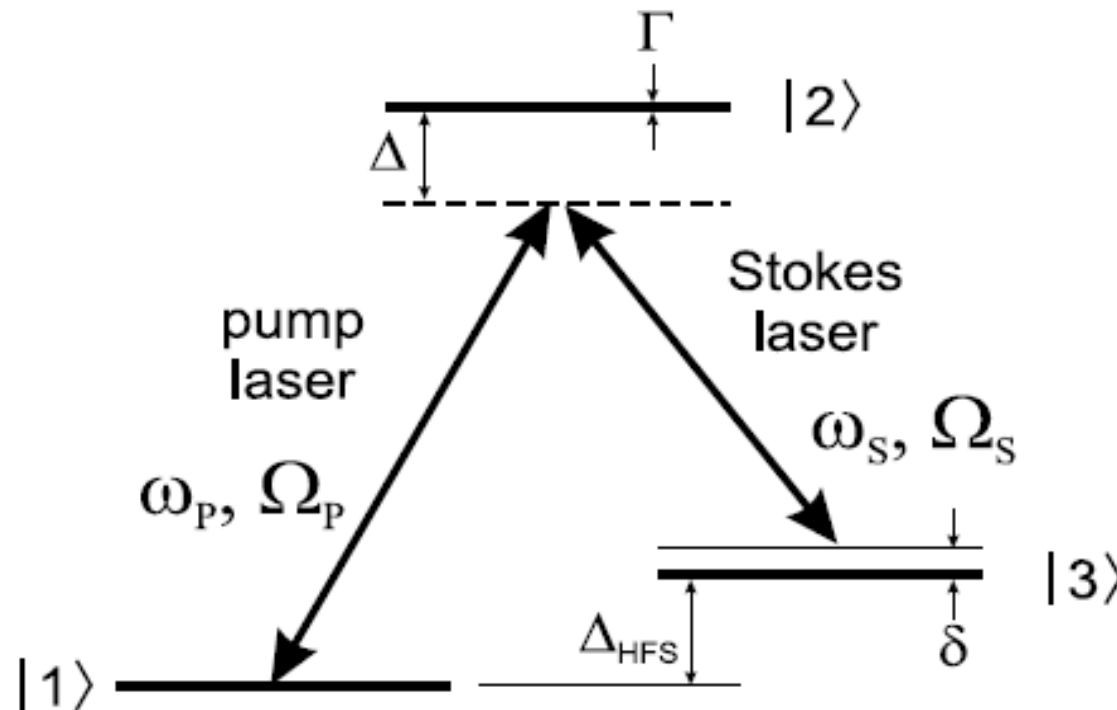
FIG. 1. Level diagram for nuclear spin-zero isotopes of Ca<sup>+</sup>, with natural lifetimes listed. The 397-nm transition is used for Doppler cooling and fluorescence detection, while metastable  $2D_{3/2,5/2}$  levels are repumped by transitions at 866 and 854 nm, respectively.

taken from the paper by F.W. Knollmann

## Raman spectroscopy

A Raman transition couples two atomic levels by the absorption of a photon from one Raman beam (pump beam) and by stimulated emission of another one into the other beam (Stokes beam).

The narrow linewidth of Raman transitions can be used to resolve atomic motional sidebands.



# dark matter and 5<sup>th</sup> force

84,86,87,88,90Sr

T. Manowitz et al., PRL 123, 203001 (2019) (Weizmann Institute of Science, Israel)

H. Miyake et al., PRR 1, 033113 (2019) (Joint Quantum Institute, USA)

**Measurement:** (1)  $^1S_0 - ^3P_1$  (689 nm, linewidth=7.4 kHz),  $^1S_0 - ^3P_0$  (698 nm, linewidth= mHz), with an uncertainty of a few kHz.

(2) electric quadrupole (0.4 Hz)  $^5S_{1/2} - ^4D_{5/2}$  with an uncertainty of 9 mHz.

**Method:** (1) laser spectroscopy in optical dipole trap.

(2) decoherence free subspaces (DFSs). Direct probe of the isotope shift with 9 mHz uncertainty.

**Results:** nonlinearity in the measured values. The problem may be  $^{87}\text{Sr}$  (center of hyperfine splitting is determined wrongly).

$^{90}\text{Sr}$  is needed (radioactive, 29 years life time).

## Outlook:

Method of decoherence free subspaces with all isotopes.

130,132,134,136,138Ba

P. Imgram et al., PRA 99, 012511 (2019) (TU Darmstadt, Germany)

**Measurement:**  $6s^2S_{1/2} - 6p^2P_{1/2}$  (D1, 493 nm),  $6s^2S_{1/2} - 6p^2P_{3/2}$  (D2, 455 nm), with accuracy of 200 kHz.

**Method:** collinear/anticollinear laser spectroscopy on collimated fast ion beams.

**Results:** uncertainty comparable to ion trap measurements on dipole transitions but far from the needed one for 5<sup>th</sup> force.

142,144,146,148,150Nd

N. Bhatt et al., ArXiv 2002.08290 (Uni of Toronto, Canada)

**Measurement:**  $4f^46s - [25044.7]_{7/2}$  (399 nm),  $4f^46s - [25138.6]_{7/2}$  (397 nm) with accuracy of a few 100 kHz.

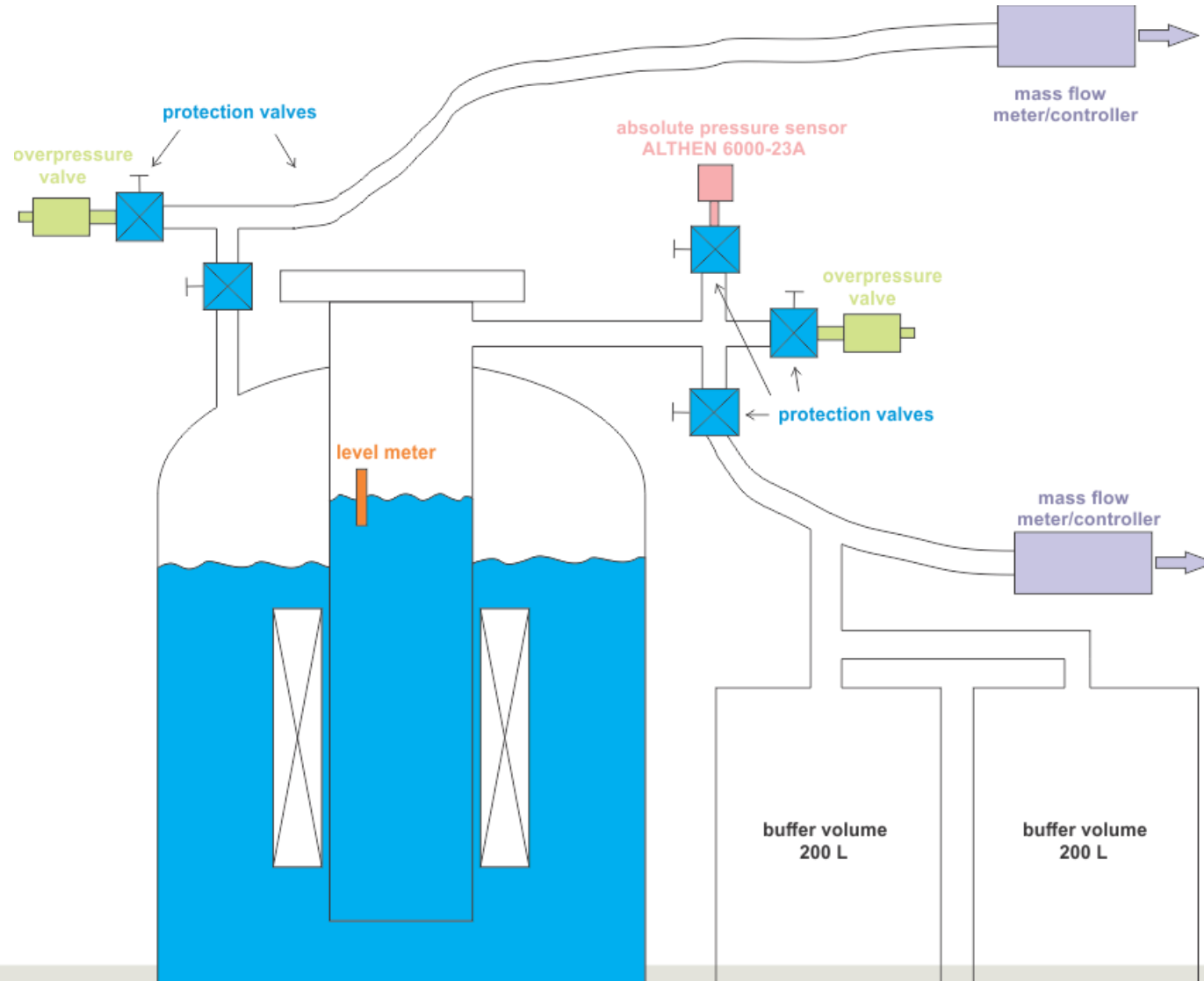
**Method:** laser absorption spectroscopy of cold ions in a neutral plasma.

**Results:** uncertainty comparable to ion trap measurements on dipole transitions but far from the needed one for 5<sup>th</sup> force.

## Outlook:

several telecommunication forbidden transitions 1500 nm with sub-Hz uncertainty.

# Stabilization of LHe level and He pressure



# Polynomial Method

Ann. Inst. Statist. Math.  
30 (1978), Part A, 9-14

## A BAYESIAN ANALYSIS OF THE MINIMUM AIC PROCEDURE

HIROTUGU AKAIKE

(Received Oct. 15, 1977; revised Apr. 24, 1978)

### Summary

By using a simple example a minimax type optimality of the minimum AIC procedure for the selection of models is demonstrated.

*Biometrika* (1989), **76**, 2, pp. 297-307  
Printed in Great Britain

## Regression and time series model selection in small samples

BY CLIFFORD M. HURVICH

*Department of Statistics and Operations Research, New York University, New York  
NY 10003, U.S.A.*

AND CHIH-LING TSAI

*Division of Statistics, University of California, Davis, California 95616, U.S.A.*

### SUMMARY

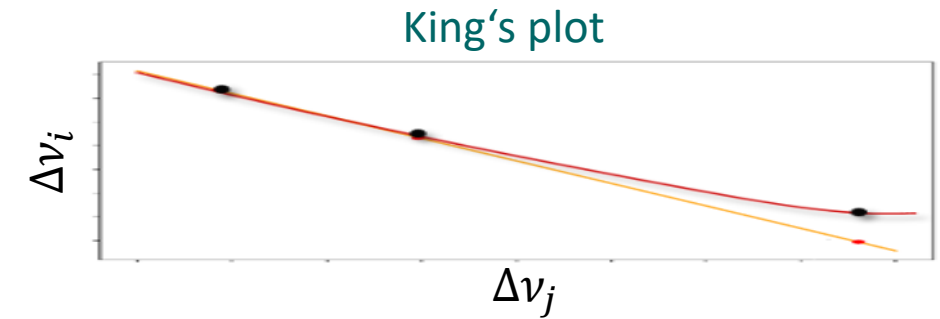
A bias correction to the Akaike information criterion,  $AIC$ , is derived for regression and autoregressive time series models. The correction is of particular use when the sample size is small, or when the number of fitted parameters is a moderate to large fraction of the sample size. The corrected method, called  $AIC_c$ , is asymptotically efficient if the true model is infinite dimensional. Furthermore, when the true model is of finite dimension,  $AIC_c$  is found to provide better model order choices than any other asymptotically efficient method. Applications to nonstationary autoregressive and mixed autoregressive moving average time series models are also discussed.

# dark matter and 5<sup>th</sup> force

$$\nu_i(\text{isotope}_1) - \nu_i(\text{isotope}_2) \equiv \Delta\nu_i = K_i \cdot \frac{m_1 - m_2}{m_1 m_2} + F_i \cdot [\langle r^2 \rangle_1 - \langle r^2 \rangle_2] + [\text{higher-order SM effects} + \text{LDM bosons}]$$

cannot be measured precisely

$$\Delta\nu_i = C_1 \cdot \frac{m_1 - m_2}{m_1 m_2} + C_2 \cdot \Delta\nu_j + [\text{higher-order SM effects} + \text{LDM bosons}]$$



one needs elements with many even-even isotopes and quadrupole (narrow optical) transitions:

168,170,172,174,176Yb  $^2S_{1/2} \leftrightarrow ^2D_{5/2}$  (411 nm)  $^2S_{1/2} \leftrightarrow ^2D_{3/2}$  (436 nm) I. Counts et al., PRL 125, 123002 (2020)

40,42,44,46,48Ca  $4s^2S_{1/2} \leftrightarrow 3d^2D_{5/2}$  (729 nm)  $4s^2S_{1/2} \leftrightarrow 3d^2D_{3/2}$  (732 nm) C. Solaro et al., PRL 125, 123003 (2020)  
F.W. Knollmann et al., PRA 100, 022514 (2019)

84,86,88,90Sr  $5S_{1/2} - 4D_{5/2}$   $1S_0 - 3P_1, 1S_0 - 3P_0$  T. Manowitz et al., PRL 123, 203001 (2019)  
H. Miyake et al., PRR 1, 033113 (2019)

142,144,146,148,150Nd

N. Bhatt et al., ArXiv 2002.08290

130,132,134,136,138Ba

P. Imgram et al., PRA 99, 012511 (2019)

**FUTURE:**

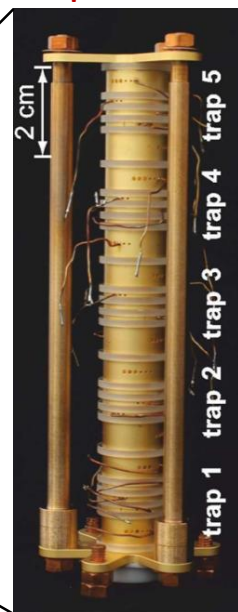
$$\delta(\Delta\nu_i) \approx 10 \text{ mHz}$$

$$\delta\left(\frac{m_1}{m_2}\right) < 10^{-11}$$

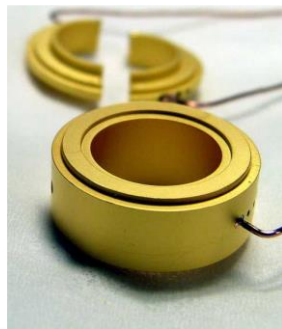
# some photos of traps and axial resonators



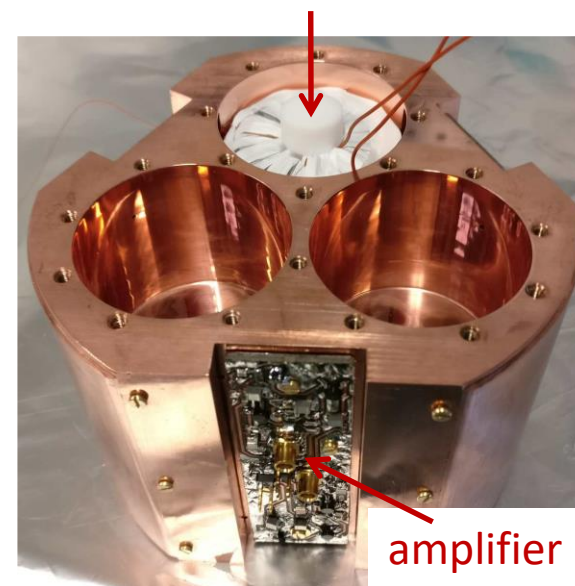
trap tower



trap electrodes



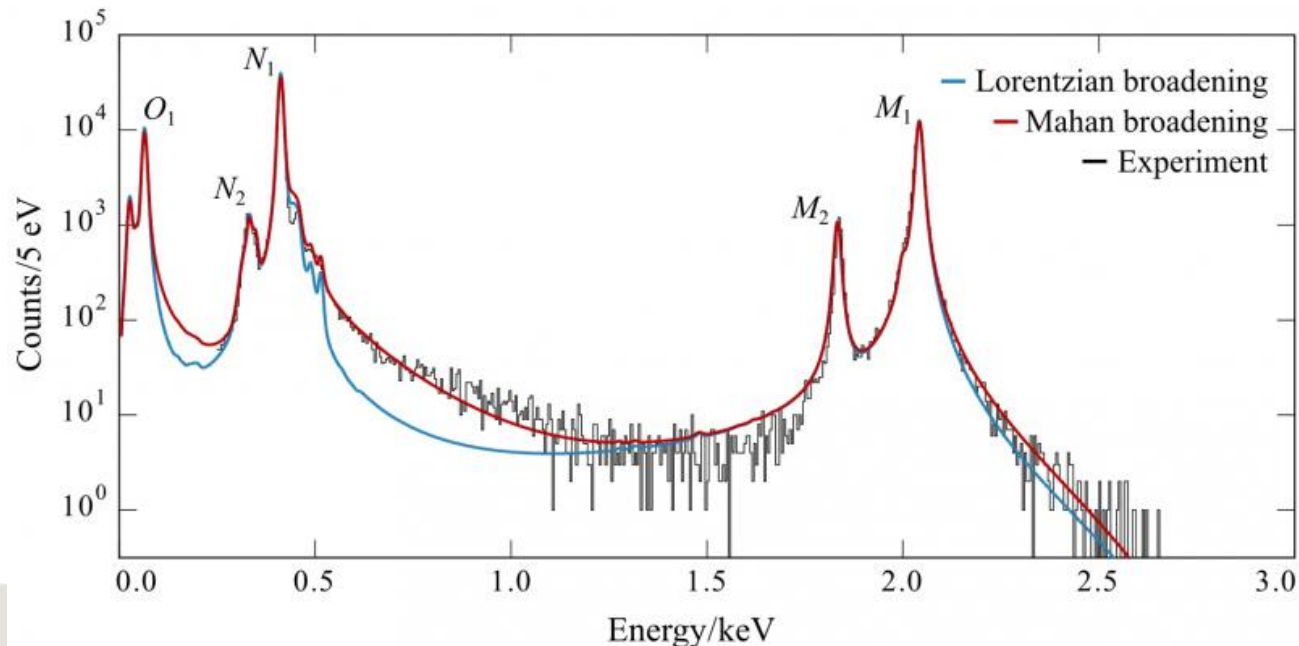
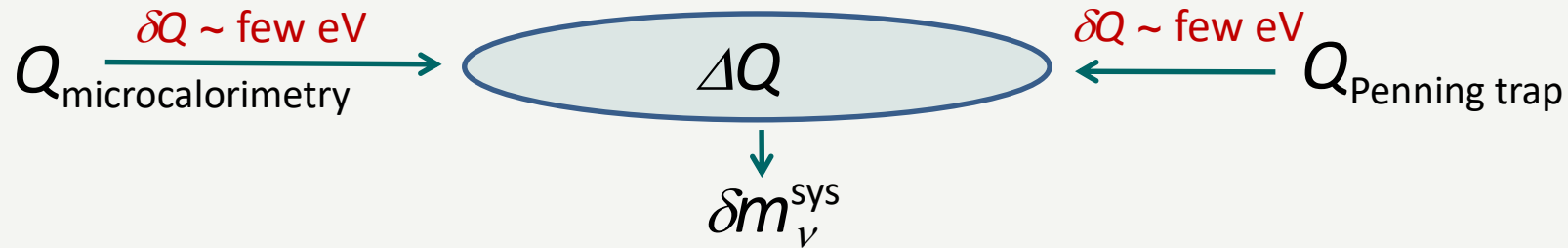
NbTi toroidal coil



amplifier

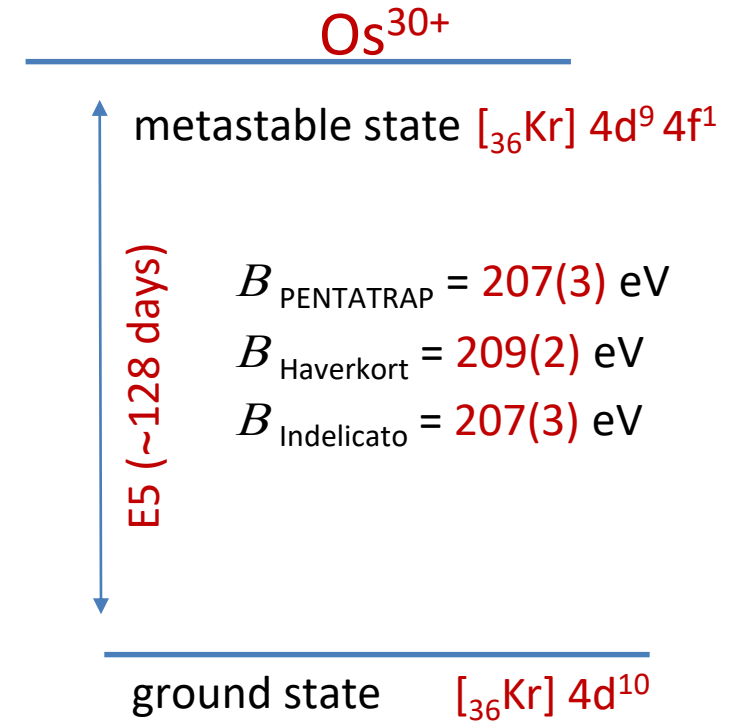
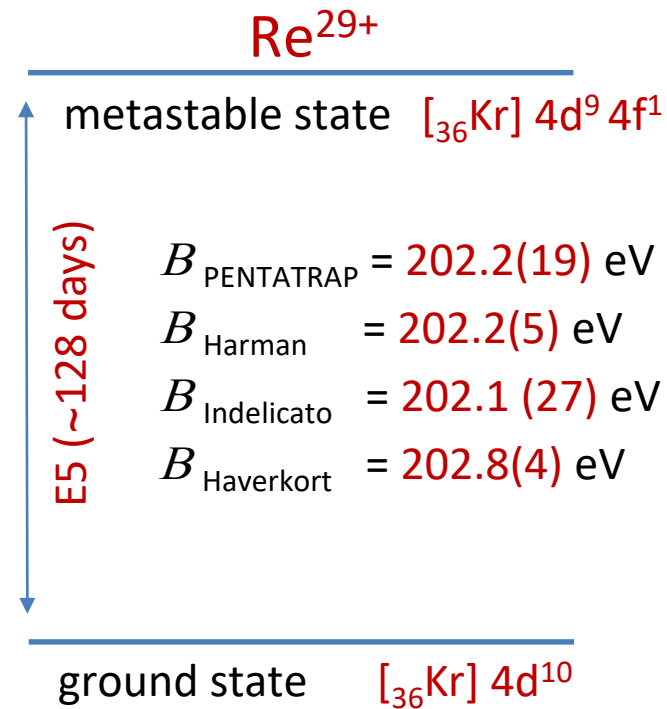
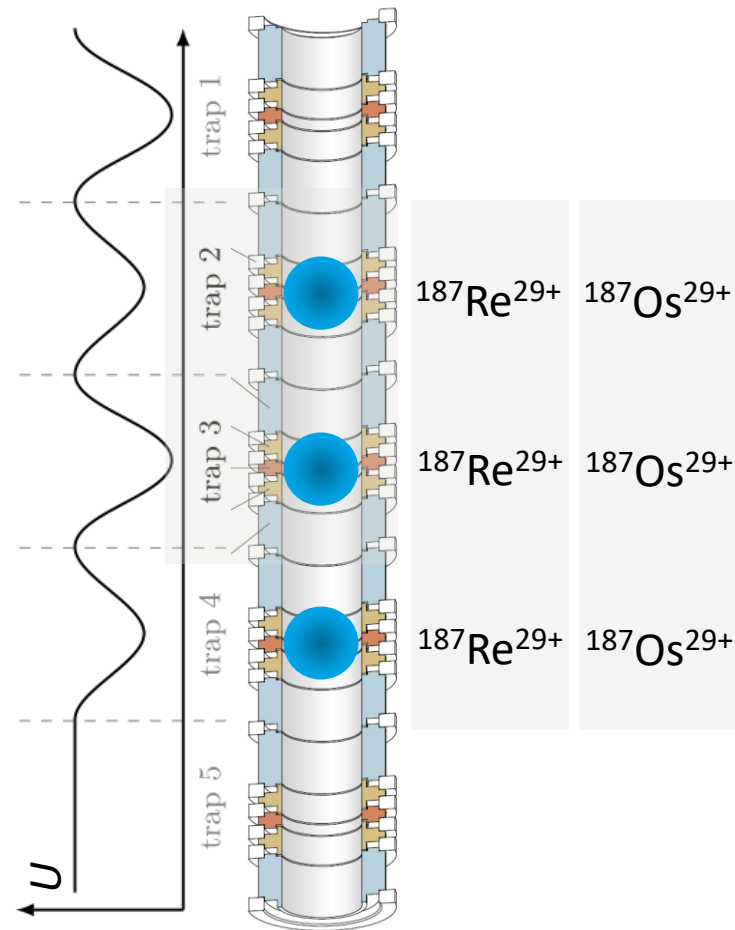
# The Electron Capture in Holmium experiment

$$\frac{dN}{dE} = A(Q - E)^2 \sqrt{1 - \frac{m_\nu^2}{(Q - E)^2}} \sum C \phi_k^2(0) \frac{\Gamma_k / 2\pi}{(E - B_k)^2 + \Gamma_k^2 / 4}$$



# excitation energies of atomic metastable states

- $\text{Os}^{29+}$  vs.  $\text{Os}^{29+}$  measurements yield always unity.
- $\text{Re}^{29+}$  vs.  $\text{Re}^{29+}$  measurements yield either unity or  $1+1.14 \cdot 10^{-9}$ .



Possible application: search for suitable clock transitions

# Data Analysis: Polynomial Method

